

Dissertation zur Erlangung des Doktorgrades  
der Fakultät für Biologie  
der Ludwig-Maximilians-Universität München

**Comparison of Genome-Wide Nucleosome Positioning  
Mechanisms in *Schizosaccharomyces pombe* and  
*Saccharomyces cerevisiae***



Alexandra Lantermann

München  
20. Mai 2010

Dissertation eingereicht am: 20. Mai 2010

Mündliche Prüfung am: 20. Juli 2010

1. Gutachter: Prof. Dr. Peter Becker
2. Gutachter: Prof. Dr. Stefan Jentsch
3. Gutachter: Prof. Dr. Dario Leister
4. Gutachter: Prof. Dr. Michael Boshart
5. Gutachter: Prof. Dr. Angelika Böttger
6. Gutachter: Prof. Dr. Dirk Eick

**Ehrenwörtliche Versicherung**

Ich versichere hiermit ehrenwörtlich, dass die vorgelegte Dissertation von mir selbständig und ohne unerlaubte Hilfe angefertigt wurde.

München, den .....

(Alexandra Lantermann)

## Erklärung

Hiermit erkläre ich, dass ich mich nicht anderweitig einer Doktorprüfung ohne Erfolg unterzogen habe.

München, den .....

(Alexandra Lantermann)

Wesentliche Teile dieser Arbeit sind in folgenden Publikationen veröffentlicht:

Lantermann, A., T. Straub, A. Stralfors, G. C. Yuan, K. Ekwall and P. Korber (2010). *Schizosaccharomyces pombe* genome-wide nucleosome mapping reveals positioning mechanisms distinct from those of *Saccharomyces cerevisiae*. Nat Struct Mol Biol 17(2): 251-257.

Lantermann, A., A. Stralfors, F. Fagerstrom-Billai, P. Korber and K. Ekwall (2009). Genome-wide mapping of nucleosome positions in *Schizosaccharomyces pombe*. Methods 48(3): 218-225.

Diese Arbeit ist Mama und Papa, Christiane und Ulf gewidmet.

## Acknowledgements

I would like to thank

Dr. Philipp Korber for giving me the opportunity to join his group, to work on this great project, for his constant support and advice throughout the thesis, and for always finding time for very stimulating discussions,

Prof. Dr. Peter Becker for following up my work and constant support, for taking over the role of an official supervisor, and for his big contribution to a stimulating scientific environment and nice atmosphere in the lab,

Prof. Dr. Stefan Jentsch for being the second member of my PhD committee,

Dr. Tobias Straub, for all his support with bioinformatical and statistical data analysis and interpretation, for his patience, for teaching me R, and for very helpful discussions,

Prof. Dr. Guo-Cheng Yuan for N-score model calculations and testing the HMM,

Prof. Dr. Karl Ekwall for collaboration on this project, stimulating discussions, and providing strains and data sets,

Annelie Strålfors for teaching me the Tiling Analysis Software, sending *S. pombe* strains and bringing my samples to the Affymetrix facility,

Prof. Hiten Madhani and Ramón Ramos Barrales for providing *S. pombe* strains,

Natalie Dutrow for advice on the analysis of transcriptome data,

Dr. Sandra Hake and Prof. Dr. Axel Imhof for being in my thesis advisory committee and for very helpful discussions,

Dr. Felix Müller-Planitz for teaching me the basics of MATLAB,

Edith Müller and Carolin Brieger from the secretary for being so well organized, helpful, and for sending away my Stockholm packages,

Dorle Blaschke, Franziska Ertel and Christian Wippo for teaching me their technical expertise, for fun in the lab, and for contributing to a great working atmosphere,

The whole North Lab and all the people from the molecular biology department who made work every day much more fun,

My parents and my sister for constant familiar support,

Ulf and my friends for constant support and non-constant distraction.

## Table of contents

<b>Summary .....</b>	<b>1</b>
<b>Zusammenfassung .....</b>	<b>2</b>
<b>1 Introduction.....</b>	<b>3</b>
1.1 Basic levels of chromatin organization in eukaryotes .....	3
1.2 Mechanisms for regulation of chromatin structure.....	5
1.3 Nucleosome positioning .....	7
1.3.1 Methods to map nucleosomes .....	9
1.3.2 Outcome of genome-wide nucleosome occupancy maps.....	10
1.3.3 Mechanisms of nucleosome positioning .....	11
1.3.3.1 The role of intrinsic DNA sequence features in nucleosome positioning.....	12
1.3.3.2 The role of trans-factors in nucleosome positioning.....	16
1.4 Aims of this work .....	19
<b>2 Materials and methods .....</b>	<b>20</b>
2.1 Materials .....	20
2.1.1 Chemicals .....	20
2.1.2 Enzymes .....	21
2.1.3 Other materials .....	21
2.1.4 Oligonucleotides and plasmids.....	22
2.1.4.1 Oligonucleotides .....	22
2.1.4.2 Plasmids .....	23
2.1.5 Bacteria and yeast strains .....	23
2.1.5.1 <i>E. coli</i> strains.....	23
2.1.5.2 <i>S. pombe</i> strains.....	23
2.1.5.3 <i>S. cerevisiae</i> strains .....	24
2.2 Media, buffers and solutions.....	24
2.2.1 Media.....	24
2.2.1.1 Media for <i>E. coli</i> .....	24
2.2.1.2 Media for <i>S. pombe</i> .....	24
2.2.1.3 Media for <i>S. cerevisiae</i> .....	25
2.2.2 Buffers and solutions.....	25
2.3 General methods for working with DNA and RNA .....	30
2.3.1 Horizontal and vertical agarose gel electrophoresis of DNA.....	30
2.3.2 Polymerase chain reaction (PCR).....	30
2.3.3 DNA purification by phenol/chloroform extraction.....	30
2.3.4 DNA precipitation with alcohol .....	30
2.3.5 DNA quantification .....	31
2.3.6 Preparation of chemically competent <i>E.coli</i> .....	31



---

2.3.7	Transformation of competent <i>E. coli</i> .....	31
2.3.8	Preparation of plasmids .....	31
2.3.9	Preparation of probe DNA.....	32
2.3.10	Southern blot .....	32
2.3.11	Northern blot .....	33
2.4	General methods for working with <i>S. pombe</i> and <i>S. cerevisiae</i> .....	33
2.4.1	Transformation of <i>S. pombe</i> .....	33
2.4.2	Transformation of <i>S. cerevisiae</i> .....	33
2.4.3	Isolation of DNA from <i>S. pombe</i> and <i>S. cerevisiae</i> .....	34
2.4.4	Isolation of RNA from <i>S. pombe</i> and <i>S. cerevisiae</i> .....	34
2.5	Preparation of yeast nuclei and yeast extract.....	35
2.5.1	Preparation of nuclei from <i>S. pombe</i> and <i>S. cerevisiae</i> .....	35
2.5.2	Preparation of whole-cell extract from <i>S. pombe</i> and <i>S. cerevisiae</i> .....	35
2.6	<i>In vitro</i> chromatin assembly .....	36
2.6.1	Purification of histone octamers from <i>Drosophila</i> embryos .....	36
2.6.2	Assembly of chromatin by salt gradient dialysis.....	37
2.6.3	Adding yeast extract to pre-assembled chromatin (reconstitution assay) .....	37
2.7	Chromatin analysis by indirect end-labeling .....	37
2.7.1	MNase digestion of <i>S. pombe</i> spheroplasts .....	37
2.7.2	MNase digestion of <i>S. pombe</i> and <i>S. cerevisiae</i> nuclei .....	38
2.7.3	DNaseI digestion of <i>S. pombe</i> and <i>S. cerevisiae</i> nuclei.....	38
2.7.4	DNA purification after DNaseI/MNase digestion.....	38
2.7.5	MNase digestion of free DNA.....	39
2.7.6	DNaseI digestion of plasmid DNA.....	39
2.7.7	Secondary cleavage .....	39
2.7.8	Generation of marker fragments.....	39
2.7.9	DNaseI digestion of <i>in vitro</i> assembled chromatin of <i>SPAC1F8.06</i> .....	40
2.8	Preparation of genome-wide nucleosome occupancy map in <i>S. pombe</i> by tiling array analysis .....	40
2.8.1	Growth and spheroplasting of <i>S. pombe</i> cells.....	40
2.8.2	MNase digestion of <i>S. pombe</i> spheroplasts .....	40
2.8.3	Purification of DNA for tiling array analysis .....	41
2.8.4	Preparation of genomic control DNA.....	41
2.8.5	DNaseI fragmentation, labeling, and hybridization to tiling arrays of mononucleosomal DNA and genomic control DNA.....	41
2.9	Bioinformatical data analysis .....	43
2.9.1	Genome versions and annotations .....	43
2.9.2	Processing of raw microarray data .....	43
2.9.3	Calculation of cumulative profiles .....	44
2.9.4	Clustering of nucleosome occupancy data .....	44

---

2.9.5	Spectral analysis .....	45
2.9.6	Hidden Markov model for NDR search .....	45
2.9.7	Analysis of DNA sequence contributions to nucleosome positioning .....	45
<b>3</b>	<b>Results .....</b>	<b>46</b>
3.1	Different nucleosome positioning at the <i>S. cerevisiae</i> <i>PHO5</i> promoter in <i>S. pombe</i> and <i>S. cerevisiae</i> .....	46
3.2	Genome-wide nucleosome occupancy map of <i>S. pombe</i> .....	51
3.3	Nucleosome occupancies vary at different genomic regions .....	60
3.4	Low nucleosome occupancy at promoters tends to correlate with high gene expression level .....	61
3.5	Nucleosome spacing is different in <i>S. pombe</i> and <i>S. cerevisiae</i> .....	63
3.6	No pronounced regular nucleosomal arrays upstream of TSSs in <i>S. pombe</i> .....	65
3.7	Different trans-factors determine nucleosome positioning .....	67
3.7.1	Transcription correlates with regular nucleosomal arrays .....	67
3.7.2	H2A.Z-containing promoters show regular upstream arrays in <i>S. pombe</i> .....	69
3.7.3	Mit1 is important for regular nucleosome spacing in <i>S. pombe</i> .....	70
3.7.4	Tup11/Tup12 target promoters show pronounced NDRs in <i>S. pombe</i> .....	72
3.8	DNA sequence has a different role in nucleosome positioning in <i>S. pombe</i> and <i>S. cerevisiae</i> .....	73
3.9	<i>In vitro</i> reconstitution of the <i>S. pombe</i> locus <i>SPAC1F8.06</i> does not generate an <i>in vivo</i> -like chromatin structure .....	77
<b>4</b>	<b>Discussion .....</b>	<b>78</b>
4.1	Consequences of the short nucleosome spacing in <i>S. pombe</i> on higher-order chromatin structure .....	78
4.2	The role of transcription in nucleosome positioning .....	80
4.3	The role of H2A.Z in nucleosome positioning .....	82
4.4	The role of DNA sequence in nucleosome positioning .....	83
4.5	The model of statistical nucleosome positioning .....	84
4.6	The evolution of nucleosome positioning mechanisms .....	86
4.7	Outlook .....	88
<b>5</b>	<b>References .....</b>	<b>89</b>
<b>6</b>	<b>Abbreviations .....</b>	<b>102</b>
	<b>Curriculum vitae .....</b>	<b>104</b>

## Summary

Positioned nucleosomes compete with DNA binding proteins for access to DNA, thereby influencing gene regulation. Information about nucleosome positions and about mechanisms determining nucleosome positioning is therefore necessary to understand gene regulation. The fission yeast *Schizosaccharomyces pombe* appeared appropriate for the study of nucleosome positioning mechanisms as it resembles higher eukaryotes more than the budding yeast *Saccharomyces cerevisiae* with regard to chromatin-related properties, like heterochromatin formation, centromere complexity and presence of RNAi, and still offers the advantages of a unicellular model organism. Further, *S. pombe* is evolutionarily far diverged from *S. cerevisiae*, and a comparative analysis of nucleosome positioning mechanisms to those in *S. cerevisiae*, where several nucleosome positioning studies already exist, allows the detection of conserved mechanisms.

A method was developed to map nucleosomes genome-wide by MNase digestion of chromatin and hybridization of mononucleosomal DNA fragments to high-resolution *S. pombe* tiling arrays. This genome-wide nucleosome occupancy map was validated by comparison to nucleosome positioning patterns generated by MNase indirect end-labeling for 19 individual loci. In order to search for stereotypical nucleosome patterns as described at the beginning and at the end of *S. cerevisiae* genes, transcription start sites (TSS) and transcription termination sites (TTS) of 4013 and 3925 *S. pombe* genes, respectively, were annotated. The TSS-aligned overlay of nucleosome occupancy profiles revealed a similar stereotypical promoter pattern as in *S. cerevisiae*, comprised of a promoter nucleosome depleted region (NDR) with the same distance to the TSS as in *S. cerevisiae*, and a translationally positioned +1-nucleosome. However, detailed analysis of the nucleosome occupancy map revealed intriguing differences compared to the nucleosome organization in *S. cerevisiae*. Regular nucleosomal arrays were only visible downstream from the promoter NDR, i.e. mainly in the direction of transcription, whereas they emanated in both directions from the promoter NDR in *S. cerevisiae*. Promoters enriched for the histone variant H2A.Z showed regular nucleosomal arrays also upstream of the promoter NDR in *S. pombe*. Regular nucleosomal arrays had a very short nucleosome repeat length of only 154 bp in *S. pombe* and the ATP-dependent remodeler Mit1 was involved in their formation. DNA sequence played a different role in nucleosome positioning in the two yeasts, as a model for the prediction of nucleosome occupancy, that was trained either for *S. pombe* or for *S. cerevisiae*, predicted the nucleosome occupancy only for the yeast that it was trained on but not for the other yeast. All in all, these results suggested that nucleosome positioning mechanisms are not universal but diverged during evolution.

## Zusammenfassung

Positionierte Nukleosomen konkurrieren mit DNA-Bindeproteinen um den Zugang zur DNA und beeinflussen dadurch die Regulation von Genen. Die Kartierung von Nukleosomen sowie ein Verständnis der Mechanismen, die die Nukleosomen-Positionierung bestimmen, sind daher notwendig, um Genregulation zu verstehen. Die Spaltheefe *Schizosaccharomyces pombe* erschien für die Untersuchung von Nukleosomen-Positionierungs-Mechanismen geeignet, da sie höheren Eukaryonten in Bezug auf Chromatin-Eigenschaften, wie Ausbildung von Heterochromatin, Komplexität der Zentromere sowie des Vorhandenseins von RNAi ähnlicher ist als die Sprossehefe *Saccharomyces cerevisiae* und dennoch die Vorteile eines einzelligen Modellorganismus bietet. Zudem sind *S. pombe* und *S. cerevisiae* evolutionär sehr unterschiedlich, und eine vergleichende Analyse der Mechanismen der Nukleosomen-Positionierung mit denen in *S. cerevisiae*, wo es bereits einige Untersuchungen zur Nukleosomen-Positionierung gibt, bot die Möglichkeit, konservierte Mechanismen zu erkennen.

Eine Methode wurde entwickelt, um mittels MNase-Verdau von Chromatin und Hybridisierung hochauflösender *S.-pombe*-Tiling-Arrays mit mononukleosomalen DNA-Fragmenten Nukleosomen genomweit zu kartieren. Diese genomweite Nukleosomen-Karte wurde durch Vergleich mit Nukleosomen-Positionierungs-Mustern, die für 19 Genregionen mittels MNase-indirekter Endmarkierung erzeugt wurden, validiert. Um nach stereotypen Nukleosomen-Mustern zu suchen, wie sie für *S. cerevisiae*-Gene am Genanfang und -ende beschrieben wurden, wurden die Transkriptions-Start- (TSS) und Transkriptions-Terminationsstellen (TTS) für 4013 bzw. 3925 Gene annotiert. Die Überlagerung der Nukleosomen-Profile an der TSS ergab ein ähnlich stereotypes Promoter-Muster wie in *S. cerevisiae*, bestehend aus einer nukleosomarmen Region (NDR) mit gleichem Abstand zur TSS wie in *S. cerevisiae*, sowie einem translational positionierten +1-Nukleosom. Eine detaillierte Analyse der Nukleosomen-Karte zeigte allerdings interessante Unterschiede im Vergleich zur Nukleosomen-Organisation in *S. cerevisiae*. Regelmäßige Nukleosomen-Anordnungen waren nur in 3'-Richtung der Promoter-NDR sichtbar, d. h. hauptsächlich in Richtung der Transkription, während sie in *S. cerevisiae* in beide Richtungen von der Promoter-NDR angingen. Promoter, an denen H2A.Z angereichert war, zeigten in *S. pombe* regelmäßige Nukleosomen-Anordnungen auch in 5'-Richtung der Promoter-NDR. Regelmäßige Nukleosomen-Anordnungen hatten einen sehr kurzen mittleren Nukleosomen-Abstand von nur 154 bp in *S. pombe*, und der ATP-abhängige „Remodeler“ Mit1 war an deren Formierung beteiligt. Die DNA-Sequenz hatte eine unterschiedliche Rolle bei der Positionierung von Nukleosomen in beiden Hefen, da ein entweder für *S. pombe* oder für *S. cerevisiae* trainiertes Modell zur Vorhersage der Nukleosomendichte zwar in der Hefe, für die es trainiert war, erfolgreich war, aber nicht in der jeweils anderen Hefe. Diese Ergebnisse ließen darauf schließen, dass die Mechanismen zur Positionierung von Nukleosomen nicht universell, sondern im Lauf der Evolution divergent entwickelt wurden.

# 1 Introduction

## 1.1 Basic levels of chromatin organization in eukaryotes

The DNA of eukaryotes is packaged into a compact DNA-protein fiber, called chromatin. Chromatin does not only allow DNA compaction to make the DNA fit into the nucleus, but also provides regulatory functions by influencing DNA accessibility. Different levels of chromatin condensation can be differentiated. The first level of DNA organization is the 10 nm fiber that appears as a ‘beads-on-a-string’-like structure, consisting of the double-stranded DNA helix (string) wrapped into nucleosomes (beads) (Fig. 1) <sup>[168]</sup>. The basic unit of this structure is the nucleosome core particle <sup>[84]</sup> and its structure was solved at high resolution by X-ray crystallography <sup>[31, 100]</sup>. The nucleosome core particle is comprised of 147 bp of DNA wrapped in 1.65 left-handed superhelical turns around a histone octamer <sup>[31, 100]</sup>. The histone octamer consists of two of each of the four core histones H2A, H2B, H3 and H4 that are rich in the basic amino acids lysine and arginine. All core histones contain a common structural motif, the histone fold, and the histone fold motives of two core histones interact with each other in a handshake-like manner to form the heterodimers H2A/H2B and H3/H4, respectively <sup>[31, 100]</sup>. Two of each of the highly positively charged H2A/H2B and H3/H4 heterodimers can combine in the presence of DNA or high salt concentrations to form a stable disc-shaped histone octamer <sup>[102]</sup>. The DNA wrapped around the histone octamer has a helical periodicity of 10.2 bp per turn <sup>[171, 179]</sup> with the minor groove of the DNA double helix being faced inward to the histone octamer surface. This conformation allows direct interaction between the histone octamer and the minor groove of the DNA double helix approximately every 10 bp, leading to fourteen contact sites within 147 bp of nucleosomal DNA. Twelve of the fourteen histone octamer-DNA contacts are formed by the histone fold motives and organize the central 121 bp of DNA within a nucleosome core. The additional 13 bp at each end of the nucleosome core are organized by an N-terminal extension of the histone fold of H3. All in all, the stabilization of DNA-histone octamer interactions and thereby of the nucleosome core is achieved by 116 direct hydrogen bonds between histones and DNA and 358 water-bridged hydrogen bonds <sup>[31, 100, 101]</sup>. All core histones also contain flexible histone tails at the N-terminus that protrude from the histone octamer surface and contain sites for posttranslational modifications. With regard to their amino acid sequence, the core histone proteins are highly conserved from yeast to humans <sup>[123]</sup> and the core histones of *Saccharomyces cerevisiae* and *Schizosaccharomyces pombe* share a homology of around 90%.

Adjacent nucleosome core particles are connected by stretches of linker DNA, and linker and nucleosome core together form the nucleosome. The linker DNA length varies from 10 bp to 80 bp between species, cell types and chromatin regions <sup>[168]</sup>. The average length of DNA in such a nucleosome is called nucleosome repeat length (NRL) or spacing and varies due to the different linker lengths. For example, the NRL is 165 bp (~18 bp linker) in *S. cerevisiae*, 175 bp (~28 bp linker) in *Drosophila melanogaster* and *Caenorhabditis elegans*, and 185 bp (~38 bp linker) in several human cell types <sup>[69]</sup>. Another histone type, the linker histone H1, can bind additional 20 bp of DNA at the entry/exit site of the nucleosome, thereby forming the chromatosome <sup>[185]</sup>.

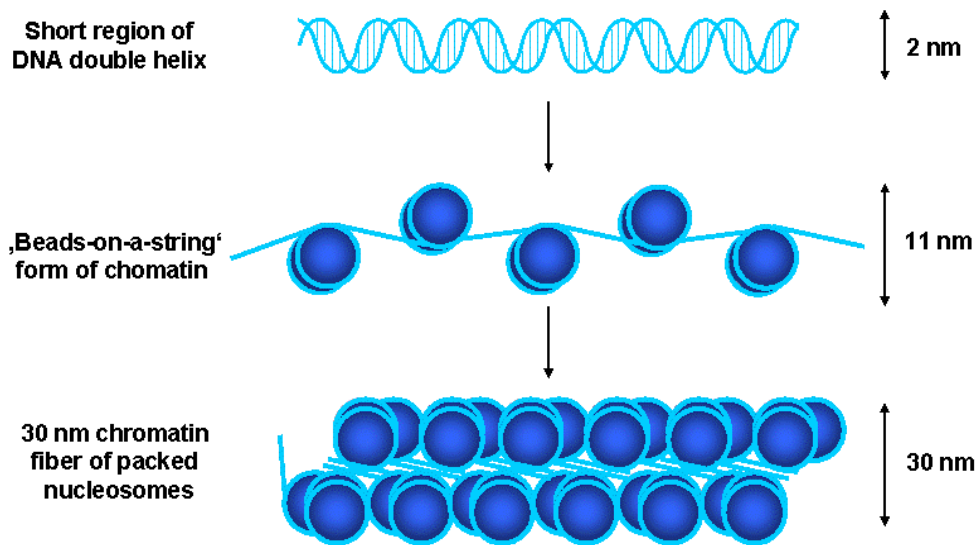


**Fig. 1: Basic levels of DNA compaction.**

The 'beads-on-a-string' form of chromatin represents the first level of chromatin, in which the DNA is wrapped in 1.65 superhelical turns around the histone octamer, thereby forming the nucleosome. Adjacent nucleosomes are connected by short stretches of linker DNA. This 'beads-on-a-string' form of chromatin is further packaged into a fiber of about 30 nm in diameter.

[Modified after Felsenfeld and Groudine <sup>[44]</sup>]

The 'beads-on-a-string'-like structure is folded into a second structural level of chromatin organization, the 30 nm chromatin fiber (Fig. 1) <sup>[186]</sup>. The structure of this 30 nm fiber has not been elucidated yet and different structural models were proposed. Two likely candidate models are the solenoid model (Fig. 2A) <sup>[34, 180]</sup> and the crossed linker model (Fig. 2B) <sup>[34, 182]</sup>. In the solenoid model, or the one-start helix, the linker DNA is bent and the nucleosomal array is coiled up so that six to eight successive nucleosomes lie adjacent to each other in one turn of the solenoid structure (Fig. 2A) <sup>[34, 180]</sup>. In the crossed linker model, or the two-start helix, the nucleosomal array is arranged in a zig-zag formation with straight linkers connecting adjacent nucleosomes located opposite of each other in the fiber (Fig. 2B) <sup>[34, 182]</sup>. Recent *in vitro* experiments provided evidence for both model types, depending on the NRL of the nucleosomal array <sup>[134, 135, 140]</sup>.

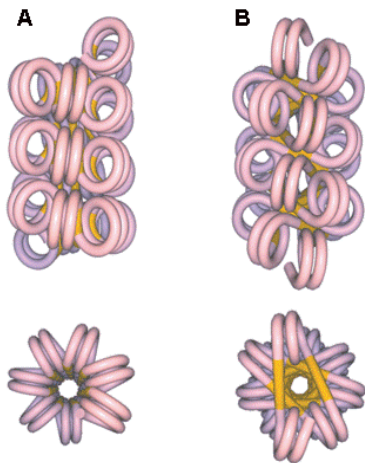


**Fig. 2: Higher-order structure models of the 30 nm chromatin fiber.** (A) One-start solenoidal <sup>[180]</sup>. (B) Two-start twisted <sup>[182]</sup>. Upper graphics show the fibers with vertical axis direction. Lower views show the fibers from the top down the fiber axis. DNA associated with the nucleosome core is pink/purple, linker DNA is yellow. [Modified after Dorigo et al. <sup>[34]</sup>]

During mitosis, further compaction beyond the 30 nm fiber is necessary for generating the highly condensed chromosomes that undergo chromosome segregation <sup>[7]</sup>. Also during interphase further compacted states were described that might be necessary for generating functionally different chromatin domains <sup>[65]</sup>. For example, gene-rich and transcriptionally active euchromatic regions are less condensed during interphase than gene-poor and mostly transcriptionally inactive heterochromatic regions <sup>[55]</sup>. Typical heterochromatic regions are centromeres and telomeres, regions of high density of repetitive DNA, and the yeast mating type locus <sup>[55]</sup>.

The mechanisms leading to further compaction are not well understood. Histone tails and their modification state may play a role in higher-order folding beyond the 30 nm fiber by mediating internucleosomal contacts <sup>[74]</sup>. During mitosis, compaction of the fiber was described to go along with a change of nucleosome positioning at some locations and with chromatin reorganization <sup>[81]</sup>. This may be achieved by chromatin remodeling factors that generate more regularly spaced nucleosomal arrays, which in turn allow more dense compaction <sup>[7]</sup>. Also the DNA structure was described to influence chromatin compaction. Certain base compositions that facilitate DNA bending were found to be enriched on average once per four nucleosomes and might also contribute to chromatin folding <sup>[79]</sup>.

## 1.2 Mechanisms for regulation of chromatin structure

Chromatin is the target of all DNA-related processes, like DNA replication, DNA repair, recombination and transcription. For the proper function of these nuclear processes, chromatin structure and thereby DNA accessibility needs to be regulated carefully. Several mechanisms are known to change chromatin structure and often work in concert with each other: DNA methylation, posttranslational modification of histones, incorporation of histone variants, ATP-dependent chromatin remodelling, and in particular the process of nucleosome positioning <sup>[20]</sup>.

DNA methylation of cytosine bases occurs in vertebrates, many plants and even some invertebrates <sup>[17]</sup>. DNA methylation results in long-term silencing of the underlying DNA sequence by inhibiting the binding of activating factors or by recruiting binding factors involved in gene silencing <sup>[49, 63]</sup>. It is important for many cellular processes, including cell differentiation, genomic imprinting, and X-chromosome inactivation <sup>[15, 17]</sup>, and is established and maintained by DNA methyltransferases (DNMTs). In *S. cerevisiae* and *S. pombe*, DNA methylation does not occur.

Another way to influence chromatin function employs post-translational modifications (PTMs) of histones, like (mono-, di-, tri-) methylation (of lysine and arginine), acetylation (of lysine), phosphorylation (of serine and threonine), ubiquitylation (of lysine), sumoylation (of lysine) and ADP-ribosylation (of glutamic acid) <sup>[85]</sup>. These PTMs of histones can cause electrostatic changes that affect chromatin structure or can influence the recruitment of non-histone proteins. PTMs of histones influence DNA replication, DNA repair and chromosome segregation, and are very important for gene regulation by leading either to activation (acetylation, phosphorylation) or repression (sumoylation) of transcription depending on the histone mark <sup>[20]</sup>. Nucleosomes containing acetylated and methylated histones were found to be enriched at promoter regions of highly transcribed genes <sup>[13, 87, 170]</sup>. However, methylation and also ubiquitylation cannot only have activating but also repressive functions, depending on the context. Most PTMs of histones occur on the histone tails, but some PTMs of histones were found that reside within the nucleosome core, e.g. the acetylation of H3 at K56 (H3K56ac). PTMs of histones within the nucleosome core change the binding affinity between histones and DNA and probably regulate nucleosome positioning by changing the relative mobility of a nucleosome along the DNA. This regulated nucleosome mobility model also involves ATP-dependent chromatin remodeling <sup>[20]</sup>.

Furthermore, canonical histones can become replaced by histone variants, which have moderate to high sequence similarity to the canonical histones <sup>[20]</sup>. Histone variants were described for the core histones H2A, H2B, H3 and the linker histone H1, but not for the core histone H4. Metazoans encode a large number of different histone variants. Most histone variants were observed for H2A, for example H2A.X, functioning as a DNA damage sensor, and H2A.Z, involved in transcriptional regulation, and for H3, for example H3.3, marking transcriptionally active regions and the centromeric CenH3, important for kinetochore formation and accurate chromosome segregation <sup>[16, 73]</sup>. *S. cerevisiae* and *S. pombe* encode only two histone variants, the centromeric H3 variant CenH3, and the H2A variant H2A.Z <sup>[105, 127]</sup>. Interestingly, the primary sequence of the core histones H2A and H3 of the two yeasts resembles more the structure of the mammalian histone variants H2A.X and H3.3, respectively <sup>[16, 58]</sup>. The histone variant H2A.Z is well conserved in all eukaryotes and is implicated in a variety of functions in different organisms, like gene activation and repression, heterochromatin silencing and chromosome segregation and



stability<sup>[197]</sup>. In general, the incorporation of histone variants causes changes in chromatin structure by altering nucleosome stability. For example, in flies, nucleosomes containing the centromeric histone variant CenH3 were described to be smaller and less stable than their canonical counterparts and were suggested to exist as tetrameric hemisomes<sup>[30]</sup>. Furthermore, CenH3 nucleosomes were shown to wrap DNA in a right-handed manner, thereby inducing positive supercoils, in contrast to canonical nucleosomes, which induce negative supercoils<sup>[50]</sup>. Also nucleosomes containing the histone variant H2A.Z were shown to be less stable<sup>[193]</sup>. The altered stability of a nucleosome might in turn influence chromatin dynamics. H2A.Z containing nucleosomes were suggested to facilitate histone eviction (nucleosome disassembly *in trans*), thereby leading to transcriptional activation *in vivo*<sup>[193]</sup>. H2A.Z was shown to be incorporated by the ATP-dependent chromatin remodeling complex Swr1 in *S. cerevisiae*<sup>[80, 86, 112]</sup> and in *S. pombe*<sup>[78, 198]</sup>, and other examples for functional connections between histone variants and chromatin remodeling complexes are known<sup>[20]</sup>.

The process of chromatin remodeling changes the packaging of chromatin and is catalyzed by chromatin remodeling factors that require energy in form of ATP hydrolysis to overcome histone-DNA interactions and are often multi-protein complexes. A number of different ATP-dependent chromatin remodeling factors were described and categorized according to their respective ATPase subunit into four subfamilies of the Swi2/Snf2 family of helicases: ISWI, SWI/SNF, CHD and INO80<sup>[29, 39]</sup>. Nucleosome remodeling can have different outcomes *in vivo*: alteration of nucleosome positions by moving the histone octamer along the DNA (nucleosome sliding)<sup>[10, 43, 77, 89]</sup>; complete loss of nucleosomes by histone eviction<sup>[18, 128]</sup>; destabilization of nucleosome structure by removing H2A-H2B dimers<sup>[21, 189]</sup>; changing nucleosome composition by exchange of H2A variants<sup>[78, 80, 86, 112, 198]</sup>.

### 1.3 Nucleosome positioning

The question to what extent nucleosomes are randomly arranged or precisely positioned has been of interest for a long time. Early studies reported the existence of well positioned nucleosomes, for example at tRNA genes<sup>[184]</sup>, at 5S rRNA genes<sup>[54, 99]</sup>, at heat shock genes in *Drosophila*<sup>[95]</sup>, and at satellite DNA in rat<sup>[67]</sup>.

A connection between nucleosome positioning and gene regulation was first suggested by the identification of a nuclease-hypersensitive site, also called nucleosome depleted region (NDR)<sup>i</sup>,

---

i: Analysis of chromatin structure by indirect end-labeling allowed the detection of chromatin regions highly accessible to nuclease digestion, termed hypersensitive sites (HS). In genome-wide analyses of chromatin structure these sites were termed nucleosome free regions (NFR)<sup>[94, 192]</sup>. The detection of more labile H3.3/H2A.Z double variant-containing nucleosomes at promoters suggested promoter regions to be rather nucleosome depleted than nucleosome free<sup>[70, 71]</sup>. Therefore, the term nucleosome depleted region (NDR) appears more appropriate, since there is rather a gradient of depletion than a total loss of nucleosomes<sup>[23]</sup>.

that occurred upon activation in the 5'-region of fruit fly heat shock genes <sup>[187]</sup> and in a globin gene of chicken red blood cells <sup>[175]</sup>. This observation implicated NDRs with gene activation and in turn the presence of nucleosomes with transcriptional repression. The repressive impact of a nucleosome was also confirmed by early *in vitro* studies, where the assembly of SV40 DNA into chromatin caused the inhibition of initiation and elongation by RNA polymerase I and II <sup>[172, 173]</sup>. Furthermore, depletion of histone H4 in *S. cerevisiae* resulted in the transcriptional activation of several genes, including the *PHO5* gene <sup>[60]</sup> under otherwise non-inducing conditions <sup>[37, 59, 98]</sup>. Since then, single gene studies *in vivo* have reported promoters comprising distinctly positioned nucleosomes, for example at the *S. cerevisiae* *PHO5* and *GALI-10* promoter and at the MMTV promoter <sup>[2, 97, 130]</sup>, and revealed that nucleosome positioning influences gene regulation.

Nucleosomal DNA is generally less accessible to DNA binding proteins than linker DNA, namely because of the close proximity to the histone protein core and to the other superhelical turn of DNA within the same nucleosome, and because of the sharp bending and altered helical twist of the nucleosomal DNA <sup>[132]</sup>.

Nucleosome positioning can be described by the translational and the rotational setting, both affecting DNA accessibility. The translational setting defines a nucleosomal midpoint relative to a given DNA locus and the nucleosome borders of perfectly translationally positioned nucleosomes have base pair precision <sup>[160]</sup>. A perfectly translationally positioned nucleosome might have repressive functions by protecting regulatory sequences of a gene <sup>[4, 169]</sup> or it might be positioned such that regulatory regions are freely accessible in the linker regions <sup>[195]</sup>. Although the presence of a nucleosome is generally implicated with repressive functions, also another example was reported for the human U6 snRNA promoter. Here, the positioning of a nucleosome between two transcription factor binding sites is essential for transcription initiation, as it allows the physical interaction of the two binding sites by wrapping the intervening DNA <sup>[157, 196]</sup>. The rotational setting defines the orientation of the DNA helix on the histone protein surface. DNA regulatory elements encoded in the nucleosomal DNA can either face inward to the histone octamer or face outward, thereby exposing it to a DNA binding protein <sup>[9]</sup>. The two parameters of translational and rotational positioning are not independent, since changing the rotational setting also changes the translational setting of the nucleosome. However, a translational shift by one helical turn of 10 bp maintains the rotational setting.

### 1.3.1 Methods to map nucleosomes

The lower accessibility of DNA within the nucleosome core particle protects it from digestion by nucleases <sup>[40, 175]</sup>. This phenomenon is exploited to map chromatin structure using both unspecific nucleases, like deoxyribonuclease I (DNaseI) or micrococcal nuclease (MNase), and specific restriction enzymes.

Most frequently, nucleosome positions were mapped locus-specifically by a combination of limited MNase or DNaseI digestion and indirect end-labeling. Both MNase and DNaseI preferentially make single strand cuts within the phosphodiester backbone of double-stranded DNA. MNase preferentially cleaves within AT-rich DNA sequences and prefers linker DNA over nucleosomal DNA. In contrast, DNaseI exhibits less strong sequence preferences and can, at sufficiently high concentrations, also cut DNA on the nucleosome surface. MNase is typically used to determine nucleosome positions, while the lower sequence specificity of DNaseI is typically used to map the full extent of nucleosome depleted regions, e.g. in regulatory regions of genes <sup>[160]</sup>.

This single gene approach has been used for a long time and has yielded valuable knowledge of chromatin structure on several loci, such as the yeast *PHO5*, *GALI-10*, and *HIS3* promoters, or the chicken beta-globin locus.

The development of high-resolution tiling arrays and high-throughput sequencing technologies in recent years allows now the analysis of nucleosome positioning on a genome-wide level. Chromatin is fragmented with MNase to an extent where 80% of the chromatin is processed into mononucleosomes. The purified mononucleosomal DNA samples can be hybridized to high-resolution tiling arrays or analyzed by high-throughput sequencing, allowing genome-wide mapping of nucleosomes <sup>[1, 69, 127, 192]</sup>.

These genome-wide approaches raised a discussion about the definition of the terms nucleosome positioning versus nucleosome occupancy. Nucleosome positioning refers to the exact borders of a nucleosome, whereas nucleosome occupancy is defined as the probability for a certain bp to be incorporated into a nucleosome core <sup>[146, 153]</sup>. Early analyses using microarrays of lower resolution were only able to map global nucleosome occupancy <sup>[14, 94]</sup>. With the improvement of the resolution of genome-wide approaches it became possible to differentiate between the borders of neighbored nucleosomes, i.e. to determine nucleosome positions. Nonetheless, the primary data of the genome-wide approaches still map nucleosome occupancy. The information on individual nucleosome positions has to be extracted from these nucleosome occupancy maps by bioinformatic algorithms that assign borders to the peaks and troughs of the nucleosome occupancy map.

### 1.3.2 Outcome of genome-wide nucleosome occupancy maps

Nucleosome occupancy was mapped genome-wide in a variety of eukaryotic organisms, like *S. cerevisiae* [46, 94, 109, 148, 176, 192], *D. melanogaster* [110], *C. elegans* [72, 167], medaka [137] and human cells [142]. This approach revealed that the majority of nucleosomes in *S. cerevisiae* is translationally positioned, i.e. the nucleosomes occupy the same DNA region in all cells throughout a population. In multicellular organisms, nucleosome positioning is more variable. In general, nucleosomes adopt stereotypical positions around promoter regions and more random positions in the interior of genes [124].

An alignment of *S. cerevisiae* nucleosome occupancy data at the transcription start site (TSS) revealed a stereotypical nucleosome occupancy pattern at gene promoters, comprised of an NDR localized just upstream of the TSS, flanked by two translationally positioned nucleosomes (Fig. 3A). The NDR flanking nucleosomes upstream and downstream of the TSS are called -1- and +1-nucleosome, respectively, and can be enriched for the histone variant H2A.Z. In principle, this stereotypical promoter pattern is conserved throughout different organisms, but there are species-specific differences (see Fig. 3B for stereotypical promoter pattern in *D. melanogaster*). For example, the position of the +1-nucleosome relative to the TSS appears to be different in *Drosophila* and human cells [110, 142]. Also the enrichment of H2A.Z at either both NDR flanking nucleosomes or only at the +1-nucleosome varies between species [1, 6, 110]. In *S. cerevisiae* and *Drosophila*, an NDR could also be observed at 3' ends of genes, although less pronounced than at promoter NDRs [110, 148, 176]. Most *S. cerevisiae* genes and many active genes in *Drosophila* and human cells display regular nucleosomal arrays over their coding regions, which start with the +1-nucleosome and decay slowly over distance [94, 110, 142].

In *S. cerevisiae*, not all promoters are characterized by the stereotypical promoter pattern, but some promoters are occupied by nucleosomes, referred to as 'covered' promoters. Whereas promoters with stereotypical chromatin pattern preferentially drive constitutive housekeeping genes, 'covered' promoters rather drive highly regulated genes [23, 46, 163]. The promoter architecture appears to influence the transcriptional activity of a gene. Promoters with a stereotypical chromatin pattern are generally accessible for transcription factors that bind to their response elements in the promoter NDR and initiate transcription. In contrast, 'covered' promoters of regulated genes are more reliant on chromatin remodelling, since nucleosomes impede the access of transcription factors to their binding sites in the promoter region [23]. Along the same line, 'covered' promoters were shown to be highly enriched for TATA boxes compared to stereotypical promoters. The access of the TATA binding protein to the TATA box probably also depends on chromatin remodelling, thereby creating another barrier for gene activation [46].

<sup>163]</sup>. A correlation between promoter chromatin architecture and gene regulation was also described in *Drosophila* and human cells and appears to constitute a conserved concept <sup>[1, 163]</sup>.

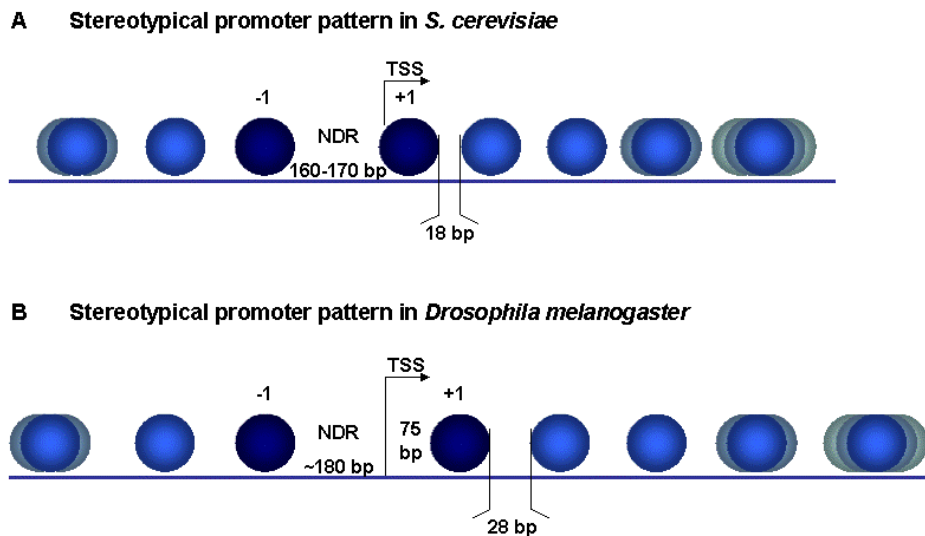


**Fig. 3: Nucleosome positioning in a stereotypical active gene of *S. cerevisiae* and *D. melanogaster*.**

An NDR is closely upstream of the TSS and flanked up- (-1) and downstream (+1) by well positioned nucleosomes. Darker nucleosomes are positioned more strongly than lighter nucleosomes. Weaker positioning with increasing distance from the NDR is illustrated by grey shadows around the nucleosomes. The average nucleosome spacing in *S. cerevisiae* (18 bp) and *D. melanogaster* (28 bp) is given.

[Modified after Radman-Livaja and Rando <sup>[124]</sup>]

### 1.3.3 Mechanisms of nucleosome positioning

These genome-wide studies on nucleosome positioning give a valuable descriptive picture of the chromatin organization throughout the genomes of different organisms. The finding of stereotypical nucleosome positions around promoter regions and less regular positions in the interior of genes leads to the question of how this pattern is generated. Two concepts were suggested: one assumes that the individual nucleosomes are positioned independently from each other (Fig. 4A). The other concept, called statistical nucleosome positioning, is based on the close packing of nucleosomes into an array (Fig. 4B). It assumes that a boundary determines the positioning of neighboring nucleosomes, because the tight packing of nucleosomes prevents their sidewise movement <sup>[69, 84]</sup>. Also a combination of the two concepts is conceivable, i.e. some nucleosomes are independently positioned and others are statistically positioned (Fig. 4C) <sup>[69]</sup>.

Two main mechanisms discussed to determine nucleosome positioning are on the one hand intrinsic DNA sequence features and on the other hand trans-factors, like ATP-dependent chromatin remodelers, transcription factors, or the process of transcription <sup>[124]</sup>. These two mechanisms are compatible with either of the two concepts described above, as they might either

determine individual nucleosome positions or might generate the boundary that passively positions neighboring nucleosomes.

In the following, the roles of the intrinsic DNA sequence features and of several trans-factors in nucleosome positioning will be discussed.

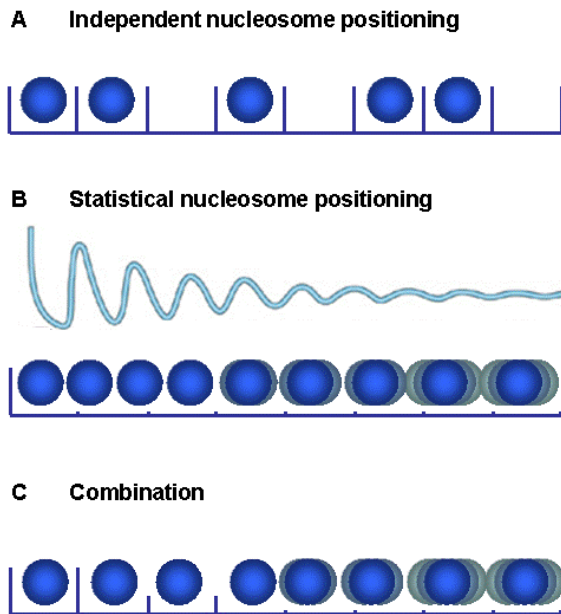


**Fig. 4: Concepts of independent and statistical nucleosome positioning.**

(A) Independent nucleosome positioning. Individual slots define the position of a nucleosome on the DNA. (B) Statistical nucleosome positioning is based on the assumption that a single barrier determines nucleosome positioning by passive ordering of the adjacent nucleosomes due to their tight packing. (C) Combination of independent and statistical nucleosome positioning.

[Modified after Jiang and Pugh <sup>[69]</sup>]

### 1.3.3.1 The role of intrinsic DNA sequence features in nucleosome positioning

Wrapping 147 bp of DNA in 1.65 superhelical turns around the histone octamer requires extensive bending of the particular DNA stretch. In general, DNA is a moderately flexible polymer that can be characterized by the bending persistence length, defining the distance over which a certain direction of the DNA strand tends to persist. The bending persistence length of an arbitrary DNA sequence over which DNA would only be gently curved, is ~50 nm or ~150 bp, which is similar to the nucleosomal DNA length of 147 bp. Therefore, a high free-energy cost is involved in DNA bending for nucleosomal DNA packaging <sup>[179]</sup>.

Another parameter characterizing the DNA molecule is the twist of the double-stranded DNA helix. The average twist for DNA in solution is about 10.5 bp/turn, whereas the average twist for nucleosomal DNA is around 10.2 bp/turn. This change of DNA twist in a nucleosome also requires free-energy cost, although less than DNA bending <sup>[179]</sup>.

Thus, major forces originating from these structural properties of the DNA work against the incorporation of DNA into a nucleosome. This energetic barrier to making nucleosomes a stable structure needs to be overcome by many stabilizing interactions between the histone octamer and the DNA in terms of hydrogen bonds or salt-bridges, hydrogen bond geometry, steric fit etc. <sup>[179]</sup>.

Therefore, DNA sequences favoring DNA distortion would reduce the energetic cost of the incorporation of DNA into a nucleosome and would yield an increased stability of the histone-DNA interactions in the nucleosome.

Indeed, the analysis of DNA sequences of nucleosome core particles isolated from chicken erythrocytes revealed a by 5 bp alternating distribution of A/T and G/C di- and trinucleotides with a periodicity of 10.2 bp and some irregularities near the dyad <sup>[36, 138]</sup>. This periodic distribution of A/T and G/C di- and trinucleotides causes DNA bending, since A/T sequences expand and G/C sequences contract the major groove of DNA. This DNA bending corresponds to a certain rotational setting with A/T sequences preferring minor groove sites facing the histone octamer and G/C sequences favoring minor groove sites facing outside <sup>[138]</sup>. A role of DNA bending in rotational nucleosome setting was also supported by *in vitro* experiments. Different artificial nucleosome positioning sequences consisting of ten repeats of (A/T)<sub>3</sub>NN(C/G)<sub>3</sub>NN sequences were designed and centered in a 163 bp long DNA fragment. *In vitro* reconstitution of these sequences into nucleosomes by salt gradient dialysis revealed a strong rotational setting, again with (A/T)<sub>3</sub> sequences facing the histone octamer and (G/C)<sub>3</sub> sequences facing outward <sup>[149]</sup>. Furthermore, calculation of the free energy for nucleosome formation of these artificial nucleosome positioning sequences revealed 100-fold more thermodynamically favored nucleosome formation compared to bulk nucleosomal DNA and other natural positioning sequences, like the sea urchin 5S rDNA <sup>[149]</sup>. These findings indicated that alternating A/T and G/C di- and trinucleotides generate a curved DNA structure that favors nucleosome formation. Also a nucleosome occupancy map obtained by *in vitro* reconstitution of the whole *S. cerevisiae* genome by salt gradient dialysis revealed a high 10.2 bp periodicity of AA and TT dinucleotides within the nucleosomes. This periodicity is lower but still observable in nucleosomes assembled *in vitro* by ACF (ATP-utilizing chromatin assembly and remodeling factor), an ATP-dependent chromatin remodeling factor that can assemble chromatin into regular nucleosomal arrays. This finding suggested that chromatin assembly and remodeling factors *in vivo* counteract the effect of DNA encoded rotational positioning <sup>[194]</sup>.

The prediction of the translational setting of nucleosomes from the DNA sequence appears to be more complicated. Poly(dA:dT) tracts were proposed to contribute to the translational setting of nucleosomes, since DNA sequence analysis from chicken erythrocyte mono- and dinucleosomal core DNA and *in vitro* reconstitution experiments found poly(dA:dT) tracts excluded from the center but enriched at the ends of nucleosomes <sup>[122, 138, 139]</sup>. Furthermore, low yields in *in vitro* reconstitution experiments using poly(dA:dT) rich sequences suggested these sequences to resist incorporation into nucleosomes <sup>[129, 151]</sup> and the rigidity of these sequences discovered by X-ray analysis supported that conclusion <sup>[114]</sup>. In addition, poly(dA:dT) stretches destabilize histone-DNA interactions <sup>[4]</sup>. Many *S. cerevisiae* promoters were shown to harbor poly(dA:dT) stretches

<sup>[154]</sup>, and recent genome-wide analyses revealed a general enrichment of poly(dA:dT) at promoter NDRs of RNA polymerase II genes in *S. cerevisiae* and *C. elegans* <sup>[46, 94, 192]</sup>.

Furthermore, *in vitro* reconstitution of the yeast *HIS3* and the *PHO84* promoter DNA into chromatin recapitulated in part the *in vivo*-like chromatin structure <sup>[147, 183]</sup>, arguing for a role of the DNA sequence in determining translational nucleosome positions.

Recent developments of high-resolution tiling arrays and high-throughput sequencing techniques and the increased number of known sequences of *in vivo* nucleosome positions reinforced the effort to predict translational nucleosome positions from DNA sequence alone. Different algorithms were developed that attempt to predict the translational nucleosome positions from DNA sequence patterns. Ioshikes et al. scanned a data set of 200 nucleosomal DNA sequences from *S. cerevisiae* for dinucleotide periodicities and found AA and TT dinucleotides occurring at a periodicity of 10 bp with a gradient of AA and TT dinucleotides from the 5' to the 3' and the 3' to the 5' end of the nucleosome, respectively. These nucleosome positioning patterns were used to generate a probabilistic model. Screening the *S. cerevisiae* genome revealed an enrichment of these sequence patterns at the +1- and the -1-nucleosome <sup>[68]</sup>. Segal et al. analyzed 199 well-positioned nucleosomes for AA/TT/AT dinucleotide distributions and found a 10 bp periodicity of these sequences with enrichment towards the nucleosome edges. Similar distributions were also found in 177 natural chicken nucleosomes and in nucleosomes reconstituted from randomly synthesized DNA *in vitro*. A probabilistic model was calculated on the basis of these dinucleotide periodicities and applied to predict the nucleosome positions from the *S. cerevisiae* genome <sup>[145]</sup>. In general, models trained with 10 bp dinucleotide periodicities alone <sup>[68, 145]</sup> performed only poorly in the prediction of the translational positions of nucleosomes. This might be due to the fact that the enrichment of AA/AT/TT dinucleotide patterns is largely limited to the -1- and +1-nucleosomes in *S. cerevisiae* and also here occurs only modestly above a random distribution <sup>[109, 145]</sup>. In general, the inclusion of nucleosome disfavoring DNA sequences for model training improved the prediction success rate, arguing for a role of the DNA sequence in nucleosome exclusion. Accordingly, the refinement of the probabilistic model from Segal et al. by including nucleosome disfavoring 5-mer sequences into the training set yielded a better prediction <sup>[46, 145]</sup>. Also Peckham et al. and Gupta et al. included nucleosome disfavoring sequences into their model <sup>[57, 119]</sup>. They used the 1000 highest and 1000 lowest scoring probes from nucleosome tiling arrays from *S. cerevisiae* <sup>[119, 192]</sup> and human cells <sup>[57, 116]</sup>, respectively, to calculate the frequency of all possible A/T or G/C-oligomers (k-mers from 1 to 6). This approach found A/T rich k-mers to be enriched in nucleosome-disfavoring and G/C rich k-mers to be enriched in nucleosome-favoring sequences, respectively. Yuan and Liu developed a model (N-score) that was based on the occurrence of dinucleotide signals within experimentally identified 199 nucleosomal <sup>[145]</sup> and 296 linker <sup>[191]</sup> sequences.



However, none of these models was able to precisely predict the *in vivo* nucleosome positions with respect to the exact borders of the nucleosomes, but only the nucleosome occupancy <sup>[146]</sup>. This was also true for another model type which was not trained with *in vivo* nucleosome occupancy data, but that calculated the deformability of a DNA sequence based on the intrinsic bendability of DNA sequences. This physical model of DNA bending around the histone octamer also only predicted the promoter NDR <sup>[111]</sup>.

Two recent studies addressed the intrinsic role of the DNA sequence by reconstituting *S. cerevisiae* genomic DNA and histone octamers by salt gradient dialysis into chromatin and mapping the nucleosomes genome-wide by high-throughput sequencing <sup>[75, 194]</sup>. One of these *in vitro* studies from Kaplan et al. claimed a good correlation between *in vitro* and *in vivo* nucleosome occupancy data, suggesting that intrinsic DNA sequence has a central role in determining nucleosome organization <sup>[75]</sup>. In contrast, the study from Zhang et al. found only poor correlation between their *in vitro* and *in vivo* nucleosome occupancy maps <sup>[194]</sup>. These different outcomes were discussed to result from different experimental conditions used for the respective *in vitro* reconstitution experiment <sup>[165, 194]</sup>. For example, differences in salt concentration, temperature and histone-DNA ratio in the *in vitro* chromatin assembly reaction influence nucleosome positioning and might lead to different outcomes of different *in vitro* experiments <sup>[165, 194]</sup>. In addition, the *in vitro* conditions may largely vary according to the conditions of nucleosome assembly *in vivo*. On this basis, direct comparisons between nucleosome positions obtained *in vitro* and *in vivo* appear arbitrary and need to be interpreted critically <sup>[165]</sup>.

According to the study from Zhang et al., only around 20% of the *in vivo* pattern of translational nucleosome positions are determined by intrinsic histone-DNA interactions <sup>[194]</sup>. Interestingly, even less nucleosome positions coincided between the *in vivo* map and the *in vitro* map obtained from chromatin assembled by ACF. In addition, *in vitro* reconstitution of the *PHO5* and *PHO8* promoters by salt gradient dialysis did not yield the *in vivo*-like chromatin pattern. Only incubation with yeast whole-cell extract in the presence of energy reconstituted the *in vivo*-like *PHO5* and *PHO8* promoter pattern, suggesting other factors in addition to the DNA sequence to determine nucleosome positioning <sup>[64, 82]</sup>. These findings suggest that remodeling or other trans-factors override nucleosome positions based only on intrinsic histone-DNA interactions, and determine nucleosome positioning. Along the same line, Kaplan et al. reported higher nucleosome occupancy at promoter NDRs in the *in vivo* map than in the *in vitro* map, suggesting a role of other factors than DNA sequence for NDR formation <sup>[75]</sup>.

All in all, DNA sequence alone is not sufficient to predict the translational setting of nucleosomes. This is probably due to trans-factors that influence nucleosome positioning, and might explain why the success rate of all models that aim to predict nucleosome positions was only modest compared to random prediction <sup>[124]</sup>.

### 1.3.3.2 The role of trans-factors in nucleosome positioning

Different DNA interacting factors were implicated in nucleosome positioning, like ATP-dependent chromatin remodeling factors, transcription factors and active RNA polymerases. Most of the observations on the contribution of these factors to nucleosome positioning were made in *S. cerevisiae*.

#### ATP-dependent chromatin remodeling factors

Isw2, one of three ISWI complexes in *S. cerevisiae*, positioned *in vivo* nucleosomes at the *POT1* promoter over sequence elements that disfavored nucleosome positioning in *in vitro* reconstitution experiments [177]. A subsequent whole-genome study *in vivo* displayed a shift of the NDR flanking nucleosomes toward the NDR at 12% of yeast promoters, so that the nucleosomes resided over unfavorable poly(dA:dT) tracts. This effect was specific to sites of Isw2 binding and was shown to be important for repression of transcription in both sense and antisense direction [176]. At individual genes, like *RNR3*, *ENAI1*, or *SUC2*, the nucleosome positioning activity of Isw2 was shown to be influenced by Tup1/Ssn6, a global corepressor complex involved in gene repression [195]. In contrast to the action of Isw2, the ATP-dependent chromatin remodeling complex RSC was shown to keep nucleosomes away from promoter NDRs [5, 61, 117]. Depletion of Sth1, the essential catalytic subunit of RSC, caused NDR shrinkage and movement of flanking nucleosomes into the NDR at 55% of analyzed promoters [61].

#### Transcription factor binding

The two essential general transcription factors Reb1 and Abf1 of *S. cerevisiae* were suggested to have a role in NDR formation, since their binding sites were more nucleosome depleted *in vivo* than *in vitro* in the absence of other factors [75]. Indeed, temperature sensitive mutants of Reb1 and Abf1 showed the same phenotype that was observed after depletion of the RSC ATPase Sth1, i.e. a shrunked NDR at a subset of promoters (12% for Reb1, 9.3% for Abf1) resulting from a shift of the flanking nucleosomes toward the NDR [61]. This movement of the NDR flanking nucleosomes propagated to the other flanking nucleosomes, whose positions were also shifted. Interestingly, the Reb1 and Abf1 NDRs are a subset of those NDRs, where the depletion of the RSC subunit Sth1 caused changed chromatin structure, arguing for a cooperation between the RSC complex and the transcription factors. A possible mechanism for NDR formation could be that Reb1 and Abf1 bind to the promoter and recruit RSC, which moves nucleosomes away, thereby generating an NDR [61]. The fact that Reb1 was shown to interact with Rsc2, Rsc3 and Npl6, i.e. all subunits of the RSC complex, supports this hypothesis [24, 25, 51].

### Histone variants

Another interesting observation from genome-wide studies on nucleosome positioning was the enrichment of NDR flanking nucleosomes for the histone variant H2A.Z [1, 6, 22, 110, 198]. *In vitro* experiments reported H2A.Z nucleosomes to be less stable, a property that could support their removal *in vivo* [193] and suggesting an important role for gene regulation. Also *in vivo* studies measuring the turnover rate of nucleosomes reported H2A.Z containing nucleosomes to be among the ‘hottest’, having the highest turnover rate [33]. H2A.Z was shown to be involved in both transcriptional activation and repression *in vivo*, and appears to be involved in other cellular processes, like chromosome segregation and heterochromatin silencing [197].

The localization of H2A.Z at NDR flanking nucleosomes was shown to be a consequence rather than an initiator of NDR formation in *S. cerevisiae* [61]. Accordingly, a recent large scale study comprising genes localized on chromosome 3 in *S. cerevisiae* deletion mutants of H2A.Z or the H2A.Z-specific remodeler Swr1 did not show changed NDR formation or nucleosome positioning [61]. A 22 bp long promoter sequence containing the Reb1 binding site followed by an adjacent poly(dT:dA) tract was able to recruit H2A.Z in *S. cerevisiae* [125].

However, the importance of H2A.Z appears to vary between different species, since H2A.Z is essential for survival in vertebrates and metazoans, but dispensable in *S. cerevisiae* and *S. pombe*. Thus, it cannot be excluded that H2A.Z might be important for nucleosome positioning in other organisms.

### Transcription by RNA polymerases

The process of transcription by RNA polymerases is a major force for shaping chromatin structure. However, since it is difficult to differentiate between effects coming from the polymerase or from polymerase-associated factors, much speculation is going on about the role of transcription in nucleosome positioning [124]. In *S. cerevisiae*, nucleosomes over highly transcribed genes were described to be more delocalized than nucleosomes over less transcribed genes [192]. Further, NDR width was shown to correlate with transcription level, which might result from eviction of the -1-nucleosome at actively transcribed genes [94]. In multicellular organisms, transcriptional gene activity varies widely between different cell types but also within one cell, which is reflected in varying nucleosome positioning profiles [142]. In addition, the position of the +1-nucleosome was slightly changed in human cells and *Drosophila* depending on whether the gene was actively transcribed or occupied by a paused polymerase [110, 142]. Inactive genes without RNA polymerase II did not have translationally well positioned nucleosomes [142]. Further, mapping nucleosome positions in the *rpb1-1* mutant of *S. cerevisiae*, carrying a temperature-sensitive allele of the large subunit of RNA polymerase II, revealed a decrease of the NDR width largely due to increased nucleosome occupancy at the -1-nucleosome position, and a shift of

coding region nucleosomes to the downstream direction <sup>[174]</sup>. This result is consistent with biochemical *in vitro* studies analyzing the mechanism of RNA polymerase transiting a nucleosome, leading to the prediction of a retrograde shift of the octamer relative to the polymerase movement <sup>[155, 156]</sup>.

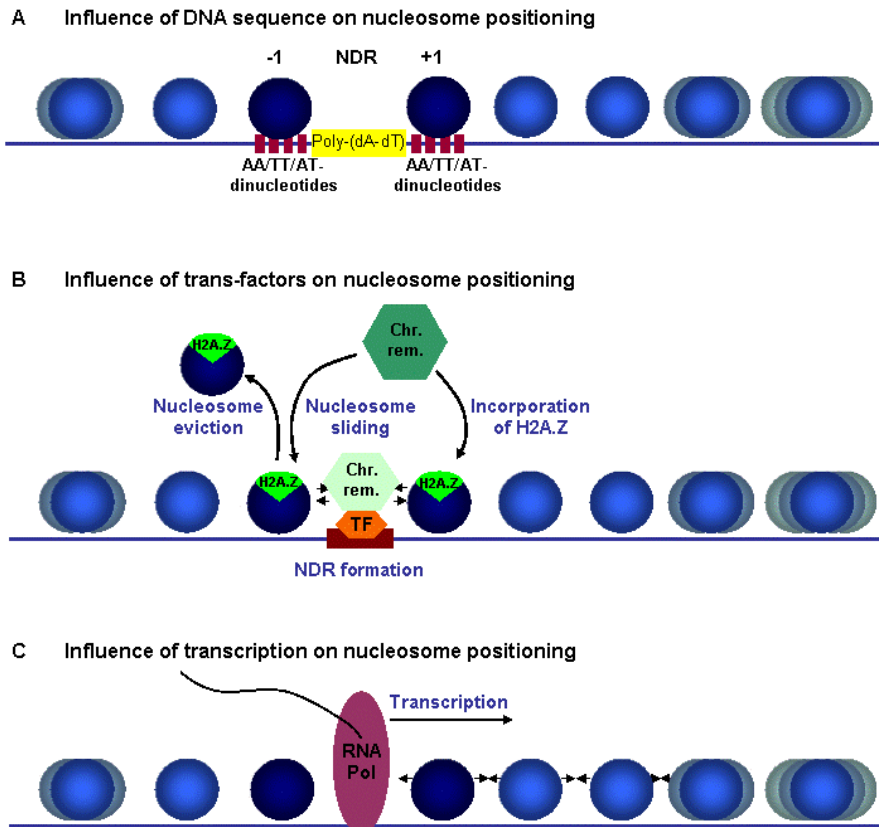


**Fig. 5: Dynamic view of chromatin structure at a typical active gene in *S. cerevisiae*.**

(A) Nucleosome positioning can be affected by the underlying DNA sequence. Unfavorable DNA sequences, e.g. poly(dA:dT) rich sequences, may inhibit nucleosome formation, whereas nucleosome positioning sequences, e.g. AA/TT/TA dinucleotides with a periodicity of 10 bp might favor nucleosome formation. (B) ATP-dependent chromatin remodelers (Chr. rem.), like RSC or Isw2, and transcription factors shape the NDR and also the positioning of adjacent nucleosomes. (C) The process of transcription might also influence chromatin structure.

[Modified after Rando and Ahmad <sup>[126]</sup>]

## 1.4 Aims of this work

Genome-wide mapping studies of nucleosome occupancy in different organisms provide a descriptive picture of nucleosome organization and set up the basis for renewed studying of nucleosome positioning mechanisms. These maps revealed communalities but also intriguing differences between nucleosome positioning patterns in different organisms. It is not clear how differences in nucleosome positioning between organisms arise or which factors determine nucleosome positioning.

The fission yeast *S. pombe* offers the advantages of a unicellular model organism that is amenable to a number of genetical and biochemical approaches and provides interesting chromatin features [11]. With regard to heterochromatin formation, the complex structure of centromeres [106] and replication origins [108], chromosome condensation during mitosis [41], and the existence of the RNAi system [106], *S. pombe* resembles metazoans more than *S. cerevisiae*. Also the mechanism of transcription initiation in *S. pombe* is more similar to metazoans than to budding yeast [28]. Further, *S. pombe* and *S. cerevisiae* separated up 420 to 330 million years ago and are evolutionary far diverged [152].

Therefore, *S. pombe* is a valuable organism to analyze nucleosome positioning. Not much previous knowledge was available on nucleosome positioning in *S. pombe*. Two early comparative studies in *S. pombe* and *S. cerevisiae* pointed to differences in nucleosome positioning mechanisms between the two yeasts and served as motivation for this work. One study used shuttle vectors and obtained different nucleosome positioning patterns over one and the same DNA sequence in *S. pombe* and *S. cerevisiae* [12]. Another study confirmed different nucleosome positioning patterns in *S. pombe* and *S. cerevisiae* at the *S. cerevisiae* *HIS3* promoter that was inserted into the *S. pombe* genome [147].

Three major questions were addressed in this thesis: First, where are nucleosomes positioned on a genome-wide scale in *S. pombe*? Second, what determines nucleosome positioning in *S. pombe*? And third, how evolutionarily conserved are nucleosome positioning mechanisms?

To address the first question, a protocol was developed to map nucleosome positions genome-wide in the fission yeast *S. pombe*. With regard to the second question, the role of DNA-sequence rules, ATP-dependent chromatin remodeling factors, and transcription, as well as a correlation of nucleosome occupancy patterns with gene expression were analyzed. The third question was addressed by a detailed comparison between genome-wide nucleosome occupancy maps of the two evolutionarily far diverged yeasts *S. pombe* and *S. cerevisiae*.

## 2 Materials and methods

### 2.1 Materials

#### 2.1.1 Chemicals

Adenine	Sigma, Taufkirchen
Agarose, ME	Biozym, Hessisch Oldenburg
Amino acids	Sigma, Taufkirchen
Ampicillin	Roth, Karlsruhe
ATP	Sigma, Taufkirchen
$\alpha$ -P <sup>32</sup> - dCTP	Hartmann Analytics
Bacto agar	Becton Dickinson, Heidelberg
Bacto peptone	Becton Dickinson, Heidelberg
Bacto tryptone	Becton Dickinson, Heidelberg
Bacto yeast extract	Becton Dickinson, Heidelberg
Bacto yeast nitrogen base	Becton Dickinson, Heidelberg
Bromophenolblue	Merck, Darmstadt
BSA, 98% pure	Sigma, Taufkirchen
BSA, purified	NEB, Frankfurt/Main
$\beta$ -mercaptoethanol	Sigma, Taufkirchen
Chloroform	Merck, Darmstadt
Complete, EDTA-free; protease inhibitor cocktail tablets	Roche, Mannheim
Creatine phosphate	Sigma, Taufkirchen
DMSO	Sigma, Taufkirchen
dNTP-mix	NEB, Frankfurt/Main
DTT	Roth, Karlsruhe
EDTA	Sigma, Taufkirchen
EGTA	Sigma, Taufkirchen
EMM broth without dextrose	ForMedium, Norfolk
Ethidiumbromide	Roth, Karlsruhe
Ficoll 400	Sigma, Taufkirchen
Formaldehyde	Sigma, Taufkirchen
Glucose, D(+)	Merck, Darmstadt
Glycogen, for molecular biology	Roche, Mannheim
Hepes	Roth, Karlsruhe
Hydroxylapatite	BioRad, Munich
Isoamylalcohol	Merck, Darmstadt
MOPS	Sigma, Taufkirchen
Myo-inositol	Sigma, Taufkirchen
NP-40	Sigma, Taufkirchen
Orange G	Sigma, Taufkirchen
Phenol for separation of DNA; pH 7.5-8.0	Sigma, Taufkirchen
Phenol for separation of RNA; pH 4.5-5.0	Roth, Karlsruhe
PEG 3350	Sigma, Taufkirchen
PEG 4000	Roth, Karlsruhe
PMSF	Sigma, Taufkirchen
PVP 40	Sigma, Taufkirchen
SDS	Serva, Heidelberg

Spermidine	Sigma, Taufkirchen
Tris	Invitrogen, Karlsruhe
Triton X-100	Sigma, Taufkirchen
Tween 20	Sigma, Taufkirchen
Uracil	Sigma, Taufkirchen
Zymolyase 100T	MP Biomedicals, Eschwege

All chemicals listed were of analytical grade. All other chemicals were purchased in analytical grade from Merck, Darmstadt.

### 2.1.2 Enzymes

Antarctic Phosphatase	NEB, Frankfurt/Main
Creatine Kinase	Roche, Mannheim
DNaseI	Roche, Mannheim
MNase	Sigma, Taufkirchen
Proteinase K	Roche, Mannheim
Restriction endonucleases	NEB, Frankfurt/Main
	Roche, Mannheim
RNase A	Roche, Mannheim
T4 DNA Ligase	NEB, Frankfurt/Main
Taq DNA Polymerase	NEB, Frankfurt/Main

### 2.1.3 Other materials

100 bp DNA Ladder	NEB, Frankfurt/Main
2-Log DNA Ladder (0.1–10.0 kb)	NEB, Frankfurt/Main
Biotinylated anti-streptavidin antibodies, P/N BA-0500	Vector Laboratories, Servion
Control Oligo B2	Affymetrix
Dialysis membrane Spectra/Por, MWCO: 3.500 Da	Roth, Karlsruhe
Fast PES Bottle Top Filter, 500ml, 0.2 µm Pore size	Nalgene, Roskilde, Denmark
GeneChip Mapping 10K Xba Assay Kit, 900441	Affymetrix
Microsep Centrifugal Concentrators, MWCO: 10.000 Da	Pall Corporation, Mexico
Miracloth	Merck, Darmstadt
Nylon Transfer membrane, Biodyne B 0.45 µm	Pall Corporation, Mexico
Prime-It II Random Primer Labeling Kit	Stratagene, La Jolla
QIAGEN Plasmid Maxi Kit	Qiagen, Hilden
QIAGEN Plasmid Midi Kit	Qiagen, Hilden
QIAGEN Plasmid Mini Kit	Qiagen, Hilden
QIAquick Gel Extraction Kit	Qiagen, Hilden
QIAquick PCR Purification Kit	Qiagen, Hilden
Quantum Prep™ Freeze 'N Squeeze DNA Gel Extraction Spin Columns	BioRad, Munich
Quick spin columns for radiolabeled DNA, Sephadex G-50 Fine	Roche, Mannheim
Siliconised reaction tubes, 1.5 ml	Biozym, Hessisch Oldenburg
<i>S. pombe</i> Tiling Array 1.0FR	Affymetrix
Streptavidin-phycoerythrin (P/N S-866)	Invitrogen, Darmstadt
Super RX Fuji medical X-ray film	Fuji, Düsseldorf

## 2.1.4 Oligonucleotides and plasmids

### 2.1.4.1 Oligonucleotides

Application	Oligonucleotide sequence (5'→3')
Probe for <i>SPAC977.12</i>	CTAGAAGTGTGATGTATGGAATCC
	GCGACCTTATTGTGTTAGTTTTGAAAT
Probe for <i>SPAC1F8.06</i>	GATCTTTAGTTAGGCGTTTCTAATTGA
	CAATCTAGCACTGATTAGAACGTG
Probe for <i>SPAC5H10.13c</i>	TCGAGATTTTCGTTTCGTTATTTTATAGG
	TGATTAACGGATGGAGTGCCAATA
Probe for <i>SPAC1751.03</i>	GGGTTTCATTCGGTTTTTCGATG
	TTCATAACTACCAAGAATTTCAAGTC
Probe for <i>SPAC22H10.12c</i>	TAGTTCATAATTTTAAAGGAAAAGATTCC
	AGTGGTGTCAAGTAGTACCATT
Probe for <i>SPAPB24D3.09c</i>	GAATCTTACTTTGTAGTCGCT
	CAAGGATTCCTGATTAATACC
Probe for <i>SPAC9E9.03</i>	CCGTGGTATCAATACCATCTACG
	CGTACAAAGTTTTAGGAGAAGCAAC
Probe for <i>SPAC14C4.03</i>	TCTAGAATAAGGATCAAGCTGAG
	AGTGAACCTTTGTTACATACGATTAT
Probe for <i>SPAC14C4.03</i>	CGATCGAAGTTTCTCCACATAAAAAG
	TCGAATCCCGGAGGGAGAG
Probe for <i>SPBC1734.15</i>	CTAGACGTTACGCTCAGAAG
	TCGAATTACAATAAGAAACCGTTCACT
Probe for <i>SPBC1734.15</i>	TTGTGGTTGATCAAACCTCTATGCT
	AGTCAACAACGGGGTGGTTAA
Probe for <i>SPBC4.04c</i>	CATTCATCTCACTGATTCCAT
	CGACATTTTCGATGTGATTGT
Probe for <i>SPBC1778.06c</i>	TCATCTAAGTCGCAATTTTGG
	CAGGGTTAAACTTTTAACTG
Probe for <i>SPBP4G3.02</i>	TGGCCAAATATTTAGTTTTGTTTCGT
	TCGTACCATAAATTTAAATTCGCG
Probe for <i>SPCC613.10</i>	TTCAAAGACTAAAGGAAGGGT
	GTGGATTTGTTTAAAAGCTAAG
Probe for <i>SPCC594.05c</i>	CAGTTGATCAAAGATTCTTCG
	CAAAAGATGCATCCTTCTGTT
Probe for <i>SPCC1322.13</i>	GAATTCAAGGTGCCTTACGAACT
	CTCGAGGCATCTGAACAATAG
Probe for <i>SPCC191.11</i>	AGATCTTGAGAGCTCAATTCATCG
	ACTATAGATGTTCCAACCTACAGAT
Probe for <i>SPAC1739.10</i>	TATAAACCCGTTAGTAAGATAAATTC
	GCAACTGAACGCTAAACATTGC
Cloning of <i>PHO5</i> promoter into YRpFB1-pUC19	TGCCATCTACTCTAGAGGGCCCCAAAAGTATTGTCTTC
	ACGTTGAGCTTCTAGAGTCGACATCGGCTAGTTTGCC
Probe for <i>PHO5</i> (~BamHI-ClaI)	CCGAAAGTTGTATTCAACAA
	CATTTAGAGATTGCCTATTC
Probe for <i>act1</i> <i>S. pombe</i>	CGAACGTGAAATTGTTTCGTG
	GGAGGAAGATTGAGCAGCAG
Probe for <i>ACT1</i> <i>S. cerevisiae</i>	ACCGCTGCTCAATCTTCTTC
	CCCAAAACAGAAGGATGGAA
Probe for pUC19	TCTAGAGTCGACCTGCAGGC
	CAGCTGGCACGACAGGTTTC
Probe for <i>URA3</i>	CATGTGGATATCTTGACTGATT
	CACGGTTCTATACTGTTGAC
Cloning of <i>SPAC1F8.06</i> into pUC19	GATTCACAGCTTCCC GGTTACTTCTTTCTTCTGTTTTGTATGGAA
	ATACGACTAACGCTGCAGAATACCAAAGTTGCTTTTTCTAAGGAA

All oligonucleotides were ordered from Eurofins MWG Operon, Ebersberg.



### 2.1.4.2 Plasmids

Plasmid type	Plasmid name	Selection marker	Source
Bacterial cloning plasmid	pUC19	amp	Invitrogen, Karlsruhe
	pBR322	tet, amp	Bolivar et al. <sup>[19]</sup>
Yeast shuttle plasmids	YRpFB1	<i>URA3</i>	Bernardi et al. <sup>[12]</sup>
	YRpFB1-pUC19	<i>URA3</i>	see description below

The backbone of the shuttle plasmid YRpFB1 <sup>[12]</sup> is pBRAT2, which is a derivative of pBR322 <sup>[19]</sup>, containing the *TRP1-ARS1* sequence and a 10 bp BamHI linker inserted in the NaeI site (nucleotide 1069 of the *TRP1-ARS1* sequence) <sup>[166]</sup>. The shuttle plasmid contained the *S. cerevisiae URA3* selection marker important for plasmid selection in auxotrophic *S. pombe* and *S. cerevisiae* strains. The BamHI linked *URA3* fragments were inserted into the BamHI site of pBRAT2 <sup>[161]</sup>. To obtain the shuttle plasmid YRpFB1-pUC19, the bacterial pBR322 sequence was replaced by the pUC19 plasmid sequence (EcoRI to XbaI). The *S. cerevisiae* and *S. pombe* origins of replication *ARS1* and *Pars772* <sup>[108]</sup>, respectively, allowed extrachromosomal maintenance of the plasmids.

### 2.1.5 Bacteria and yeast strains

#### 2.1.5.1 *E. coli* strains

<i>E. coli</i> strains	Selection marker	Source
DH5 $\alpha$	amp	Genentech, San Francisco
XL1-Blue	tet, amp	Stratagene, La Jolla

#### 2.1.5.2 *S. pombe* strains

<i>S. pombe</i> strains	Genotype	Source
wt-41	<i>h-, leu-, ura-</i>	Ramón Ramos Barrales; group of J.J. Ibeas, Universidad Pablo de Olavide, Sevilla, Spain
wt (HU303)	<i>h-</i>	Karl Ekwall; Karolinska Institutet, Department of Biosciences and Nutrition, Huddinge, Sweden
<i>mit1</i> (HU1295)	<i>h-, mit1::kanMX6, leu1-32, ade6-210, ura4-DS/E</i>	Karl Ekwall; Karolinska Institutet, Department of Biosciences and Nutrition, Huddinge, Sweden
<i>fft3</i> (HU1939)	<i>h-, fft3::hph, leu1-32, ade6-210, ura4-DS/E or D18</i>	Karl Ekwall; Karolinska Institutet, Department of Biosciences and Nutrition, Huddinge, Sweden
<i>tup11 tup12</i> (HU0946)	<i>h+, tup11::ura4, tup12::ura4, ade6-M210, leu1-32, ura4-D18</i>	Karl Ekwall; Karolinska Institutet, Department of Biosciences and Nutrition, Huddinge, Sweden
<i>clr3</i> (PM0564)	<i>clr3::clr3D232N-natMX smt0</i>	Hiten Madhani; Department of Biochemistry and Biophysics, University of California, San Francisco, USA

### 2.1.5.3 *S. cerevisiae* strains

<i>S. cerevisiae</i> strains	Genotype	Source
CY337	MATa, <i>ura-53</i> , <i>lys2-801</i> , <i>ade2-101</i> , <i>his3-Δ200</i> , <i>leu2-Δ1</i>	Richmond and Peterson <sup>[131]</sup>
BY4741 (Y0000)	MATa, <i>his3Δ1</i> , <i>leu2Δ0</i> , <i>met15Δ0</i> , <i>ura3Δ0</i>	EUROSCARF ( <a href="http://web.uni-frankfurt.de/fb15/mikro/euroscarf/index.html">http://web.uni-frankfurt.de/fb15/mikro/euroscarf/index.html</a> )

## 2.2 Media, buffers and solutions

### 2.2.1 Media

#### 2.2.1.1 Media for *E. coli*

##### Luria-Bertani (LB) medium

- 1.0% (w/v) Bacto tryptone
- 1.0% (w/v) NaCl
- 0.5% (w/v) Bacto yeast extract
- adjust to pH 7.0 with 10 M NaOH

The medium was autoclaved for 20 min at 120°C. For preparing plates, the LB medium was mixed with 1.5% Bacto agar.

#### 2.2.1.2 Media for *S. pombe*

##### YES medium

- 0.5% (w/v) Bacto yeast extract
- 3.0% (w/v) glucose
- 0.7 g/l amino acid mix (adenine, leucine, histidine, uracil, lysine, arginine, glutamine)
- sterile filtered (fast PES bottle top filter)

##### EMM (Edinburgh Minimal Medium)

- 12.3 g/l EMM without dextrose
- 2.0% (w/v) glucose
- 250 mg/l uracil, leucine, histidine, lysine or adenine (depending on auxotrophy)

##### Low-glucose EMM

- 12.3 g/l EMM without dextrose
- 0.5% (w/v) glucose
- 250 mg/l uracil, leucine, histidine, lysine or adenine (depending on auxotrophy)

*S. pombe* media were autoclaved for 20 min at 120°C. Glucose was added afterwards using autoclaved 50% (w/v) glucose solution. For preparing plates, medium was mixed with 2.4% Bacto agar.

### 2.2.1.3 Media for *S. cerevisiae*

#### Amino acid drop-out mix (without histidine, uracil, leucine, tryptophan = -HULT)

2 g adenine, 2 g alanine, 2 g arginine, 2 g asparagine, 2 g aspartate, 2 g cysteine, 2 g glutamine, 2 g glutamate, 2 g glycine, 2 g myo-inositol, 2 g isoleucine, 2 g lysine, 2 g methionine, 0.2 g p-aminobenzoic acid, 2 g phenylalanine, 2 g proline, 2 g serine, 2 g threonine, 2 g valine, 2 g tyrosine

#### Phosphate free medium

2.0% (w/v) glucose, 1.6 g/l amino acid drop-out mix, 2.0 g/l L-asparagine, 500 mg/l MgSO<sub>4</sub> x H<sub>2</sub>O, 100 mg/l NaCl, 100 mg/l CaCl<sub>2</sub> x 2 H<sub>2</sub>O, 2.0 mg/l myo-inositol, 500 µg/l H<sub>3</sub> BO<sub>3</sub>, 40 µg/l CuSO<sub>4</sub> x H<sub>2</sub>O, 100 mg/l KJ, 200 µg/l Fe(III)Cl<sub>3</sub> x 6 H<sub>2</sub>O, 400 mg/l MnSO<sub>4</sub> x H<sub>2</sub>O, 200 µg/l (NH<sub>4</sub>)<sub>6</sub>Mo<sub>7</sub>O<sub>27</sub> x 4 H<sub>2</sub>O, 200 mg/l ZnSO<sub>4</sub> x 7 H<sub>2</sub>O, 200 µg/l riboflavin, 200 µg/l p-aminobenzoic acid, 2.0 µg/l biotin, 2.0 µg/l folic acid, 400 µg/l nicotin acid, 400 µg/l pyridoxin-HCl, 400 µg/l thiaminchlorid, 13.4 mM KCl, 50 mM natriumcitrate pH 5.0

#### YNB (yeast nitrogen base) medium

6.7 g/l Bacto yeast nitrogen base w/o amino acids

2.0% (w/v) glucose

1.6 g/l amino acid drop-out mix

→ add histidine, uracil, leucine or tryptophan according to auxotrophy

#### YPDA medium

1.0% (w/v) Bacto yeast extract

2.0% (w/v) Bacto peptone

2.0% (w/v) glucose

100 mg/l adenine

*S. cerevisiae* media were autoclaved for 20 min at 120°C. For preparing plates, medium was mixed with 2.4% Bacto agar.

### 2.2.2 Buffers and solutions

AE-buffer	50 mM Na acetate, pH 5.3 10 mM EDTA, pH 8.0
Buffer A	10 mM Tris/HCl, pH 8.0 150 mM NaCl 5 mM KCl 1 mM EDTA, pH 8.0 added freshly: 1 mM PMSF
Denaturing buffer	0.5 M NaOH 1.5 M NaCl

---

Denhardt's (10x)	5% (w/v) SDS 10 mM EDTA, pH 8.0 0.2% (w/v) BSA 0.2% (w/v) Ficoll 0.2% (w/v) PVP40
Dialysis buffer	20 mM Hepes/KOH, pH 7.5 20% glycerol 50 mM NaCl 1 mM EGTA, pH 8.0 added freshly: 5 mM DTT Complete protease inhibitor (1 tablet for 50 ml)
DNaseI buffer (10x)	150 mM Tris/HCl, pH 7.4 750 mM NaCl 30 mM MgCl <sub>2</sub> 0.5 mM CaCl <sub>2</sub> 10 mM β-mercaptoethanol
DTT stock solution	1 M DTT in H <sub>2</sub> O → storage at -20°C
Ex50 buffer	10 mM Hepes/NaOH, pH 7.6 50 mM NaCl 1.5 mM MgCl <sub>2</sub> 0.5 mM EGTA, pH 8.0 10% (v/v) glycerol added freshly: 1 mM DTT 0.2 mM PMSF
Extraction buffer	0.2 M Tris/HCl, pH 7.5 10 mM MgSO <sub>4</sub> 20% glycerol 1 mM EDTA, pH 8.0 390 mM (NH <sub>4</sub> ) <sub>2</sub> SO <sub>4</sub> added freshly: 1 mM DTT Complete protease inhibitor (1 tablet for 50 ml)
Ficoll buffer	18% Ficoll 20 mM KH <sub>2</sub> PO <sub>4</sub> 1 mM MgCl <sub>2</sub> 0.25 mM EGTA, pH 8.0 0.25 mM EDTA, pH 8.0 pH 6.8 adjusted with KOH

---

High-salt buffer	10 mM Tris/HCl, pH 7.6 2 M NaCl 1 mM EDTA, pH 8.0 1 mM $\beta$ -mercaptoethanol 0.05% Nonidet P40
IAC	4% isoamylalcohol 96% chloroform
K-PO <sub>4</sub> buffer (1M)	280 mM KH <sub>2</sub> PO <sub>4</sub> 720 mM K <sub>2</sub> HPO <sub>4</sub>
LiAc/EDTA buffer	100 mM lithium acetate 1 mM EDTA, pH 8.0 pH 4.9
Loading buffer (5x)	50% (v/v) glycerol 5 mM EDTA, pH 8.0 0.3% (w/v) xylene cyanol, bromophenol blue and/or orange G
Loening buffer (10x)	0.4 M Tris 0.2 M NaOAc(3 H <sub>2</sub> O) 0.01 M EDTA, pH 8.0 2% (v/v) acetic acid
Low-salt buffer	10 mM Tris/HCl, pH 7.6 50 mM NaCl 1 mM EDTA, pH 8.0 1 mM $\beta$ -mercaptoethanol 0.05% Nonidet P40
Lysis buffer	15 mM Hepes/KOH, pH 7.5 10 mM KCl 5 mM MgCl <sub>2</sub> 0.05 mM EDTA, pH 8.0 0.25 mM EGTA, pH 8.0 10% glycerol added freshly: 1 mM DTT 0.2 mM PMSF Complete protease inhibitor (1 tablet for 50 ml)
MNase buffer (10x)	150 mM Tris/HCl, pH 7.4 500 mM NaCl 14 mM CaCl <sub>2</sub> 2 mM EGTA, pH 8.0 2 mM EDTA, pH 8.0 50 mM $\beta$ -mercaptoethanol

---

MNase stock solution (Sigma)	MNase resuspended in 850 $\mu$ l Ex50 buffer → 100 $\mu$ l aliquots → storage at -20°C
MNase and DNaseI dilution buffer	10 mM Tris/HCl, pH 7.4 0.1 mg/ml BSA (NEB)
MOPS buffer (10x)	200 mM MOPS 50 mM Na-acetate 10 mM EDTA, pH 8.0
NP buffer	1 M sorbitol 50 mM NaCl 10 mM Tris/HCl, pH 7.4 5 mM MgCl <sub>2</sub> 1 mM CaCl <sub>2</sub> 0.75% (v/v) NP-40 added freshly: 1 mM $\beta$ -mercaptoethanol 500 $\mu$ M spermidine
PMSF stock solution	200 mM PMSF in 2-propanol → storage at 4°C
Prehybridization solution	2x SSC 1x Denhardt's 0.1 mg/ml herring sperm DNA
Preincubation solution 1	2.8 mM EDTA, pH 8.0 0.7 mM $\beta$ -mercaptoethanol in dH <sub>2</sub> O
Preincubation solution 2	20 mM Na <sub>2</sub> HPO <sub>4</sub> 20 mM citric acid 40 mM EDTA, pH 8.0 28.6 mM $\beta$ -mercaptoethanol
Proteinase K stock solution	20 mg/ml in 10 mM Tris/HCl, pH 8.0 → storage at -20°C
RNase A stock solution	10 mg/ml in 5 mM Tris/HCl, pH 7.5 → heat 10 min at 100°C → 1 ml aliquots → storage at -20°C
RNA loading buffer	50% glycerol 1 mM EDTA, pH 8.0 0.4% bromophenolblue
Sorbitol/ $\beta$ -ME	1 M sorbitol 5 mM $\beta$ -mercaptoethanol

---

Sorbitol/Phosphate buffer	0.9 M sorbitol 50 mM Na <sub>2</sub> PO <sub>4</sub> , pH 7.5 140 mM β-mercaptoethanol
Sorbitol/Tris/β-ME buffer	1 M sorbitol 50 mM Tris/HCl, pH 7.4 10 mM β-mercaptoethanol
SSC (20x)	3 M NaCl 0.3 M Na citrate (dihydrate)
STE buffer	0.1 M NaCl 10 mM Tris/HCl, pH 8.0 1 mM EDTA, pH 8.0
Sucrose containing buffer	15 mM Hepes/KOH, pH 7.5 10 mM KCl 5 mM MgCl <sub>2</sub> 0.05 mM EDTA, pH 8.0 0.25 mM EGTA, pH 8.0 1.2% sucrose added freshly: 1 mM DTT 0.2 mM PMSF Complete protease inhibitor (1 tablet for 50 ml)
TAE buffer	40 mM Tris acetate 1 mM EDTA, pH 8.0
TE buffer, pH 7.4	10 mM Tris/HCl, 7.4 1 mM EDTA, pH 8.0
TFBI buffer	30 mM K acetate 100 mM KCl 50 mM MnCl <sub>2</sub> 15% (v/v) glycerol → pH 5.8, adjusted with acetic acid → sterile filtered: 0.2 μm, keep at 4°C
TFBII buffer	10 mM MOPS/NaOH, pH 7.0 75 mM CaCl <sub>2</sub> 10 mM KCl 15% (v/v) glycerol → sterile filtered: 0.2 μm, keep at 4°C

## 2.3 General methods for working with DNA and RNA

### 2.3.1 Horizontal and vertical agarose gel electrophoresis of DNA

Agarose gel electrophoresis was used to separate DNA fragments according to their size and to analyze the quality and quantity of the DNA [136]. Horizontal agarose gel electrophoresis was performed in TAE buffer. Ethidiumbromide (EthBr) was added to the gel at a final concentration of 0.5 µg/ml. DNA samples were supplied with 5x loading buffer. Electrophoresis was performed at 10-12 V/cm. DNA was visualized by UV-light (254-366 nm) due to the fluorescence of the DNA bound ethidiumbromide, and the gels were documented by a gel documentary system (Peqlab).

For analysis of *in vitro* DNaseI indirect end-labeling, vertical gel electrophoresis systems prepared by the in-house workshop were used. For one gel, 400 ml of 1.5% (w/v) agarose solved in 1x Loening buffer were used. Electrophoresis was performed at 100 V.

### 2.3.2 Polymerase chain reaction (PCR)

The total volume of a standard PCR reaction was 50 µl, containing ~50 ng of template DNA, 100 pmol of each primer, 1 U of DNA polymerase, 200 µM dNTPs and the appropriate PCR buffer.

### 2.3.3 DNA purification by phenol/chloroform extraction

NaClO<sub>4</sub> was added at a final concentration of 1 M. The high salt concentration helps to separate the phases during phenol extraction and provides salt for the following ethanol (EtOH) precipitation. One volume of phenol was added, and the sample was vortexed vigorously. Then one volume of IAC was added, the sample was vortexed vigorously, and centrifuged (5 min, 16.000 x g, RT, Eppendorf 5415D). The supernatant was transferred into a fresh microcentrifuge tube, vortexed vigorously with one volume of IAC, centrifuged, and the supernatant was transferred to a fresh microcentrifuge tube.

### 2.3.4 DNA precipitation with alcohol

DNA was precipitated by adding NaCl to a final concentration of 0.2 M and either 2.5 volumes of EtOH (RT) or 0.7 volumes of isopropanol (RT). Depending on the DNA concentration the



samples were incubated on ice for 10 min or over night (o/n) at -20°C and centrifuged afterwards (20 min, 20.000 x g, 4°C, Eppendorf 5417R). The precipitated DNA was washed with 70% EtOH (RT), air-dried, and resuspended in TE buffer, pH 7.4 or dH<sub>2</sub>O.

### **2.3.5 DNA quantification**

DNA amount was estimated by agarose gel electrophoresis in comparison to marker DNA and quantified by spectrophotometry (Nanodrop ND1000, Peqlab) measuring the absorption at a wavelength of 260 nm ( $A_{260}$ ), where nucleic acids have their absorption maximum. An  $A_{260}$  of 1 corresponds to a concentration of 50 µg DNA/ml. Since proteins and RNAs have a maximal absorbance at 280 nm, the DNA purity can be judged by the ratio  $A_{260}/A_{280}$ . A ratio of  $A_{260}/A_{280}$  between 1.8 and 2.0 indicates pure DNA.

### **2.3.6 Preparation of chemically competent *E.coli***

100 ml of a logarithmic *E. coli* culture, grown in LB medium to an  $OD_{600}$  of 0.5 (Spectrophotometer, Pharmacia Biotech, Ultrospec 2000), were centrifuged (15 min, 6000 x g, 4°C, Heraeus Kendro Cryofuge 6000i), resuspended in 30 ml ice cold TFBI buffer, and incubated for 30 min on ice. Cells were centrifuged again (5 min, 1000 x g, 4°C, Eppendorf 5810R), resuspended in 4 ml ice cold TFBII buffer, and incubated for 10 min on ice. Aliquots of 200 µl were shock frozen in liquid nitrogen and stored at -80°C.

### **2.3.7 Transformation of competent *E. coli***

After thawing on ice, 100 µl of chemically competent *E. coli* were added to 30 µl plasmid DNA containing 50-500 ng of DNA. Samples were mixed gently, incubated 30 min on ice, heat shocked for 45 s at 42°C, and incubated again on ice for 3 min. 900 µl LB-medium were added, and the cells were incubated at 37°C for 30 min. Finally, bacteria were streaked out on agar plates containing appropriate antibiotics and incubated overnight at 37°C.

### **2.3.8 Preparation of plasmids**

Plasmids were prepared using the Qiagen Plasmid Mini, Midi and Maxi kits following the manufacturer's instructions.

### 2.3.9 Preparation of probe DNA

The preparation of radioactively labeled probes for hybridization of Southern blots was performed using the Prime-It II Random Primer Labeling Kit (Stratagene). 10 µl of random oligonucleotide primers were added to 24 µl probe DNA solution containing 25-30 ng of probe DNA. The reaction was heated for 5 min at 95°C and placed back on ice for 5 min. 10 µl of 5x dCTP primer buffer, 5 µl of  $\alpha$ -<sup>32</sup>P labeled dCTP, and 1 µl of 5 U/µl Exo(-)Klenow enzyme were added, mixed thoroughly, and incubated for 10 min at 37°C. 50 µl of STE buffer were added, and the mixture was purified by a Sephadex QuickSpin G-50 column (Roche). The 70-100 µl flow-through containing the radioactively labeled probe was transferred to a fresh microcentrifuge tube. Before hybridization, the probe was denatured for 5 min at 95°C.

### 2.3.10 Southern blot

Southern blotting was used to transfer DNA from agarose gels to a nylon membrane. Agarose gels were soaked for 20 min in denaturing buffer. The agarose gel was laid on top of thick Whatman papers soaked with 20x SSC with the ends of the Whatman papers hanging into a bath of 20x SSC buffer. The membrane was laid on top of the agarose gel followed by three thick Whatman papers soaked with 20x SSC and a stack of filter tissues. Weight was put on top of the blotting construction to ensure even pressure on the gel and allow constant DNA transfer onto the membrane. The transfer of DNA from the agarose gel onto the membrane occurred *o/n* by capillary action. The following day the membrane was baked for 2h at 80°C to permanently immobilize the DNA on the membrane.

The baked membrane was washed for 30 min in 3x SSC and for 2 h in 3x SSC/1x Denhardt's at 68°C. The membrane was transferred to a 200 ml cylinder and pre-hybridized for 1 h at 68°C in 25 ml prehybridization solution in the presence of herring sperm DNA, which reduced unspecific binding of probe DNA. For hybridization, half of the probe was added to 5 ml prehybridization solution per cylinder, and hybridization was carried out *o/n*. The cylinder was flushed 3 times with 2x SSC and the membrane was washed three times for 30 min at 68°C with 2x SSC/1x Denhardt's. The washed membrane was wrapped into plastic wrap (Saran) and exposed to an X-ray film.

To remove bound probes from the membrane, blots were washed three times in 0.4 M NaOH for 30 min at 45°C. The membrane was neutralized two times for 15 min at 45°C with 0.1x SSC/0.1% SDS and hybridized with another probe.

### 2.3.11 Northern blot

Agarose gels (1.2%) were prepared in 1x MOPS buffer and 7.4% (v/v) formaldehyde without EthBr. RNA samples were prepared as follows: 6  $\mu$ l RNA sample, containing 10-24  $\mu$ g of RNA, were mixed with 15  $\mu$ l formamid, 5  $\mu$ l 37% formaldehyde, and 3  $\mu$ l 10x MOPS, and incubated for 15 min at 65°C. Samples were placed back on ice for 5 min and 1  $\mu$ l EthBr was added. 3  $\mu$ l RNA loading buffer were added to the sample before loading the samples onto the gel. Electrophoresis was performed at 4 V/cm. Northern blotting was performed analogous to Southern blotting described in 2.3.10, but incubation in denaturing solution was omitted. Instead, the agarose gel was washed in dH<sub>2</sub>O for 5 min, and then capillary blotting onto a nylon membrane o/n was performed. Baking, washing, and hybridization of Northern blots were performed as described in 2.3.10.

To rehybridize the Northern blot with another probe, the probe bound to the membrane was removed by shaking the membrane two times for 5 min in boiling 0.1% (w/v) SDS solution. The SDS solution and the membrane were cooled down to RT and the blot was hybridized again.

## 2.4 General methods for working with *S. pombe* and *S. cerevisiae*

### 2.4.1 Transformation of *S. pombe*

A 10 ml *S. pombe* culture was grown in low-glucose EMM medium to an OD<sub>600</sub> of 0.5-1 (Spectrophotometer, Pharmacia Biotech, Ultrospec 2000). Cells were washed with 10 ml dH<sub>2</sub>O, resuspended in 1 ml dH<sub>2</sub>O, and transferred to a microcentrifuge tube. Cells were pelleted briefly, washed with 200  $\mu$ l LiAc/EDTA buffer, and resuspended in 50  $\mu$ l LiAc/EDTA buffer. 1  $\mu$ g plasmid DNA in a volume of 30  $\mu$ l and 300  $\mu$ l 40% (w/v) PEG 3350 in LiAc/EDTA buffer were added and incubated for 30 min with agitation at 30°C. Cells were heat shocked for 15 min at 42°C in a water bath and pelleted briefly by centrifuging (1 min, 1500 x g, RT, Eppendorf 5415D). Cells were resuspended in 400  $\mu$ l TE buffer, pH 7.4 and 200  $\mu$ l aliquots were streaked out on EMM plates selective for the plasmid marker.

### 2.4.2 Transformation of *S. cerevisiae*

A 10 ml culture of *S. cerevisiae* was grown to an OD<sub>600</sub> of 2-3 (Spectrophotometer, Pharmacia Biotech, Ultrospec 2000) in YPDA medium or selective YNB medium. Cells were washed with 50 ml TE buffer, pH 7.4 and resuspended in TE buffer, pH 7.4 to a concentration of 30 OD cells

per ml. 500  $\mu$ l of this cell suspension were mixed with 500  $\mu$ l 0.2 M LiAc and vigorously shaken for 1 h at 30°C in a water bath. 100  $\mu$ l of the cell suspension was transferred into a microcentrifuge tube containing 30  $\mu$ l of plasmid DNA (1-2  $\mu$ g DNA) and incubated for 30 min at 30°C without shaking. 130  $\mu$ l of 60% (w/v) PEG 4000 were added, and after intense vortexing the mixture was incubated for 1 h at 30°C. Cells were heat shocked for 10 min at 42°C in a water bath, centrifuged (1 min, 1500 x g, RT, Eppendorf 5415D), and washed with 1 ml dH<sub>2</sub>O. Cells were centrifuged again, resuspended in 100  $\mu$ l dH<sub>2</sub>O, and streaked out on YNB plates selective for the plasmid marker.

### 2.4.3 Isolation of DNA from *S. pombe* and *S. cerevisiae*

A 10 ml yeast culture was grown to an OD<sub>600</sub> of 5-8 (Spectrophotometer, Pharmacia Biotech, Ultrospec 2000), washed with dH<sub>2</sub>O, and resuspended in 250  $\mu$ l Sorbitol/Phosphate buffer. 0.2 mg zymolyase 100T (fresh solution in dH<sub>2</sub>O) was added and cells were spheroplasted for 40 min at 37°C. 50  $\mu$ l Proteinase K (20 mg/ml), 60  $\mu$ l 0.2 M EDTA, pH 8.0, and 44  $\mu$ l 20% (w/v) SDS were mixed with the spheroplasts, and incubated for 30 min at 37°C. After adding 1 M NaClO<sub>4</sub> and phenol/chloroform extraction, the supernatant was transferred to a fresh microcentrifuge tube and EtOH precipitated. The pellet was resuspended in 250  $\mu$ l TE buffer, pH 7.4 and incubated with 20  $\mu$ l RNase A (10 mg/ml) for 1 h at 37°C. The sample was EtOH precipitated, and the DNA pellet was resuspended in 100  $\mu$ l TE buffer, 7.4.

### 2.4.4 Isolation of RNA from *S. pombe* and *S. cerevisiae*

Preparation of total RNA from *S. cerevisiae* and *S. pombe* was performed as described [141]. All buffers and solutions used for RNA isolation were prepared with DEPC-dH<sub>2</sub>O. 10 ml of *S. pombe* and *S. cerevisiae* were grown to an OD<sub>600</sub> of 2-4 (Spectrophotometer, Pharmacia Biotech, Ultrospec 2000). Cells were harvested by centrifugation (5 min, 3000 x g, RT, Eppendorf 5810R), resuspended in 400  $\mu$ l AE-buffer, and transferred to a 1.5 ml microcentrifuge tube. The suspension was supplied with 40  $\mu$ l 10% SDS, vortexed, and one volume of phenol was added for separation of RNA. The mixture was vortexed again, incubated at 65°C for 4 min, rapidly chilled in a dry ice/EtOH bath until phenol crystals appeared, and then centrifuged (2 min, 16000 x g, RT, Eppendorf 5415D) to separate the aqueous and phenol phase. The upper aqueous phase was phenol/chloroform extracted, the supernatant was transferred to a fresh microcentrifuge tube, and precipitated with 0.3 M Na acetate and 2.5 volumes of EtOH. The RNA pellet was washed with 80% EtOH, air-dried, resuspended in sterile dH<sub>2</sub>O, and the RNA solution was stored at -80°C.

## 2.5 Preparation of yeast nuclei and yeast extract

### 2.5.1 Preparation of nuclei from *S. pombe* and *S. cerevisiae*

Nuclei from *S. cerevisiae* and *S. pombe* were prepared as described [3, 12]. 0.5-1 l yeast were grown to an OD<sub>600</sub> of 2-4 (yeast in log phase) (Spectrophotometer, Pharmacia Biotech, Ultrospec 2000), harvested (10 min, 6000 x g, RT, Heraeus Kendro Cryofuge 6000i), and washed once with dH<sub>2</sub>O. After centrifugation (5 min, 3000 x g, RT, Eppendorf 5810R) and determining the wet weight of the pellet, the cells were resuspended in 2 volumes of preincubation buffer 1 and incubated for 30 min in a 30°C water bath with vigorous shaking. Yeasts were centrifuged and the pellet was washed with 1 M sorbitol and resuspended in 5 ml Sorbitol/β-ME per g wet weight. Spheroplasts were obtained by adding zymolyase 100T to a final concentration of 2 mg zymolyase 100T per g wet weight for *S. cerevisiae* and 8 mg zymolyase 100T per g wet weight for *S. pombe* and vigorous shaking for 30 min at 30°C in a water bath. For *S. cerevisiae*, the efficiency of the yeast cell wall digestion by zymolyase can be visualized by a decreased absorbance at OD<sub>600</sub> and should lie between 60% and 95%. In *S. pombe*, the zymolyase digest does not yield a change in the absorbance at OD<sub>600</sub>. The spheroplasts were washed in 1 M sorbitol, and cell lysis was performed by resuspending the spheroplasts in a hypotonic ficoll buffer. 1 g aliquots of yeast nuclei were pelleted by centrifugation (30 min, 24.000 x g, 4°C, Sorvall Kendro RC6PLUS). Finally, the yeast nuclei were frozen for 10 min in EtOH/dry ice and stored at -80°C.

### 2.5.2 Preparation of whole-cell extract from *S. pombe* and *S. cerevisiae*

Whole-cell extract from *S. pombe* was prepared as described for *S. cerevisiae* [64, 82]. The protocol was based on the protocol from Schultz et al. [143, 144] with modifications by S.E. Kong and J. Q. Svejstrup. Cells were grown to an OD<sub>600</sub> of 2-4 (Spectrophotometer, Pharmacia Biotech, Ultrospec 2000) and centrifuged (5 min, 3000 x g, RT, Eppendorf 5810R). The cell pellet was washed with dH<sub>2</sub>O and extraction buffer and shock frozen in liquid nitrogen. The frozen yeast cells were lysed by grinding in a mortar in liquid nitrogen with some additional extraction buffer. The lysed cells were thawed slowly at 4°C and centrifuged (2 h, 100.000 x g, 4°C, SW60Ti-rotor, Optima LE-80K Ultracentrifuge, Beckman Coulter). The middle part of the supernatant containing the soluble proteins was withdrawn with a syringe, leaving behind the cloudy layer on top of the pellet and the lipid-rich layer at the meniscus. Proteins were precipitated by adding 337 mg/ml (NH<sub>4</sub>)<sub>2</sub>SO<sub>4</sub> while stirring until complete dissolution and centrifuged (20 min, 41.000 x g, 4°C, TLA55-rotor, Optima MAX-E Ultracentrifuge, Beckman Coulter). The pellet was

resuspended in 500-700  $\mu$ l dialysis buffer and dialyzed three times for 30 min against the same buffer. Aliquots of the extract were frozen in liquid nitrogen and stored at  $-80^{\circ}\text{C}$ .

## 2.6 *In vitro* chromatin assembly

### 2.6.1 Purification of histone octamers from *Drosophila* embryos

Purification of *Drosophila* embryo histone octamers was performed as described by Simon and Felsenfeld <sup>[150]</sup>. Collected *Drosophila* embryos were washed in tap water and 0.7% NaCl/0.04% Triton-X100, incubated for 3 min with 3% hypochlorite, and frozen in 100 g aliquots at  $-80^{\circ}\text{C}$ . 100 g *Drosophila* embryos were thawed at  $4^{\circ}\text{C}$ , resuspended in 40 ml lysis buffer, and homogenized (Yamamoto homogenizer) by 6 strokes at 1000 rpm. The homogenized embryos were centrifuged (10 min, 10.000 x g,  $4^{\circ}\text{C}$ , Sorvall Kendro RC6PLUS) resulting in three fractions: a solid pellet, a soft layer on top of the pellet containing the nuclei, and a supernatant layer. The supernatant layer was carefully removed. The nuclei layer was resuspended in 50 ml sucrose buffer, transferred to new tubes, and centrifuged again (10 min, 10.000 x g,  $4^{\circ}\text{C}$ , Sorvall Kendro RC6PLUS). This washing step was repeated. The nuclei pellet was resuspended in sucrose buffer to a final volume of 30 ml, and 90  $\mu$ l of 1 M  $\text{CaCl}_2$  were added. The nuclei digest was performed with approximately 200 U/ $\mu$ l MNase for 10 min at  $26^{\circ}\text{C}$ , stopped with 10 mM EDTA, pH 8.0, and centrifuged (10 min, 10.000 x g,  $4^{\circ}\text{C}$ , Sorvall Kendro RC6PLUS). The resulting pellet was resuspended in 6 ml TE buffer, pH 7.6 with 1 mM DTT and 0.2 mM PMSF and lysed by rotation for 30-45 min at  $4^{\circ}\text{C}$ . After lysis, the nuclei were centrifuged (30 min, 23.000 x g,  $4^{\circ}\text{C}$ , Sorvall Kendro RC6PLUS) and the supernatant was withdrawn. The salt concentration of the supernatant, containing the mononucleosomes, was adjusted to 0.63 M KCl. The supernatant was loaded on a hydroxylapatite column. The histone octamers were eluted with a salt gradient between 0.63 M and 2 M KCl (octamers usually eluted at approximately 1 M KCl). The fractions containing the histone octamers were pooled and concentrated with Microsep Centrifugal Concentrators (10 kD cut off, Pall Corporation). Glycerol concentration was adjusted to 40-50% and supplemented with DTT and Complete protease inhibitor without EDTA and kept at  $-20^{\circ}\text{C}$ . Concentration was estimated by SDS-PAGE in comparison to other histone preparations.

## 2.6.2 Assembly of chromatin by salt gradient dialysis

Salt gradient dialysis was performed as described previously by Längst et al <sup>[91]</sup>. A typical assembly reaction contained 10 µg of supercoiled plasmid DNA, 20 µg bovine serum albumine, and 6-10 µg of *Drosophila* embryo histone octamers (preparation see 2.6.1) in 100 µl high salt buffer. This mixture was dialyzed for 15 h at RT while slowly diluting 300 ml of high-salt buffer with 3 l of low-salt buffer using a peristaltic pump. A final 1 h dialysis step versus low-salt buffer yielded a final concentration of 50 mM NaCl. Chromatin was stored at 4°C.

## 2.6.3 Adding yeast extract to pre-assembled chromatin (reconstitution assay)

1 µg of salt gradient dialysis chromatin was incubated with or without *S. pombe* or *S. cerevisiae* extract (~ 250 µg protein) and with or without a regenerative energy system in assembly buffer. This reconstitution assay was performed in a volume of 100 µl in assembly buffer for 2 h at 30°C.

### Regenerative energy system

3 mM ATP  
3 mM MgCl<sub>2</sub>  
30 mM creatine phosphate  
50 ng/µl creatine kinase

### Assembly buffer (1x)

12% glycerol  
2.5 mM DTT  
20 mM HEPES, pH 7.5  
0.5 mM EGTA, pH 8.0  
80 mM KCl

## 2.7 Chromatin analysis by indirect end-labeling

### 2.7.1 MNase digestion of *S. pombe* spheroplasts

Growth and permeabilization of *S. pombe* cells was performed as described under 2.8.1, but crosslinking was omitted and the washed spheroplast pellet was resuspended in 1.5 ml NP-buffer to give a final volume of 1.8 ml. 300 µl aliquots were digested with MNase (10 min, 37°C) using MNase concentrations of 50-400 U/ml.

For generating MNase ladders, 300 µl aliquots were digested for 10 min at 37°C with MNase concentrations between 600 and 2000 U/ml. The reaction was stopped with 1% SDS/10 mM EDTA, pH 8.0 and samples were put back on ice. DNA was purified as described in 2.7.4 and the DNA pellet was finally resuspended in 50 µl.

### 2.7.2 MNase digestion of *S. pombe* and *S. cerevisiae* nuclei

1 g of *S. cerevisiae* nuclei (see 2.5.1 for preparation), stored at  $-80^{\circ}\text{C}$ , was thawed and washed with 6 ml 1x MNase buffer. After centrifugation (5 min, 3000 x g,  $4^{\circ}\text{C}$ , Eppendorf 5810R), the nuclei were resuspended in 1x MNase buffer to a final volume of 1.8 ml. 300  $\mu\text{l}$  aliquots of *S. cerevisiae* nuclei were digested with different MNase concentrations between 0.125 and 1 U/ml for 20 min at  $37^{\circ}\text{C}$ . For generating MNase ladders from *S. cerevisiae* nuclei, MNase concentrations of 2-16 U/ml were used.

1 g of *S. pombe* nuclei (see 2.5.1 for preparation), stored at  $-80^{\circ}\text{C}$ , was thawed and washed with 6 ml buffer A according to Bernardi et al <sup>[12]</sup>. After centrifugation (5 min, 3000 x g,  $4^{\circ}\text{C}$ , Eppendorf 5810R), nuclei were resuspended in buffer A to a total volume of 2.1 ml. The cell suspension was divided into six 350  $\mu\text{l}$  aliquots and a final concentration of 5 mM  $\text{CaCl}_2$  was added to each aliquot. The MNase digestion was performed for 5 min at  $37^{\circ}\text{C}$  using concentrations of 25-450 U/ml. MNase digestion was stopped with 0.5% SDS/4 mM EDTA, pH 8.0 for *S. cerevisiae* samples, and 1% SDS/10 mM EDTA, pH 8.0 for *S. pombe* samples.

### 2.7.3 DNaseI digestion of *S. pombe* and *S. cerevisiae* nuclei

DNase indirect end-labeling was performed as described by Almer and Horz <sup>[2]</sup>. 1 g of yeast nuclei (see 2.5.1 for preparation), stored at  $-80^{\circ}\text{C}$ , was thawed and washed with 6 ml 1x DNaseI buffer. After centrifugation (5 min, 3000 x g,  $4^{\circ}\text{C}$ , Eppendorf 5810R), the nuclei were resuspended in 1x DNaseI buffer to a final volume of 1.8 ml for *S. cerevisiae* and 2.1 ml for *S. pombe*. Six 300  $\mu\text{l}$  aliquots of *S. cerevisiae* nuclei were digested with different concentrations of DNaseI ranging from 0.1-4 U/ml for 20 min at  $37^{\circ}\text{C}$ . For *S. pombe*, six 350  $\mu\text{l}$  aliquots were digested with 1-30 U/ml of DNaseI for 5 min at  $37^{\circ}\text{C}$ . DNaseI digestion was stopped with 0.5% SDS/4 mM EDTA, pH 8.0 for *S. cerevisiae* samples, and 1% SDS/10 mM EDTA, pH 8.0 for *S. pombe* samples.

### 2.7.4 DNA purification after DNaseI/MNase digestion

The stopped DNaseI/MNase digestion solutions were mixed with 5% (v/v) Proteinase K (20 mg/ml) and incubated for 1 h at  $37^{\circ}\text{C}$ . 1 M  $\text{NaClO}_4$  was added and samples were phenol/chloroform extracted and EtOH precipitated. The DNA pellet was resuspended in 250  $\mu\text{l}$  TE buffer, pH 7.4, and 20  $\mu\text{l}$  RNase A (10 mg/ml) was added and incubated for 1 h at  $37^{\circ}\text{C}$ .



Finally, the samples were EtOH precipitated and the DNA pellet was resuspended in 50  $\mu$ l TE buffer, pH 7.4.

### **2.7.5 MNase digestion of free DNA**

Genomic DNA was prepared from 500 ml of *S. pombe* culture divided into 6 aliquots as described in 2.7.1, but instead of MNase treatment 1% SDS/10 mM EDTA, pH 8.0 stop buffer was added immediately. Purification of the DNA as described in 2.7.4 yielded six 50  $\mu$ l aliquots of genomic DNA. 20  $\mu$ l of purified DNA were digested with 0.025/0.05 U/ml MNase in a volume of 50-100  $\mu$ l (filled up with NP-buffer), stopped with 1/10 volume 0.2 M EDTA, pH 8.0, and purified by EtOH precipitation. The DNA pellet was resuspended in 20  $\mu$ l TE buffer, pH 7.4.

### **2.7.6 DNaseI digestion of plasmid DNA**

10  $\mu$ g of plasmid DNA were digested with DNaseI in a volume of 50  $\mu$ l in 1x DNaseI buffer. DNaseI digestion was performed for 20 min at 37°C, using concentrations of 0.01, 0.05, 0.1, 0.2 U/ml DNaseI, and stopped with 4  $\mu$ l of 0.2 M EDTA, pH 8.0.

### **2.7.7 Secondary cleavage**

25-50  $\mu$ l of the DNaseI/MNase digested and purified DNA was used for secondary cleavage with a restriction enzyme. The restriction enzyme digestion was performed for 2 h in a volume of 150  $\mu$ l using 40 U of an appropriate restriction enzyme. The restriction enzyme cleavage site was located 500-1500 bp up- or downstream of the region of interest. After restriction enzyme digestion, samples were EtOH precipitated, and DNA was resuspended in 20  $\mu$ l TE buffer, pH 7.4.

### **2.7.8 Generation of marker fragments**

Two to four appropriate restriction enzymes cutting within the region of interest were chosen and 3  $\mu$ l of the purified genomic DNA were digested separately with each enzyme and with the secondary cleavage restriction enzyme.

### 2.7.9 DNaseI digestion of *in vitro* assembled chromatin of SPAC1F8.06

A 4 kb region around the *S. pombe* locus SPAC1F8.06 was cloned over SmaI and PstI into the pUC19 plasmid and assembled into salt gradient dialysis chromatin. The *in vitro* assembled chromatin was digested with different amounts of DNaseI for 5 min at RT. The reaction was stopped with 0.5% SDS/2 mM EDTA, pH 8.0, and after addition of 3  $\mu$ l Proteinase K (20 mg/ml) and 1  $\mu$ l glycogen (20 mg/ml) incubated for 12-15 h at 37°C. The DNA was EtOH precipitated, resuspended in 20  $\mu$ l TE buffer, pH 8.0, and for secondary cleavage digested with BglIII. Marker fragments were generated with MscI and HpaI, cleaving 227 bp and 891 bp behind the ATG of SPAC1F8.06, respectively.

## 2.8 Preparation of genome-wide nucleosome occupancy map in *S. pombe* by tiling array analysis

### 2.8.1 Growth and spheroplasting of *S. pombe* cells

The protocol used for preparation of mononucleosomal DNA was modified from Yuan et al. and Whitehouse et al. [176, 192] and adapted for *S. pombe* [92]. *S. pombe* was grown o/n for 15-17 h in 500 ml YES medium to an OD<sub>600</sub> of ~0.45-0.5 (Spectrophotometer, Pharmacia Biotech, Ultrospec 2000). Cells were crosslinked with 0.5% (v/v) formaldehyde for 20 min and crosslinking was stopped with 125 mM glycine. Cells were centrifuged (10 min, 4°C, 3000 x g, Eppendorf 5810R) and washed with 45 ml dH<sub>2</sub>O. After centrifugation, cells were resuspended in 20 ml preincubation buffer 2 and incubated for 10 min at 30°C in a water bath while vigorous shaking. Cells were centrifuged again, resuspended in 10 ml Sorbitol/Tris/ $\beta$ -ME buffer, and spheroplasted with 8 mg zymolyase 100T at 30°C for 30 min. *S. pombe* spheroplasts were centrifuged (10 min, 4°C, 3000 x g, Eppendorf 5810R), washed with cooled 1 M Sorbitol/Tris, and resuspended in a total volume of 7.5 ml NP buffer.

### 2.8.2 MNase digestion of *S. pombe* spheroplasts

100  $\mu$ l MNase (50 U/ $\mu$ l) were added to 7.5 ml of *S. pombe* spheroplasts resuspended in NP-buffer. MNase digestion was performed in a water bath at 37°C for 20 min and yielded an appropriate chromatin digestion degree of around 80% mononucleosomal DNA. MNase digestion was stopped with 1 ml 5% SDS/100 mM EDTA, 8.0.

### 2.8.3 Purification of DNA for tiling array analysis

400  $\mu$ l RNase A (10 mg/ml) were added to the MNase digested sample and incubated for 45 min at 37°C. 450  $\mu$ l Proteinase K (20 mg/ml) were added and incubated o/n for ~15 h at 65°C. During this step, proteins became digested and crosslinking was reversed. Samples were cooled for 10 min on ice. 2.5 ml of 3 M KAc, pH 5.5 (Quiagen buffer P3) were added, and the sample was incubated for 10 min on ice. Samples were centrifuged (10 min, 4°C, 3000 x g, Eppendorf 5810R) and the supernatant was phenol/chloroform extracted. The volume of the upper phase was filled up to 15 ml with 200 mM NaCl, 100  $\mu$ g glycogen and dH<sub>2</sub>O, and the sample was precipitated by adding 10.7 ml isopropanol, incubating for 1 h at -20°C, and centrifuging (1 h, 4°C, 3000 x g, Eppendorf 5810R). The pellet was washed with 5 ml 70% EtOH (RT), air-dried, resuspended in 200  $\mu$ l TE buffer, pH 7.4, and shaken for 3-5 h at 37°C to allow proper resuspension. The resuspended DNA sample was supplied with loading buffer, loaded onto a 1.8% agarose gel, and electrophorized until mono-, di- and trinucleosomal bands were separated. The mononucleosomal DNA bands were cut out with a clean scalpel and chopped into small pieces. The DNA was eluted from the agarose gel pieces using the Quantum Prep™ Freeze 'N Squeeze DNA Gel Extraction Spin Columns (Bio-Rad) following the manufacturer's instructions. The flow-through was collected, precipitated with isopropanol o/n, and the final DNA pellet was resuspended in 100  $\mu$ l TE buffer, pH 7.4. The mononucleosomal DNA in the sample was derived from 500 ml of an OD<sub>600</sub> of 0.45-0.5 *S. pombe* cells, had a concentration of 150-400 ng/ $\mu$ l, and an absorption ratio A<sub>260</sub>/A<sub>280</sub> of 1.85-2.0 indicative of sufficient purity.

### 2.8.4 Preparation of genomic control DNA

For the preparation of the genomic control DNA the same protocol was used as described in 2.8.1-2.8.3, but the crosslinking step, the MNase treatment, and the gel purification step were omitted.

### 2.8.5 DNaseI fragmentation, labeling, and hybridization to tiling arrays of mononucleosomal DNA and genomic control DNA

The isolated mononucleosomal DNA fragments and the genomic control DNA were fragmented with DNaseI and biotin labeled with terminal deoxynucleotidyl transferase using the Affymetrix GeneChip Mapping 10K Xba Assay Kit. Samples were prepared according to GeneChip Mapping 10K 2.0 Assay Manual and Affymetrix Chromatin Immunoprecipitation Assay Protocol. 22.5  $\mu$ l containing 10  $\mu$ g of mononucleosomal or genomic control DNA were mixed with 2.5  $\mu$ l of 10x Fragmentation buffer and 2.5  $\mu$ l of Fragmentation reaction mix and incubated for 1 h at 37°C. The

enzyme was heat inactivated for 15 min at 95°C. This fragmentation step was intended to yield fragments between 25 and 60 bp, and the fragment size was checked with an Agilent Bioanalyzer following the manufacturer's instructions. For the DNA labeling, 25.3 µl of DNaseI fragmented DNA sample were mixed with 9.7 µl Master mix and incubated for 2 h at 37°C. The Master mix contained terminal deoxynucleotidyl transferase (TdT) and biotin labeled dNTPs. The TdT incorporated the biotin labeled dNTPs at DNA fragment ends.

For array hybridization, 28 µl of the DNaseI fragmented and biotin labeled DNA were mixed with 14 µl DMSO, 100 µl 2x Hybridization mix, 3.3 µl Control Oligo B2, and 54.7 µl H<sub>2</sub>O. This 200 µl hybridization mix was heated for 5 min at 99°C, cooled for 5 min at 45°C, and centrifuged (1 min, 16000 x g, RT, Eppendorf 5415D). The hybridization mix was injected into the Affymetrix GeneChip *S. pombe* Tiling 1.0FR array, and the array was rotated for 16 h at 60 rpm and 45°C.

After hybridization, the arrays were washed and stained with streptavidin-phycoerythrin (SAPE). The signals were amplified with biotinylated anti-streptavidin antibodies in an Affymetrix Fluidics 450 wash station. Finally, the arrays were scanned in a 3000 7G scanner, and the signal was quantified with the Affymetrix GeneChip Command Console Software (AGCC) to generate CEL files.

#### Fragmentation reaction mix

2.2 µl Fragmentation reagent/ DNaseI (2.75 U/µl)  
122.8 µl 1x Fragmentation buffer

#### Master mix

14 µl 5x TdT buffer  
2 µl 5 mM GeneChip DNA Labeling Reagent  
3.4 µl 30 U/µl TdT

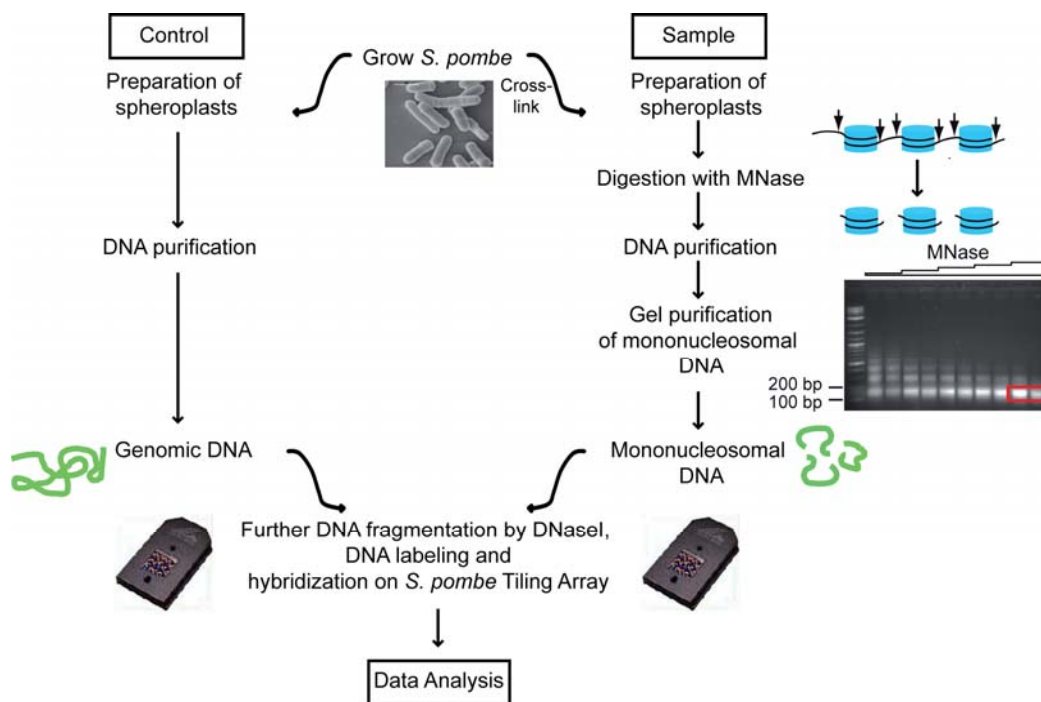


**Fig. 6: Workflow for processing of mononucleosomal and genomic control DNA from *S. pombe*.**

## 2.9 Bioinformatical data analysis

Bioinformatical data analysis was mainly conducted by Dr. Tobias Straub.

### 2.9.1 Genome versions and annotations

Information about *S. pombe* genome sequences and annotations (version of 16<sup>th</sup> July 2008) were obtained from the Sanger Genome Project ([www.sanger.ac.uk/Projects/S\\_pombe](http://www.sanger.ac.uk/Projects/S_pombe)). The probes on the Affymetrix GeneChip *S. pombe* Tiling 1.0FR array matched the 2004 genome version of *S. pombe* and were remapped to the genome dated 16<sup>th</sup> July 2008 using NCBI MegaBlast (<http://www.ncbi.nlm.nih.gov/blast/megablast.shtml>). Redundant probes on the array that matched more than one genomic location were removed. Also replication origins<sup>[62]</sup> matched the 2004 genome version and were remapped to the genome dated 16<sup>th</sup> July 2008. Transcriptome data from Dutrow et al.<sup>[38]</sup> matched the genome version of 2007, which is compatible with the genome version of 16<sup>th</sup> July 2008 in terms of gene coordinates.

Information about *S. cerevisiae* genome sequences and annotations were obtained from Saccharomyces Genome Database (SGD: <http://www.yeastgenome.org/>). The probes on the *S. cerevisiae* tiling array matched the 2003 genome version.

For annotating TSS and TTS of *S. pombe* transcripts, transcriptome data from Dutrow et al.<sup>[38]</sup> were used. Data were loaded into the Integrated Genome Browser (<http://www.bioviz.org/igb/>) and analyzed by eye. TSS and TTS were annotated where the signal of two subsequent probes was decreased by more than half compared to the average signal over the transcript. If transcripts of closely neighbored genes merged and did not allow clear discrimination between the two transcripts, TSS and TTS were not annotated.

For *S. cerevisiae*, TSS and TTS annotations from David et al. were used<sup>[32]</sup>.

### 2.9.2 Processing of raw microarray data

R/Bioconductor ([www.r-project.org](http://www.r-project.org), [www.bioconductor.org](http://www.bioconductor.org)) was used for the processing of raw microarray data. The raw tiling array data (Tab. 1) were normalized using the ‘vsn’ algorithm<sup>[66]</sup> and the nucleosome occupancy was calculated as log<sub>2</sub>-ratio of averaged mononucleosome to the averaged signals of all four genomic DNA replicates.

<i>S. pombe</i> strain	Replicates of mononucleosomal DNA	Replicates of genomic DNA
wt	4	3
<i>mit1</i> mutant	3	1
<i>ffi3</i> mutant	2	---
<i>tup11 tup12</i> mutant	2	---
<i>clr3</i> mutant	2	---

**Tab. 1: Tiling array data generated by hybridization of *S. pombe* mononucleosomal and genomic DNA.**

Processing of external *S. pombe* ChIP data (Tab. 2), i.e. normalization and calculation of the log<sub>2</sub> ratio of sample versus input, was performed in an analogous manner. Also the processing of *S. cerevisiae* nucleosome occupancy data from Lee et al. <sup>[94]</sup> and Yuan et al. <sup>[192]</sup> was performed as for *S. pombe*. For the processing of RNA expression data ‘gcrma’ was applied using default parameters.

Organism	Data set	Source
<i>S. pombe</i>	RNA expression wt	Dutrow et al. <sup>[38]</sup>
	RNA expression wt	Karl Ekwall; Karolinska Institutet, Department of Biosciences and Nutrition, Huddinge, Sweden Affymetrix yeast genome 2.0 array
	RNA polymerase II ChIP	Wilhelm et al. <sup>[181]</sup>
	H2A.Z ChIP	Buchanan et al. <sup>[22]</sup>
	Tup11 and Tup12 ChIP	Fagerstrom-Billai et al. <sup>[42]</sup>
	H3K9me2 ChIP	Cam et al. <sup>[26]</sup>
<i>S. cerevisiae</i>	Nucleosome occupancy	Lee et al. <sup>[94]</sup>
	Nucleosome occupancy	Yuan et al. <sup>[192]</sup>
	RNA expression wt	David et al. <sup>[32]</sup>

**Tab. 2: External data sources.**

RNA expression data, chromatin immunoprecipitation (ChIP) data, and *S. cerevisiae* nucleosome occupancy data used for analyses are listed.

### 2.9.3 Calculation of cumulative profiles

In cumulative profiles, normalized and averaged nucleosome occupancy profiles were overlaid by aligning at certain reference points, such as TSS, TTS, ATG, NDRs (see 2.9.6) or replication origins. A sliding window approach, using a window size of 50 bp and a 10 bp step size, calculated the average values of all overlaid signals within each 50 bp window in a 10 bp step along the genome relative to the reference point.

### 2.9.4 Clustering of nucleosome occupancy data

Clustering was used to determine regions of similar nucleosome occupancy profiles and to cluster them on this basis into distinct groups. Normalized and averaged nucleosome occupancy profiles were first scaled and then the Ward’s minimum variance method in ‘hclust’ (R package ‘Stats’) was used to cluster on the basis of similar nucleosome occupancy patterns within the region from -370 to +500 bp relative to the TSS.

### 2.9.5 Spectral analysis

Spectral densities were calculated using ‘spec.pgram’ (R package ‘Stats’) on equally spaced nucleosome occupancy data (50 bp window, 10 bp step size) including demeaning, a padding proportion of 1, and Daniell smoothers widths of 5. Spectral densities were sampled for 1 kb windows with a 500 bp overlap all along the chromosomes.

### 2.9.6 Hidden Markov model for NDR search

For Fig. 26A, NDRs were defined by a Hidden Markov model (HMM) calculated with TileMap (<http://biogibbs.stanford.edu/~jihk/TileMap/index.htm>). All signals revealing a strong depletion of the nucleosome density over ten or more following probes were defined as NDR. In total, 2839 NDRs were identified this way, two thirds of them localized in promoter regions (-500 bp to +100 bp relative to TSS). For the alignment in Fig. 26A, only NDRs that could be assigned as being closest to the TSS were used. Of the other identified NDRs, 73 were localized within transcripts (+100 bp relative to TSS to -100 bp relative to TTS), 43 in the 3'-region of genes (- 100 bp to +200 bp relative to TTS), and 586 somewhere else.

### 2.9.7 Analysis of DNA sequence contributions to nucleosome positioning

To calculate predicted nucleosome occupancy on the basis of DNA sequence, the N-score algorithm was applied <sup>[190, 191]</sup>. Two different N-score models were generated in a collaboration with Guo-Cheng Yuan, who developed the N-score algorithm <sup>[191]</sup>. One was trained with *S. pombe*, the other with *S. cerevisiae* nucleosome occupancy data. 8000 probes each corresponding to the highest or lowest log ratio in the tiling array data were selected for training. For *S. cerevisiae*, the nucleosome occupancy data from Lee et al. <sup>[94]</sup> were used. From each locus the centered 129 bp genomic sequence was extracted, converted into 16 dinucleotide frequencies, and wavelet-transformed with the Haar basis. Then a stepwise logistic regression classification model was built by combining three types of sequence features as predicting variables, namely wavelet energies, word counts <sup>[119]</sup>, and structural parameters <sup>[94, 121]</sup>. Each model was applied to calculate the genome-wide scores for both species.

To search for an enrichment of certain DNA sequence words within NDRs as defined by the HMM (see 2.9.6), all probes matching the NDR regions were extracted. All other probes were used as reference set. The search for frequencies of DNA sequence words was performed using algorithms developed by Karlin et al. and Yuan et al. <sup>[76, 192]</sup>.

## 3 Results

### 3.1 Different nucleosome positioning at the *S. cerevisiae* *PHO5* promoter in *S. pombe* and *S. cerevisiae*

In chromatin structure analyses of the *S. cerevisiae* genes *LEU2* and *SUC2* <sup>[107, 120]</sup> and of the *S. pombe* genes *ade6* and *ura4* <sup>[11]</sup>, the same chromatin structure was observed for the chromosomal and the extrachromosomal gene location. These results demonstrated that extrachromosomal plasmid DNA becomes packaged into chromatin, and that the nucleosome positions on a gene are largely independent of its surrounding context (Bernardi et al., 1991). In a next step, the group of Fritz Thoma compared the chromatin structure at genes localized extrachromosomally on shuttle plasmids in the two different yeast species *S. pombe* and *S. cerevisiae*. Interestingly, the indirect end-labeling of the respective genes, the *S. pombe* gene *ade6* and the *S. cerevisiae* gene *URA3*, showed different nucleosome positioning patterns in the two yeasts, speaking for species-specific nucleosome positioning mechanisms <sup>[12]</sup>. One drawback of this analysis was that it was not tested, if the genes localized on the shuttle plasmids had different transcription efficiencies in the two yeasts, which could lead to different chromatin structures. In another study, chromatin structure analysis of the *S. cerevisiae* gene *HIS3* after stable insertion into the *S. pombe* genome yielded different chromatin structures in *S. pombe* compared to *S. cerevisiae* <sup>[147]</sup>.

The *PHO5* promoter is a well established model system for chromatin structure analysis in *S. cerevisiae*. Depending on the intracellular phosphate level, the *PHO5* promoter can be strongly induced <sup>[115]</sup> resulting in changes in promoter chromatin structure. Under repressing conditions in the presence of phosphate, the gene is lowly transcribed and the promoter is packaged into four well positioned nucleosomes <sup>[3, 159]</sup> interrupted by a short 80 bp hypersensitive region between nucleosome -2 and -3 <sup>[2]</sup>. Upon activation of *PHO5* in the absence of phosphate, the positioned nucleosomes become remodeled, thereby generating a large nuclease hypersensitive site (Fig. 7) <sup>[2, 3]</sup>.

The well established *PHO5* promoter model was considered appropriate for a comparative analysis of chromatin structure in *S. pombe* and *S. cerevisiae* for mainly two reasons. First, the *PHO5* gene is not transcribed under repressive conditions in *S. cerevisiae*. And second, there was a chance that *PHO5* is also not transcribed in *S. pombe*, since promoter regions of *S. pombe* and *S. cerevisiae* are often not compatible <sup>[52]</sup>. This would allow comparing the chromatin structure of a region of the same transcription level, i.e. not expressed, in the two yeasts. If different transcription levels were excluded by this approach, this would argue more directly for species-specific nucleosome positioning mechanisms.



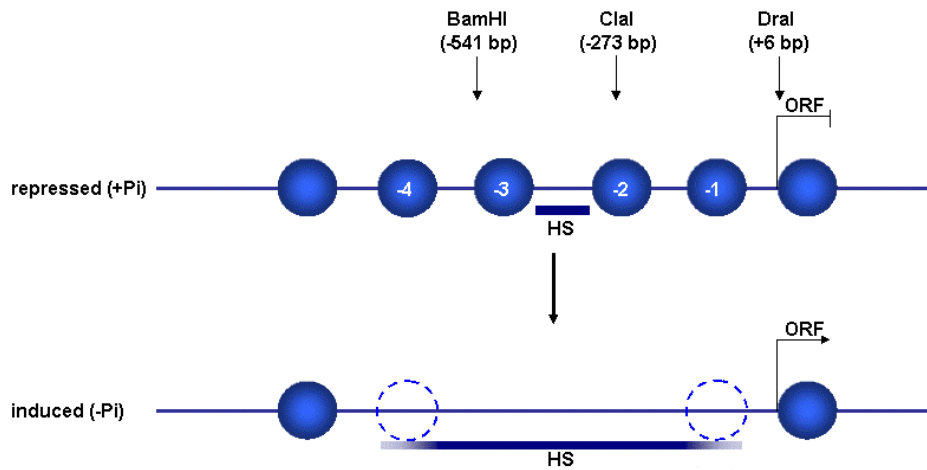


**Fig. 7: Chromatin structure at the *PHO5* promoter in its repressed and induced state.**

In the repressed state, four positioned nucleosomes are localized at the *PHO5* promoter, numbered -1 to -4 according to their position relative to the TSS. Phosphate starvation leads to induction of the *PHO5* promoter and to nucleosome loss *in trans* and the establishment of a large hypersensitive site. On average three nucleosomes are lost from the *PHO5* promoter<sup>[18, 83]</sup> and the less remodeled nucleosomes are illustrated with stippled lines. The restriction enzyme cleavage sites for BamHI, ClaI and DraI that are used for generation of marker fragments and their position relative to the ATG are given.

Therefore, the *S. cerevisiae* *PHO5* promoter was cloned into the YRpFB1-pUC19 shuttle plasmid, which can be maintained and packaged into chromatin both in *S. pombe* and *S. cerevisiae*<sup>[12]</sup>. Two shuttle plasmids were constructed, which allowed the analysis of the *PHO5* promoter chromatin structure (Fig. 8).

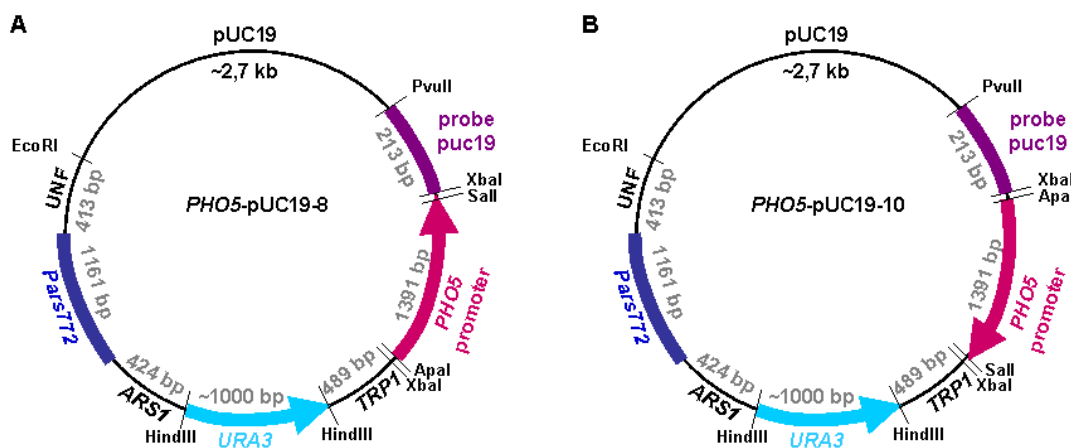


**Fig. 8: Two shuttle plasmids *PHO5*-pUC19-8 and *PHO5*-pUC19-10 containing the *PHO5* promoter in opposite orientations.**

(A and B) *PHO5*-pUC19-8 and *PHO5*-pUC19-10, respectively, containing the *PHO5* promoter in opposite directions. The *PHO5* promoter (ApaI to Sall) was cloned by XbaI into the shuttle plasmid YRpFB1-pUC19 resulting in the two shuttle plasmids *PHO5*-pUC19-8 and *PHO5*-pUC19-10. See 2.1.4.2 for description of the shuttle plasmid YRpFB1-pUC19.

The chromatin structure at the *PHO5* promoter revealed different nucleosome positioning patterns in *S. pombe* and *S. cerevisiae* independent of from which side the promoter was analyzed. In *S. cerevisiae*, the *PHO5* promoter chromatin structure was the same as known for the chromosomal

*PHO5* locus under repressive conditions, in *S. pombe*, the pattern was different and neither resembled the repressed nor the active state in *S. cerevisiae* (Fig. 9).

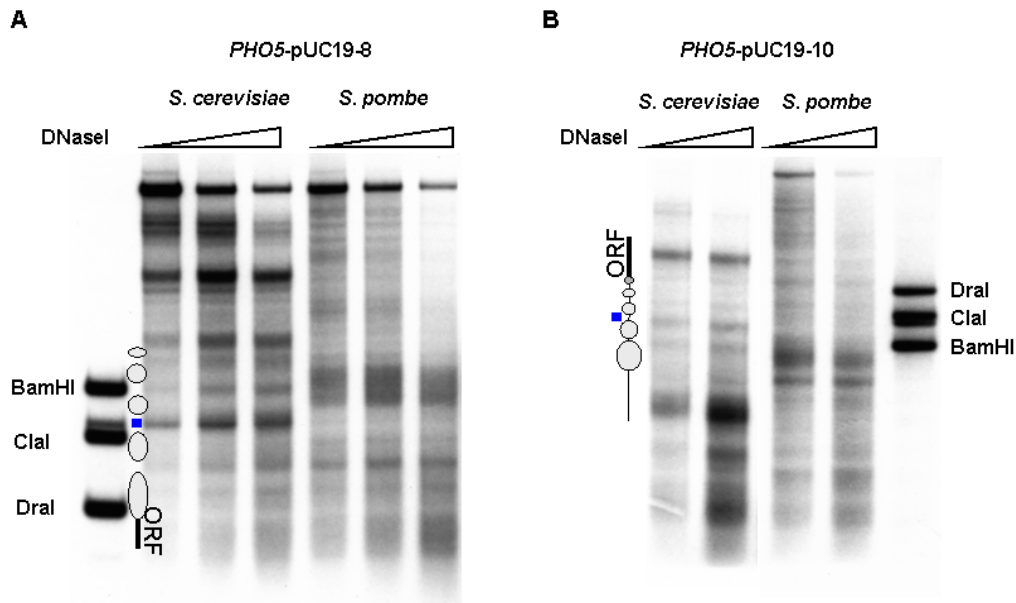


**Fig. 9: DNaseI indirect end-labeling at the *PHO5* promoter revealed a different chromatin structure in *S. pombe* and *S. cerevisiae*.**

(A and B) Indirect end-labeling of the *PHO5* promoter from the 3' direction (*PHO5*-pUC19-8) and 5' direction (*PHO5*-pUC19-10), respectively. PvuII site of pUC19 was used for secondary cleavage and DraI, ClaI and BamHI served as marker (see Fig. 7 for cut sites). Probe pUC19 was used for hybridization. Increasing DNaseI concentrations are indicated by ramps on top of the lanes.

To check for the transcription level of the *PHO5* promoter region on the shuttle plasmids, RNA was extracted from *S. pombe* cells (plus phosphate) and from induced (minus phosphate) and repressed (plus phosphate) *S. cerevisiae* cells. The Northern blot was hybridized with four different probes: the pUC19 probe, the *PHO5* promoter probe, binding transcripts of the BamHI-ClaI *PHO5* promoter region, the *URA3* probe, binding *URA3* transcripts, and the actin probe against *S. pombe* and *S. cerevisiae* chromosomal actin transcripts (see Fig. 8). The pUC19 probe, the *PHO5* promoter probe, and the *URA3* probe recognized regions transcribed from the shuttle plasmid. The actin probe served as positive control for the RNA preparation and gave a clear signal both in *S. pombe* and *S. cerevisiae*. In *S. pombe*, the RNA signal for actin was stronger (4.3-4.5-fold) and more smeary than in *S. cerevisiae* (Fig. 10A). Since the identical RNA amount was loaded for *S. pombe* and *S. cerevisiae* samples, the stronger signal could argue for higher transcription levels in *S. pombe* compared to *S. cerevisiae*, or could result from different hybridization efficiencies. The more smeary pattern might be due to faster RNA degradation in *S. pombe*. Induced *S. cerevisiae* cells (minus phosphate) usually have a reduced metabolism and accordingly lower RNA levels were observed.

Hybridization with the probes against the *PHO5* promoter and the pUC19 plasmid sequence gave a very prominent and smeary RNA pattern of three relatively large bands in *S. pombe* but no

signal in *S. cerevisiae* (Fig. 10B and C). These high transcription levels in *S. pombe* were not expected for the bacterial pUC19 sequence or the *S. cerevisiae* *PHO5* promoter region. Hybridization with the *URA3* probe (Fig. 10D) showed *URA3* transcripts both in *S. pombe* and *S. cerevisiae*. This was expected, as *URA3* was used as selection marker and needs to be transcribed in both yeasts. But also the *URA3* signal appeared differently in the two yeasts: in *S. cerevisiae* the *URA3* signal was visible as single band and was relatively weak, whereas in *S. pombe* the same RNA pattern appeared as after hybridization with the *PHO5* promoter probe and pUC19 probe. In general, as can be seen from Northern blot hybridizations with probes recognizing shuttle plasmid regions, plasmid *PHO5*-pUC19-10 showed higher expression levels than plasmid *PHO5*-pUC19-8 in *S. pombe* (3.5-, 4.2-, 7.0-fold) (Fig. 10B, C, D, and E). This was not due to generally higher RNA expression levels, since the actin transcript levels originating from the chromosomal location were comparable in *S. pombe* cells transformed with the shuttle plasmid *PHO5*-pUC19-8 and *PHO5*-pUC19-10.

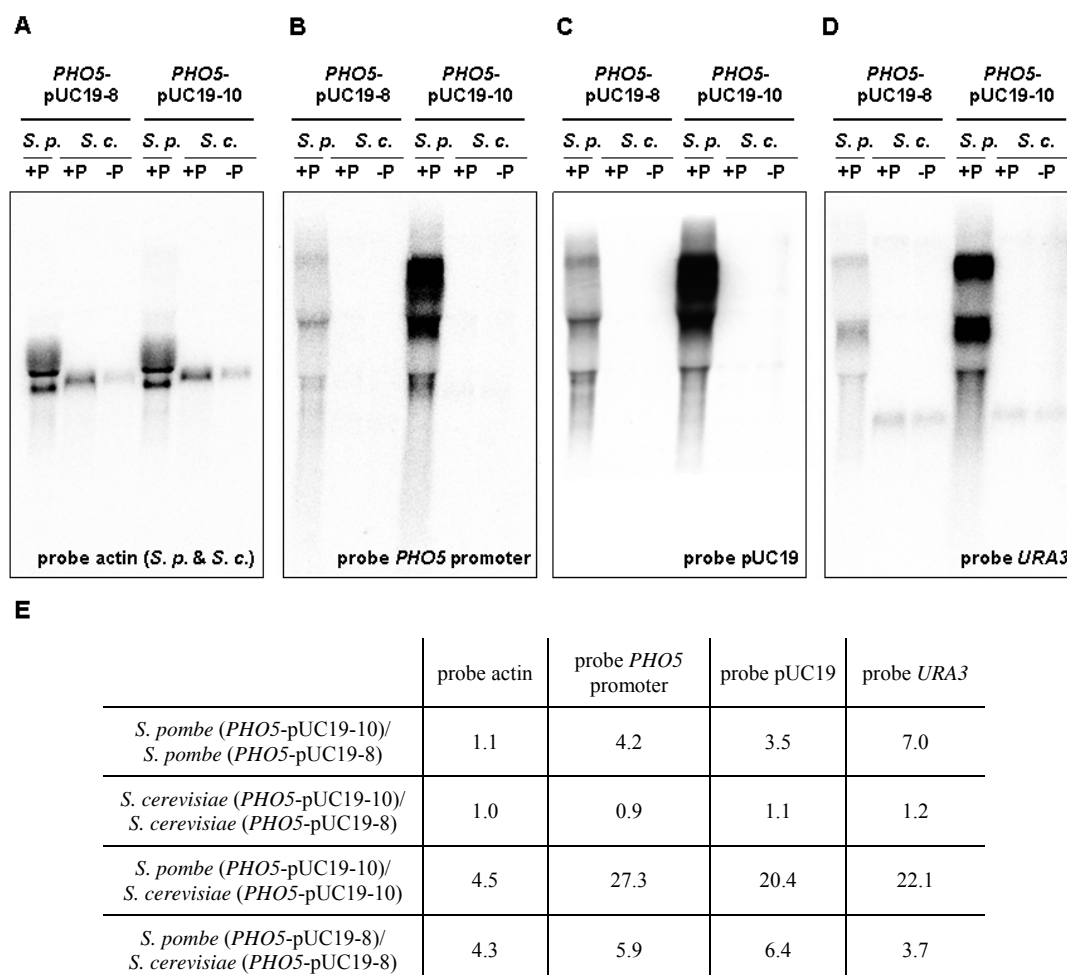


**Fig. 10: Analysis of RNA expression levels by Northern blot showed RNA signals for the *PHO5* promoter region in *S. pombe* but not in *S. cerevisiae*.**

RNA was isolated from *S. pombe* cells and induced and repressed *S. cerevisiae* cells and analyzed by Northern blot. (A) Northern blot hybridization with a probe recognizing the chromosomal actin transcripts of *S. pombe* and *S. cerevisiae*. (B-D) Northern blot hybridizations with probes against *PHO5* promoter, pUC19, or *URA3* transcripts, respectively, all originating from the shuttle plasmids. (E) Quantitative comparison of the Northern blot signals.

To test if the different transcription levels were due to different copy numbers of the shuttle plasmids, DNA was isolated from *S. cerevisiae* and *S. pombe* cells transformed with the shuttle plasmids and from non-transformed wt cells serving as negative control (Fig. 11). As expected, hybridization with the probe pUC19 revealed no signal in the non-transformed wt *S. cerevisiae* and *S. pombe* cells. For the shuttle plasmid *PHO5*-pUC19-8, the signal intensity was comparable in *S. pombe* and *S. cerevisiae* (Fig. 11A), and an exact quantification of the signals revealed a slight enrichment of 1.6-fold in *S. pombe* (Fig. 11B). In contrast, shuttle plasmid *PHO5*-pUC19-10 clearly gave a higher signal intensity in *S. pombe* compared to *S. cerevisiae*, and additionally a second band above the main plasmid band was visible in *S. pombe*. Using only the main plasmid band for quantification gave an enrichment of 4.7-fold in *S. pombe* compared to *S. cerevisiae*, including the second band for quantification gave a 6.3-fold enrichment. Further, the copy number of plasmid *PHO5*-pUC19-10 was higher than the copy number of plasmid *PHO5*-pUC19-8 in *S. pombe* (Fig. 11A and B).

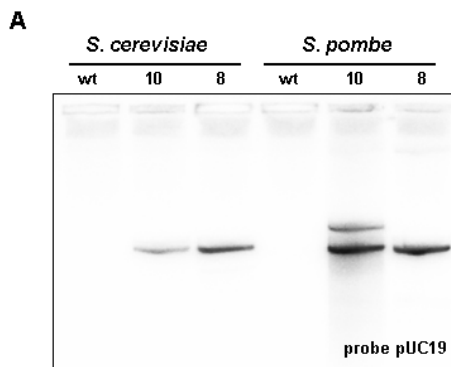


**Fig. 11: Copy number analysis of the two shuttle plasmids *PHO5*-pUC19-8 and *PHO5*-pUC19-10 in *S. pombe* and *S. cerevisiae*.**

(A) DNA was isolated from wt and transformed *S. pombe* and *S. cerevisiae* cells. Plasmid copy number was analyzed by Southern blot hybridized with the probe pUC19. (B) Comparative quantification of Southern blot signals.

**B**

	main band of plasmid <i>PHO5</i> -pUC19-10 in <i>S. pombe</i>	both bands of plasmid <i>PHO5</i> -pUC19-10 in <i>S. pombe</i>
<i>S. pombe</i> ( <i>PHO5</i> -pUC19-10)/ <i>S. pombe</i> ( <i>PHO5</i> -pUC19-8)	1.5	1.9
<i>S. cerevisiae</i> ( <i>PHO5</i> -pUC19-10)/ <i>S. cerevisiae</i> ( <i>PHO5</i> -pUC19-8)	0.5	---
<i>S. pombe</i> ( <i>PHO5</i> -pUC19-10)/ <i>S. cerevisiae</i> ( <i>PHO5</i> -pUC19-10)	4.7	6.3
<i>S. pombe</i> ( <i>PHO5</i> -pUC19-8)/ <i>S. cerevisiae</i> ( <i>PHO5</i> -pUC19-8)	1.6	1.6

The higher copy number of plasmid *PHO5*-pUC19-10 compared to plasmid *PHO5*-pUC19-8 in *S. pombe* could explain its higher transcript level observed by Northern blot analysis. However, the large difference in RNA transcript levels of the pUC19 and *PHO5* promoter plasmid regions between *S. pombe* and *S. cerevisiae* could probably not just be explained by the different plasmid copy numbers. Especially for shuttle plasmid *PHO5*-pUC19-8, the differences of RNA transcript levels between *S. pombe* and *S. cerevisiae* (5.9 to 6.4-fold enrichment in *S. pombe* compared to *S.*

*cerevisiae*) were much more pronounced than differences in copy number (1.6-fold enrichment in *S. pombe* compared to *S. cerevisiae*).

A more likely explanation for the higher transcription levels of plasmid regions in *S. pombe* is a read-through from the *S. cerevisiae URA3* marker on the shuttle plasmids. This read-through could be observed on both shuttle plasmids independently of the orientation of the *PHO5* promoter. Auxotrophic *S. pombe* cells can use the *S. cerevisiae URA3* marker gene despite the heterologous promoter to survive in uracil depleted medium but they seem to transcribe beyond the transcription termination sites of the *URA3* region, which appear to be heterologous, too. A read-through effect from the *URA3* gene in *S. pombe* is supported by several arguments: First, the hybridizations with all three probes recognizing plasmid transcripts, i.e. pUC19, *PHO5* promoter, and *URA3*, gave the same RNA pattern of three different bands in the Northern blot. Second, the three bands of RNA were relatively large in size, which could be explained by the 10 kb length of the shuttle plasmid leading to long transcripts if read-through occurs. Third, the RNA pattern appeared more smeary for RNAs transcribed from the shuttle plasmids than from other genomic regions, such as the actin transcripts. This could be explained by different sites at which transcription terminates, thereby leading to different transcript lengths.

In summary, it is still not clear if the different nucleosome positioning patterns at one and the same DNA sequence in *S. pombe* and *S. cerevisiae* were due to different nucleosome positioning mechanisms or were a consequence of different transcriptional activities. In the two evolutionary far diverged yeasts, regulatory regions are usually not compatible, e.g. *S. pombe* promoters<sup>[52]</sup> or replication origins<sup>[108]</sup> generally cannot be used by *S. cerevisiae* and vice versa. It may be difficult to find a locus that behaves equally in terms of transcription level in the two yeasts.

### 3.2 Genome-wide nucleosome occupancy map of *S. pombe*

In order to understand which factors determine nucleosome positioning, it was mandatory to first get a descriptive view of the nucleosome organization in *S. pombe*. Therefore, a method was developed to map nucleosomes genome-wide in *S. pombe*<sup>[92]</sup>. Several replicates of mononucleosomal DNA sample, obtained by digestion of chromatin with MNase, and of genomic DNA, serving as input control, were prepared from *S. pombe* wt cells and hybridized to an *S. pombe* tiling array (Tab. 1). The tiling array was comprised of 1.2 million probes of 25 bp tiled for both strands of the complete *S. pombe* genome and had a resolution of 20 bp. The raw signals obtained from hybridization were normalized, and the nucleosome occupancy was calculated as log<sub>2</sub>-ratio of mononucleosomal to genomic DNA signals.

During the development of the method it became clear that further DNaseI fragmentation of the mononucleosomal DNA to a fragment size of around 50 bp before hybridization was mandatory to obtain an accurate nucleosome occupancy map. Omitting this step caused a shift of nucleosomal peaks by half a nucleosome in comparison to the DNaseI fragmented mononucleosomal DNA sample (Fig. 12), and the peaks did not correlate with nucleosome positions mapped by indirect end-labeling. The effect of DNA fragment size on the array signal was also described by others, who reported a ~2-fold greater hybridization efficiency for the ends than for the mid points of full-length (~150 bp) mononucleosomal DNA fragments [176]. A possible explanation for this might be a steric effect caused by the relatively short length of oligonucleotides on the tiling array.

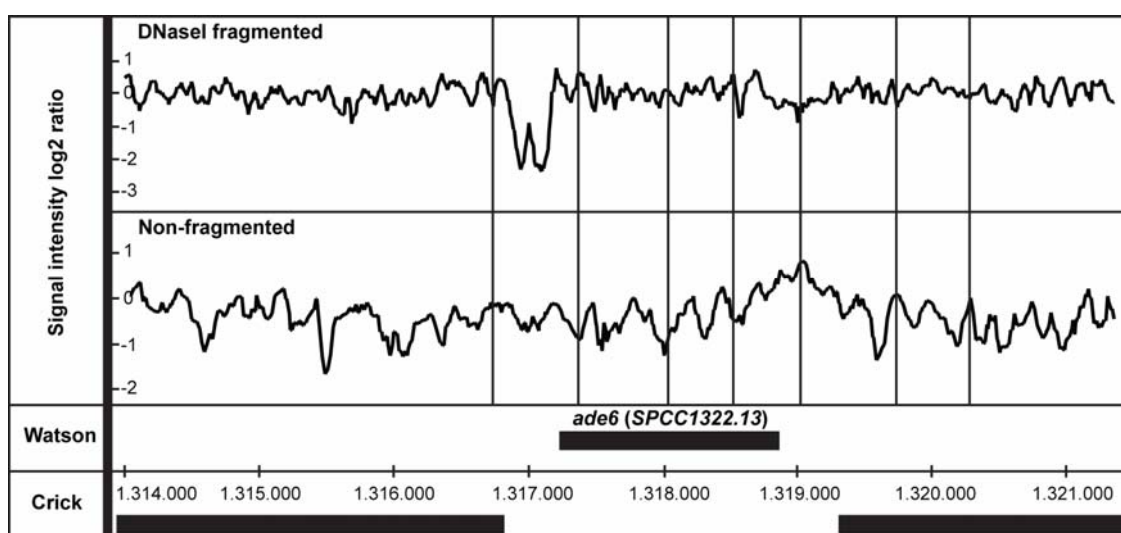
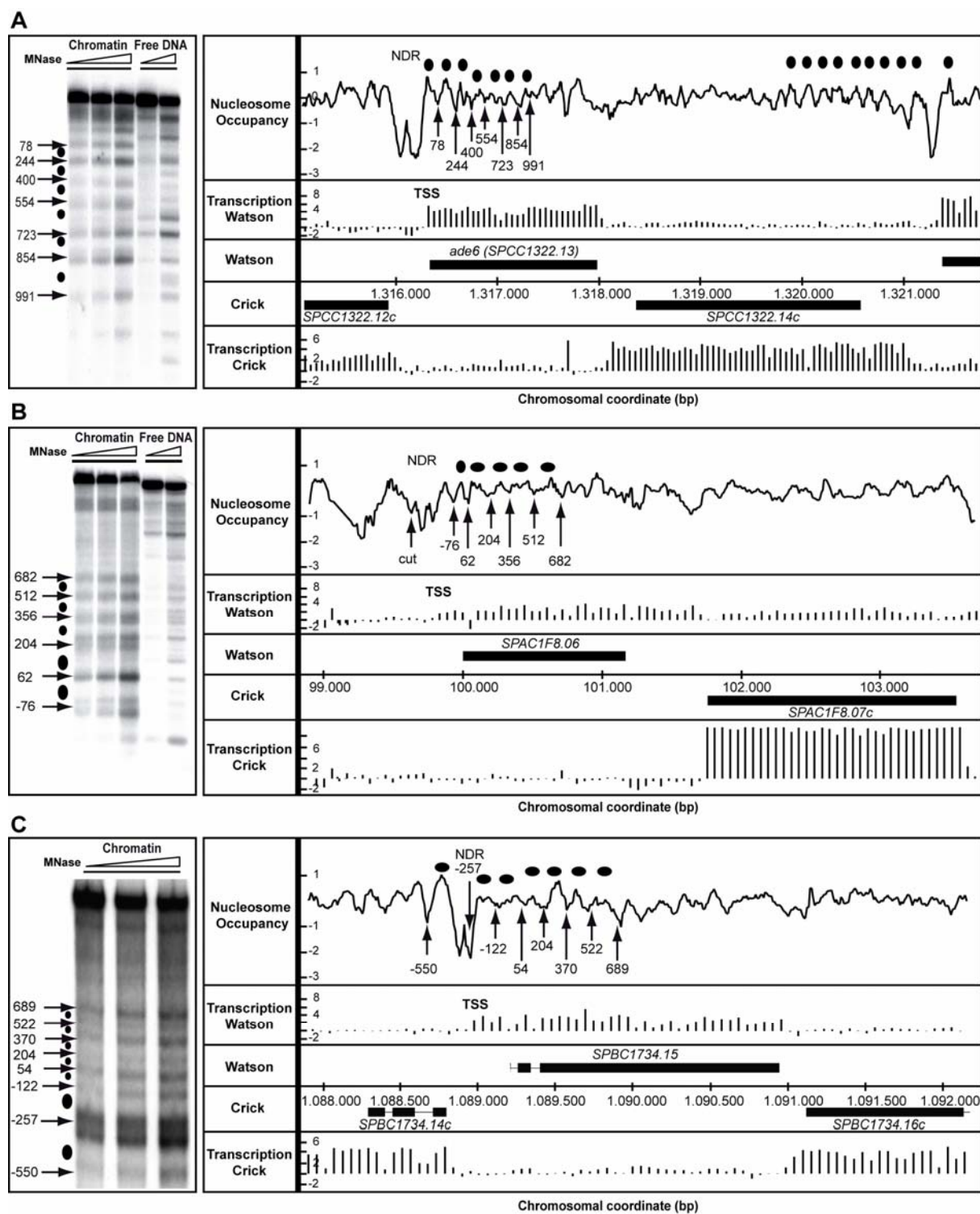


**Fig. 12: Comparison of hybridization data for DNaseI fragmented and non-fragmented mononucleosomal DNA at the *ade6* locus.**

The y-axis displays the signal intensity calculated as  $\log_2$  ratio for the average of three replicates of non-fragmented mononucleosomal DNA and of DNaseI fragmented mononucleosomal DNA to four replicates of genomic DNA signals. Examples of prominent differences in the hybridization profiles are indicated by thin vertical lines.

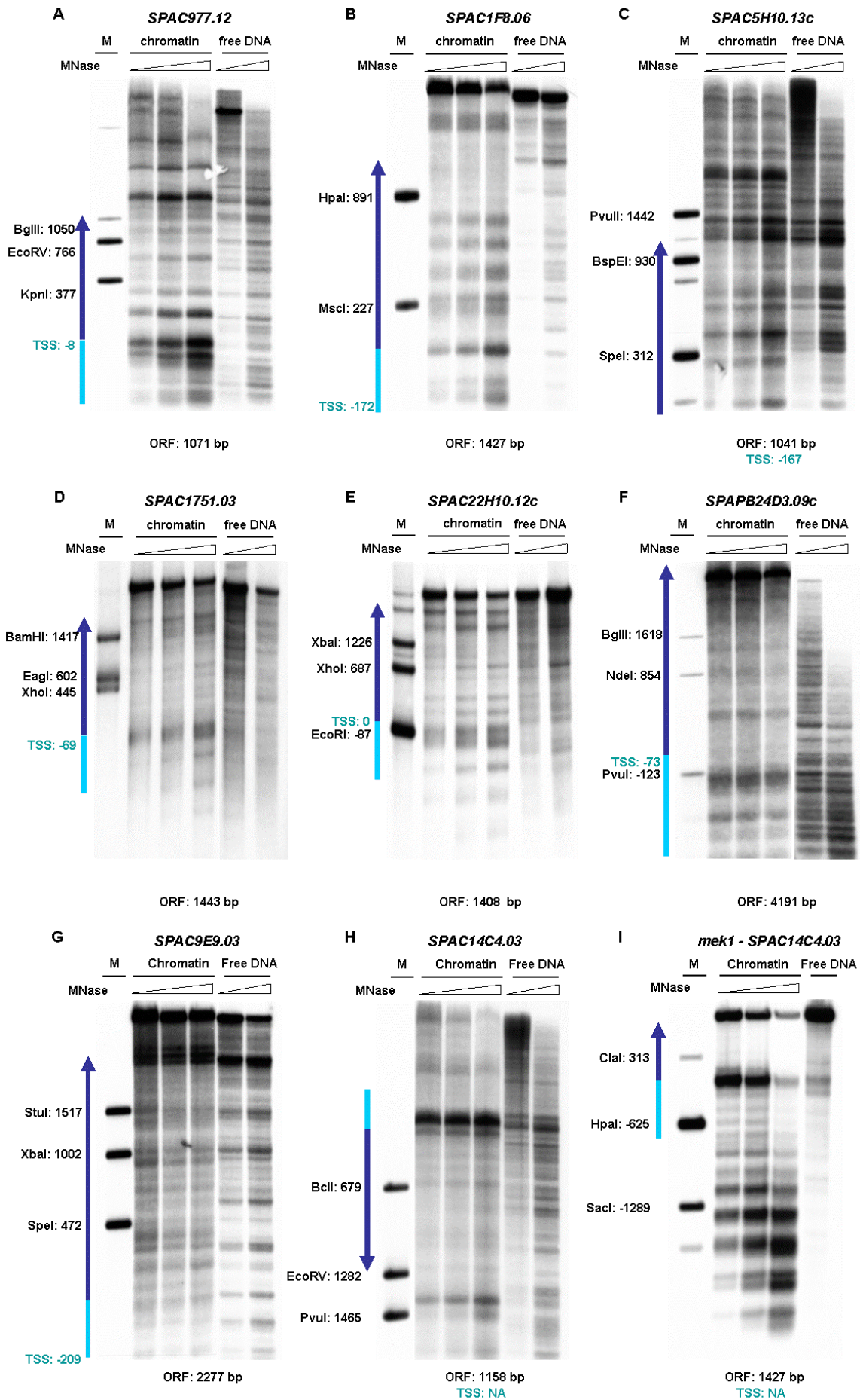
The nucleosome occupancy map revealed a pattern of peaks and troughs with peaks of a width of around 150 bp representing nucleosomes, and small troughs in between representing linker regions. Also very deep and broad troughs, called NDRs, were observed (Fig. 13).

In order to validate the nucleosome occupancy map obtained by tiling array analysis, the chromatin structure of 19 individual loci was mapped by indirect end-labeling (Fig. 14). The positions of 154 indirect end-labeling bands representing linker regions were determined and compared to the positions of troughs in the nucleosome occupancy map (Tab. 3, Fig. 13). Allowing a variation of  $\pm 20$  bp for indirect end-labeling bands due to the lower resolution of the agarose gel compared to the tiling array, a very good correlation of 94%, with a variation of  $\pm 40$  bp an even better correlation of 99% was obtained (Tab. 3, Fig. 13).

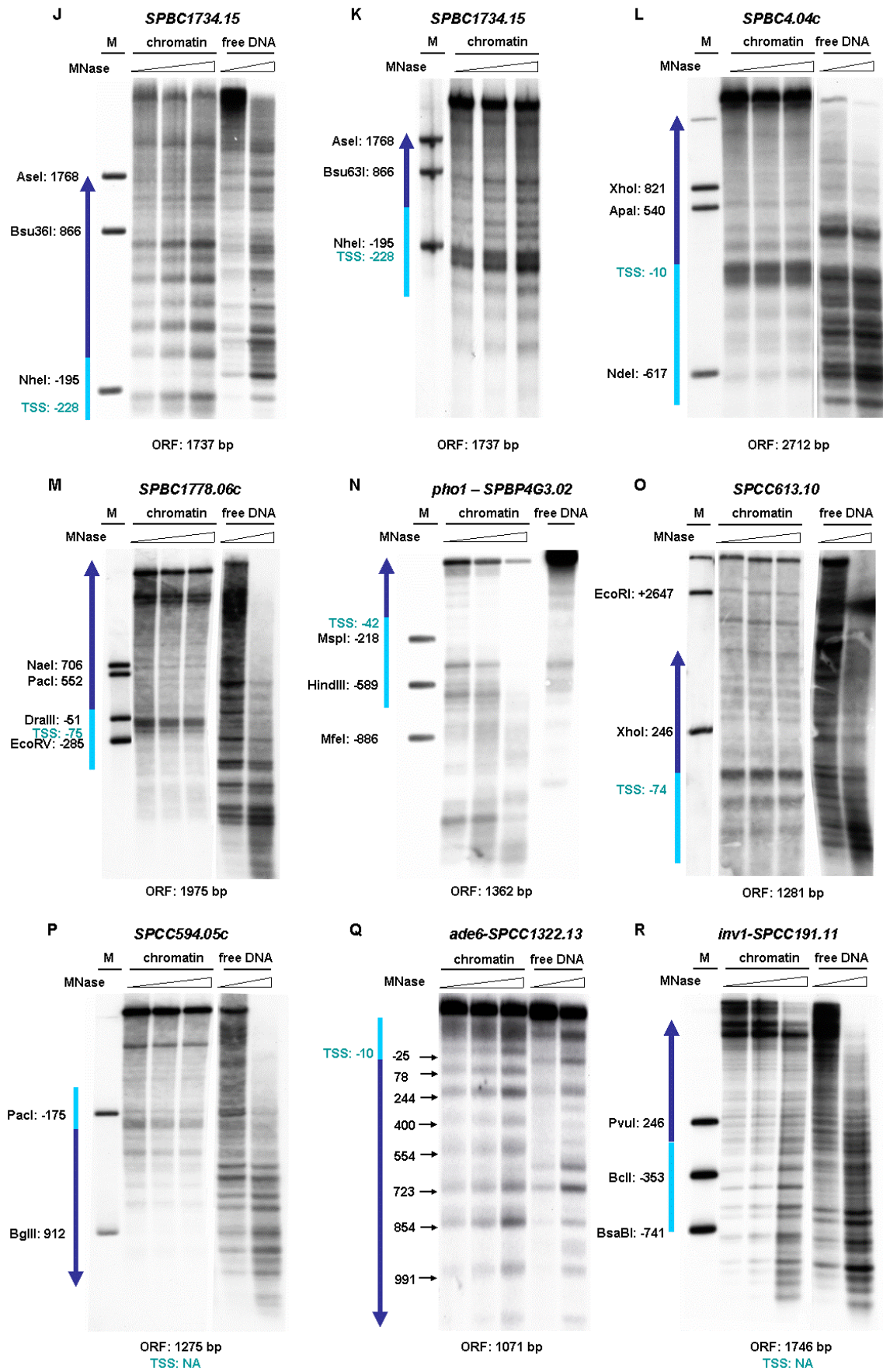


**Fig. 13: Good correlation between the nucleosome positioning patterns obtained by MNase indirect end-labeling (left) and tiling array analysis (right), as shown for the three *S. pombe* loci *SPCC1322.13*, *SPAC1F8.06* and *SPBC1734.15*.**

NDRs coincide well with TSSs. The positions of the indirect end-labeling bands marked by arrows are given in bp relative to the ATG and were determined relative to size markers for the respective locus. Identical positions are marked by arrows in the nucleosome occupancy profile along the chromosomal coordinate. Coding regions are denoted by black boxes and black ovals illustrate positioned nucleosomes. Indirect end-labeling patterns for MNase digested chromatin and free DNA are shown (left). Ramps on top of the indirect end-labeling lanes indicate increasing MNase concentrations. Transcriptome data from Dutrow et al. [38] are given for the Watson and Crick strand. (A) *SPCC1322.13*. (B) *SPAC1F8.06*. (C) *SPBC1734.15*.







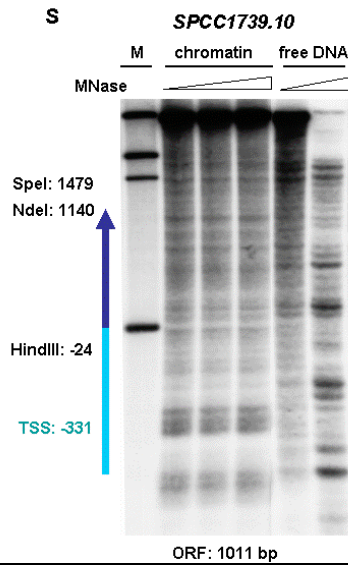


**Fig. 14: Mnase indirect end-labeling patterns of 19 *S. pombe* loci.** Indirect end-labeling patterns are shown for wt chromatin and for free DNA. The positions of the marker bands are given in bp relative to the ATG. Ramps on top of the indirect end-labeling lanes indicate increasing Mnase concentrations. The TSSs for the respective genes are given except if not available (NA). Graphical illustrations on the left represent the promoter (light blue) and the coding regions (dark blue) of the respective loci.

Gene	Chrom. coord.	Gene length (bp)	Secondary cleavage: cleavage site rel. to start codon	TSS rel. to start codon	TTS rel. to stop codon	Marker bands rel. to start codon	Number of bands	Bands coinciding with troughs	
								+/-20 bp	+/-40 bp
SPAC977.12	57269-60157	1071	XbaI: -482	-8	148	KpnI: +377 EcoRV: +766 BglII: +1050	7	7	7
SPAC1F8.06 (fta5)	100835-101699	1158	BglII: -376	-172	485	MscI: +227 HpaI: +891	6	6	6
SPAC5H10.13c (gmh2)	168716-170486	1041	XhoI: -165	-167	NA	SpeI: +312 BspEI: +930 PvuII: +1442	9	7	9
SPAC1751.03	386614-389247	1443	EcoRV: -1037	-69	30	XhoI: +445 EagI: +602 BamHI: +1417	10	10	10
SPAC22H10.12c (gdi1)	2394660-2398219	1408	PvuII: -1007	0	261	EcoRI: -87 XhoI: +687 XbaI: +1226	9	9	9
SPAPB24D3.09c (pdr1)	2967335-2968414	4191	PvuII: -745	-73	135	PvuI: -123 NdeI: +854 BglII: +1618	5	5	5
SPAC9E9.03 (leu2)	4441082-4442159	2277	EcoRI: -321	-209	102	SpeI: +472 XbaI: +1002 StuI: +1517	8	8	8
SPAC14C4.03 (mek1)	5230544-5231930	1427	XbaI: -2000	NA	NA	SacI: -1289 HpaI: -625 ClaI: 313	9	9	9
SPAC14C4.03 (mek1)	5231894-5233477	1427	SmaI: +1800	NA	NA	PvuI: +1465 EcoRV: +1282 BclI: +679	7	7	7
SPBC1734.15 (rsc4)	1089299-1090777	1737	SpeI: -1285	-228	16	NheI: -195 Bsu63I: +866 AseI: +1768	7	6	7
SPBC1734.15 (rsc4)	1089820-1091484	1737	XbaI: -464	-228	16	NheI: -195 Bsu36I: +866 AseI: +1768	9	9	9
SPBC4.04c (mcm2)	1193989-1195628	2712	BamHI: -996	-10	82	NdeI: -617 ApaI: +540 XhoI: +821	10	10	10
SPBC1778.06c (fim1)	3109400-3111093	1975	XbaI: -1191	-75	259	EcoRV: -285 DraIII: -51 PacI: +552 NaeI: +706	10	9	10
SPBP4G3.02 (pho1)	4448159-4449886	1362	MscI: -1456	-42	81	MfeI: -886 HindIII: -633 MspI: -218	6	4	6
SPCC613.10	96478-99101	1281	NdeI: -867	-74	0	XhoI: +245 EcoRI: +2647	8	7	8
SPCC594.05c (spf1)	364640-367234	1275	XbaI: +1329	NA	NA	BglII: +912 PacI: -175	12	11	11
SPCC1322.13 (ade6)	1317288-1318234	1659	XhoI: +1466	-10	0	-----	7	6	7
SPCC191.11 (inv1)	1724335-1725963	1746	BglII: -1189	NA	NA	BsaBI: -741 BclI: -353 PvuI: +246	8	8	8
SPCC1739.10 (mug33)	2048320-2049499	1011	EcoRI: -815	-331	201	HindIII: -24 NdeI: +1140 SpeI: +1479	7	7	7
Sum							154	145	153
Percent							100%	94%	99%

**Tab. 3: Validation of the nucleosome occupancy map obtained by tiling array analysis by comparison with indirect end-labeling chromatin patterns.**

Individual examples of *S. cerevisiae* genes were shown to have an NDR over their promoter region upstream of the TSS residing within the +1-nucleosome [93, 94, 192]. To see if *S. pombe* genes have a similar promoter architecture, nucleosome occupancy data were compared to RNA transcript data [38]. Single gene comparisons showed a similar result for *S. pombe* (Fig. 13 and Fig. 15), i.e. an NDR over the promoter, and the TSS being localized within the +1-nucleosome. Even for genes with long untranslated regions (UTRs) at the 5' region such patterns were observed (Fig. 15).

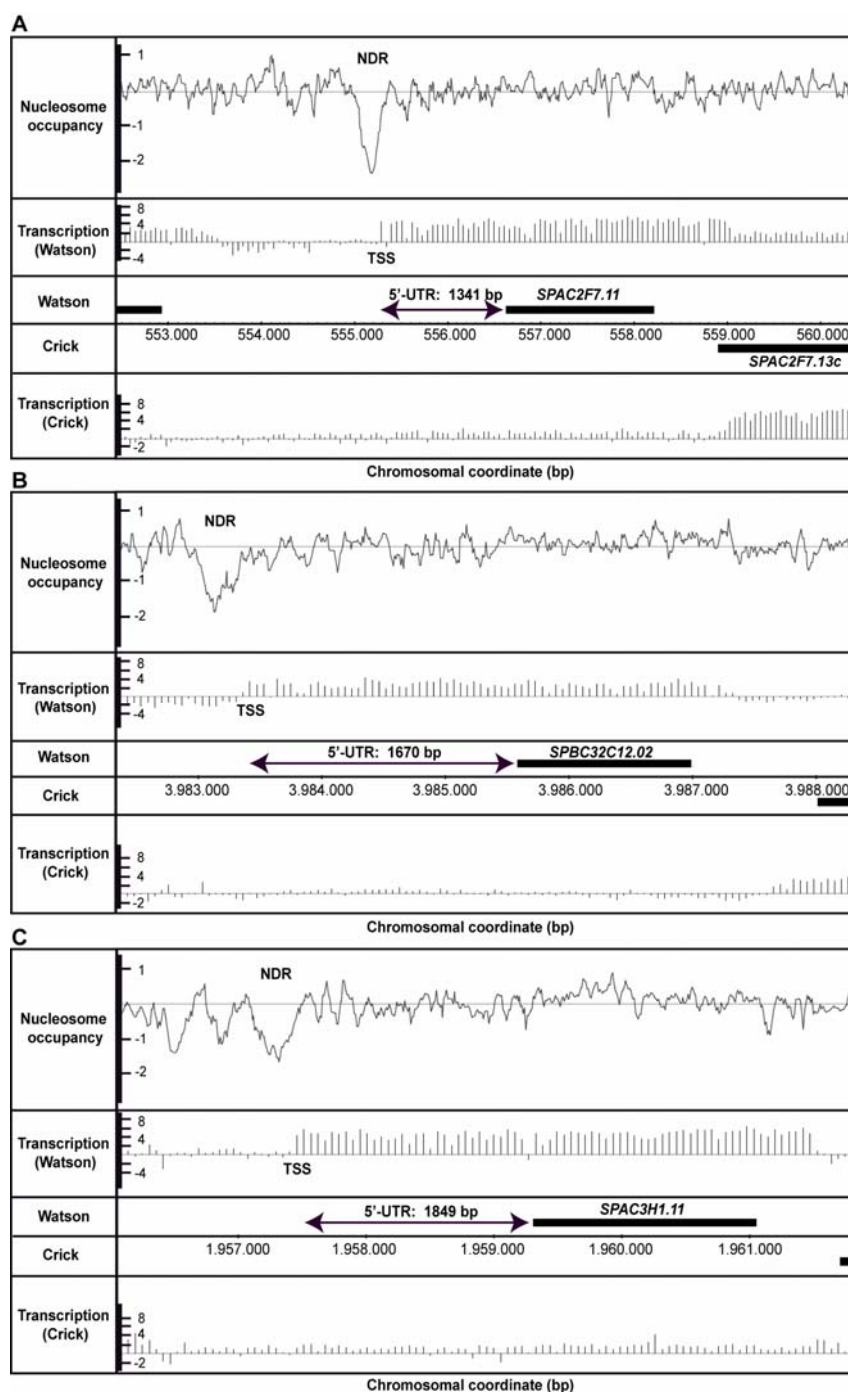


**Fig. 15: Even at genes with long 5'-UTRs NDRs coincide with annotated TSS.**

Nucleosome occupancy data and transcriptome data [38] for the Watson and Crick strand at three genomic regions were plotted as in Fig. 13. Coding regions are denoted by black boxes above the chromosomal coordinate. The 5'-UTR is indicated by double headed arrows. (A) *SPAC2F7.11*. (B) *SPBC32C12.02*. (C) *SPAC3H1.11*.

The promoter organization observed for individual *S. cerevisiae* genes appeared to be stereotypical, since an alignment of nucleosome occupancy data of many *S. cerevisiae* genes at their TSS showed the same pattern of a promoter NDR, flanked at both sides by positioned nucleosomes<sup>[94, 192]</sup>. To see if also an overlay of *S. pombe* nucleosome occupancy data after TSS-alignment generated such a stereotypical promoter pattern, both the TSS and the TTS were annotated for *S. pombe* using the RNA transcript map from Dutrow et al.<sup>[38]</sup>. The median 5' UTR length of 4013 genes was 85 bp and the median 3' UTR length of 3925 genes was 149 bp (Fig. 16). The median UTR length of both 5'- and 3'UTRs was longer than in *S. cerevisiae*, where the median 5' UTR was 68 bp and the median 3' UTR was 91 bp in length<sup>[32]</sup>.

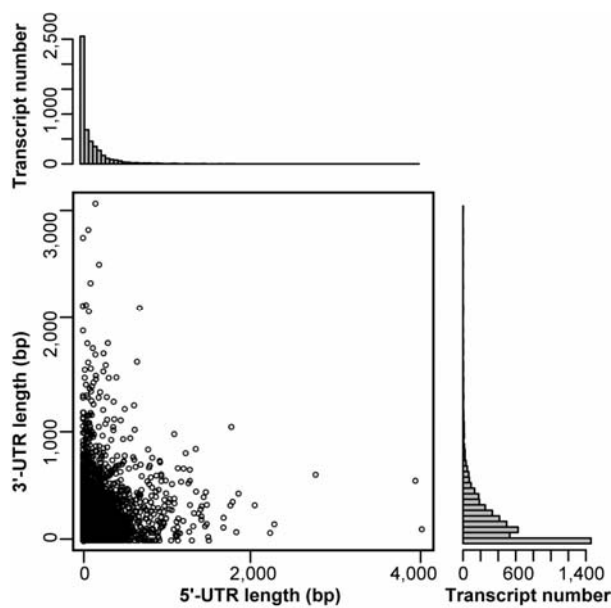


**Fig. 16: Distribution of 5' and 3' UTR lengths in *S. pombe* genes.**

The transcriptome data of Dutrow et al.<sup>[38]</sup> were used for the annotation of TSS of 4013 genes and TTS of 3925 genes. The median 5'-UTR of *S. pombe* transcripts was 85 bp, the median 3'-UTR length was 149 bp.

The TSS-aligned overlay of nucleosome occupancy data of 4013 *S. pombe* genes gave a similar stereotypical promoter pattern for *S. pombe* compared to *S. cerevisiae*<sup>[94]</sup>, with an NDR over the promoter and a well positioned +1-nucleosome followed by a regular nucleosomal array in the downstream direction over the gene body (Fig. 17).

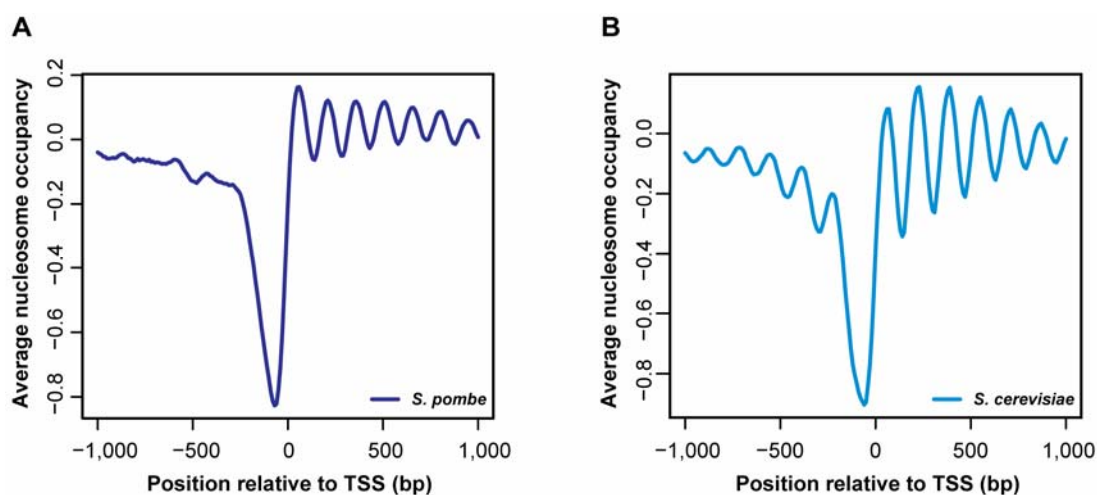


**Fig. 17: Alignment of nucleosome occupancy profiles at the TSS revealed a prominent NDR upstream and a regular nucleosomal array downstream of the TSS of *S. pombe* and *S. cerevisiae* genes.**

(A) Overlay of nucleosome occupancy profiles of 4013 *S. pombe* genes after TSS-alignment. (B) As A, but for 5838 *S. cerevisiae* genes.

An overlay of nucleosome occupancy data at the TTS showed an NDR at the end of genes downstream of the TTS in *S. pombe* and *S. cerevisiae* (Fig. 18), but this NDR was much less pronounced than promoter NDRs (compare to stippled lines representing TSS-aligned overlay of nucleosome occupancy profiles). For *S. cerevisiae* and *Drosophila*, an NDR at gene ends was described before, and in addition a positioned nucleosome upstream of this NDR was reported [110, 148]. A positioned nucleosome at gene ends could neither be observed after TTS-alignment of *S. pombe* nor *S. cerevisiae* nucleosome occupancy data [94].

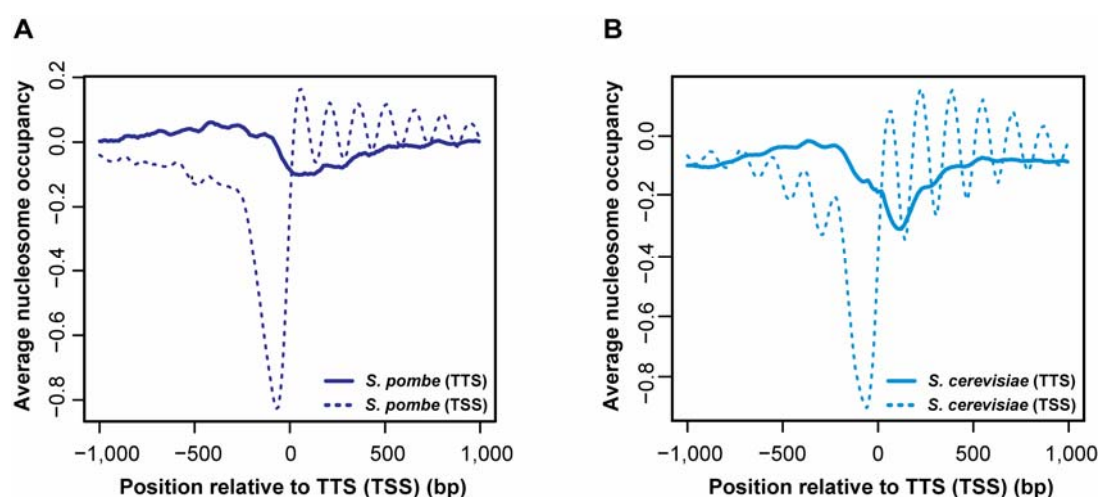


**Fig. 18: Alignment of nucleosome occupancy profiles at the TTS revealed an NDR at gene ends both for *S. pombe* and *S. cerevisiae*.**

(A) Overlay of nucleosome occupancy profiles of 3925 *S. pombe* genes after alignment at the TTS. Stippled lines indicate TSS-aligned overlay of nucleosome occupancy profiles (Fig. 17). (B) Same as in A, but for 5015 *S. cerevisiae* genes.

### 3.3 Nucleosome occupancies vary at different genomic regions

It was shown for *S. cerevisiae* that the nucleosome occupancies vary at different genomic regions. For example, intergenic regions were depleted of nucleosomes compared to genic regions<sup>[94]</sup>. For *S. pombe* the analysis of nucleosome occupancies at different genomic regions also gave a higher nucleosome occupancy for genic regions (TSS to TTS, red) than for intergenic regions (blue). This is probably due to the presence of NDRs at 5' and 3' regions of genes. Accordingly, promoter regions from -200 to TSS (green) show on average the lowest nucleosome occupancy probably due to the very prominent NDR over promoters (Fig. 19).

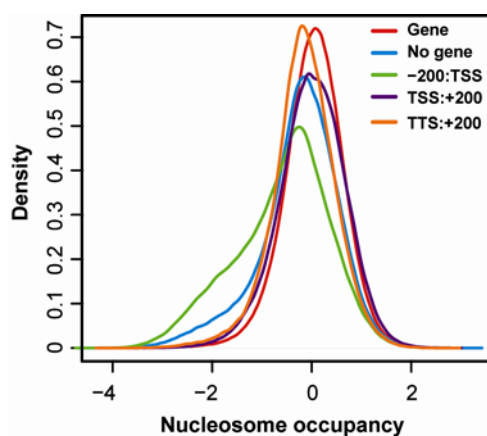


**Fig. 19: Nucleosome occupancy is higher in genic than in intergenic regions.**

Distribution of nucleosome occupancy for probes clustered according to their location within or outside of genes, upstream (-200 to 0 bp relative to TSS) or downstream (0 to +200 bp from TSS) of TSS, and downstream of TTS (0 to +200 bp from TTS).

In *S. cerevisiae*, replication origins were reported to be depleted of nucleosomes<sup>[46, 109]</sup>. Also in *S. pombe*, replication origins, mapped by Heichinger et al.<sup>[62]</sup>, were nucleosome depleted. This effect was of a different quality compared to promoter NDRs, since the NDR trough was much less pronounced (Fig. 20A; note the scale of the y-axis). In order to analyze if nucleosome occupancy correlated with origin efficiency, *S. pombe* replication origins were divided into two groups of high efficiency (50% of origins above the median efficiency) and low efficiency (50% of origins below the median efficiency), respectively. Indeed, origins of high efficiency were more depleted of nucleosomes than origins of low efficiency (p-value < 2.2 e-16, two-sided Wilcox test) (Fig. 20A and B)<sup>[46]</sup>. These findings confirmed an earlier study in which a model trained on *in vivo* nucleosome occupancy data from *S. cerevisiae* also predicted a higher degree of nucleosome depletion over origins of high efficiency than over origins of low efficiency. Although the observed effects were small, competition between nucleosomes and factors for DNA access might be one mechanism to influence replication origin efficiency.

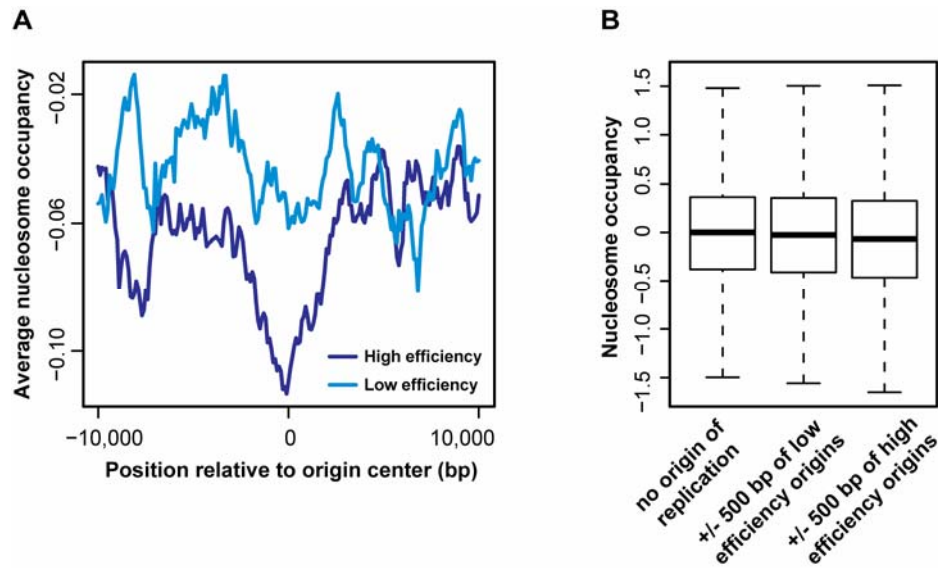


**Fig. 20: Lower nucleosome occupancy around high efficiency origins than around low efficiency origins.** (A) Overlay of nucleosome occupancy profiles after alignment at the center of high and low efficiency replication origins. (B) Box plot analysis of nucleosome occupancy in a 1 kb window around high and low efficiency origins of replication compared to nucleosome occupancy in all genomic regions without replication origins (p-value < 2.2 e-16, two-sided Wilcox test).

### 3.4 Low nucleosome occupancy at promoters tends to correlate with high gene expression level

Nucleosomes are often implicated with a repressive function as they are thought to compete with other factors for access to the DNA. For *S. cerevisiae*, it was reported that gene expression at promoters correlated inversely with nucleosome occupancy, and highly expressed genes were shown to contain more prominent NDRs than genes expressed at low levels [14, 192]. To look for such a correlation between promoter nucleosome occupancy and gene expression in *S. pombe*, genes were clustered on the basis of nucleosome occupancy surrounding their TSS into six groups. The generated gene clusters were characterized by a prominent difference in the NDR pronunciation and the two clusters 2 and 6 with the least prominent NDRs displayed lower average expression levels than clusters 1, 3, 4 and 5 with well pronounced NDRs (Fig. 24A-C). The same was true when the analysis was performed the other way round, i.e. genes were first grouped according to their steady state expression levels, and then the average promoter nucleosome occupancy was calculated for the different groups. Also here higher average expression correlated with lower promoter nucleosome occupancy and vice versa (Fig. 21A) and this was confirmed for *S. cerevisiae* using data from Lee et al. (Fig. 21B) [94]. However, a gene-by-gene comparison of the nucleosome occupancy at promoters to the steady state expression level revealed only a very poor correlation (Fig. 21C, E). Mainly silent genes of *S. pombe* usually showed high nucleosome occupancy at promoters and followed the trend (Fig. 21C). Also the

correlation of promoter nucleosome occupancy with RNA polymerase II occupancy, which should not be effected by posttranscriptional processes and therefore may represent chromatin effects better than steady state RNA expression level, was only poor (Fig. 21D). This reflects that the trend of averages does not necessarily need to apply on a single gene basis. RNA expression level or RNA polymerase II occupancy cannot be predicted accurately by nucleosome occupancy at promoters and vice versa.

No correlation was found between the nucleosome occupancy over coding regions and the gene expression levels (Fig. 21F). This was in contrast to *S. cerevisiae*, where highly expressed genes seemed to have higher nucleosome occupancy in coding regions<sup>[94]</sup>.

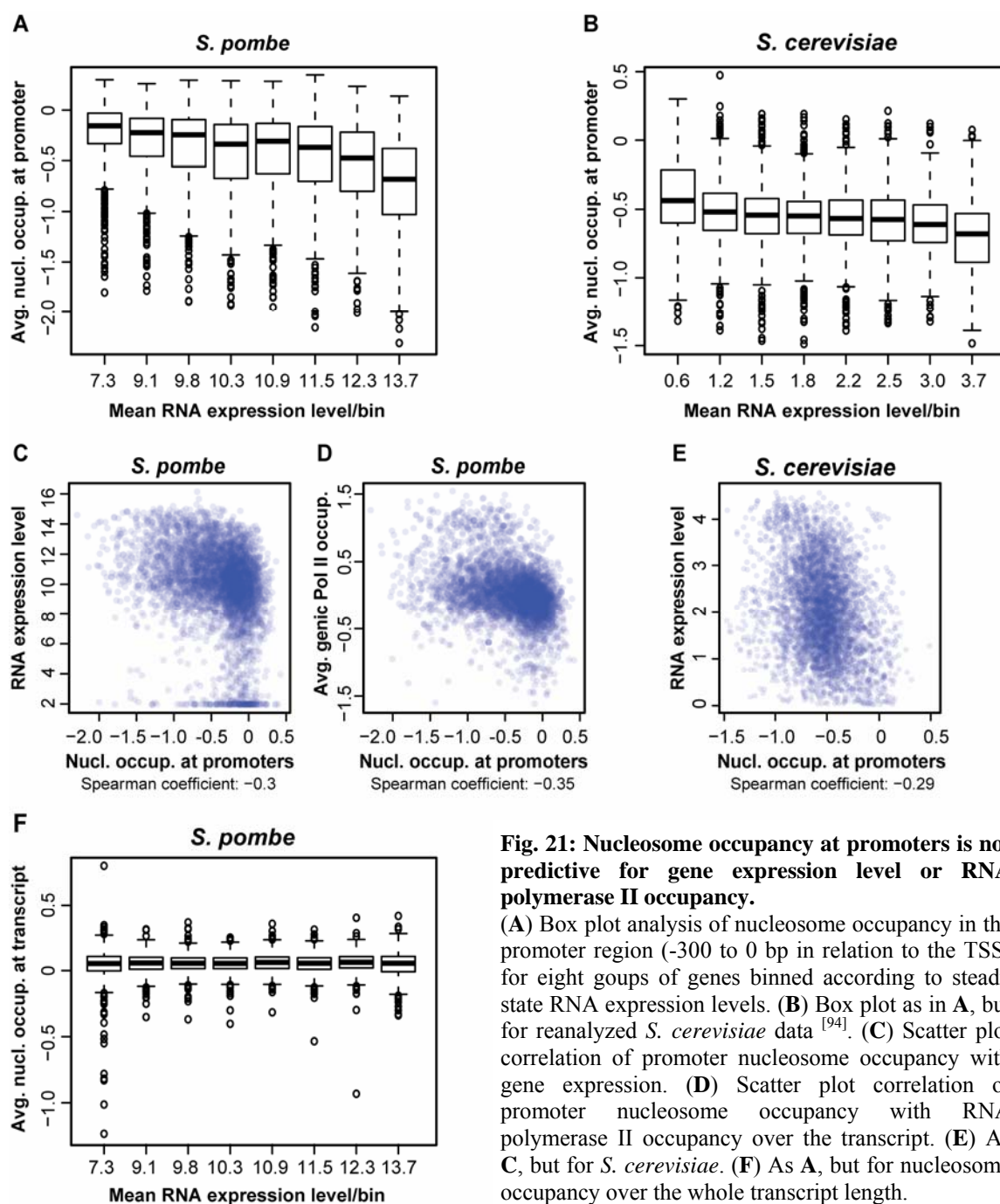


**Fig. 21: Nucleosome occupancy at promoters is not predictive for gene expression level or RNA polymerase II occupancy.**

(A) Box plot analysis of nucleosome occupancy in the promoter region (-300 to 0 bp in relation to the TSS) for eight groups of genes binned according to steady state RNA expression levels. (B) Box plot as in A, but for reanalyzed *S. cerevisiae* data<sup>[94]</sup>. (C) Scatter plot correlation of promoter nucleosome occupancy with gene expression. (D) Scatter plot correlation of promoter nucleosome occupancy with RNA polymerase II occupancy over the transcript. (E) As C, but for *S. cerevisiae*. (F) As A, but for nucleosome occupancy over the whole transcript length.



### 3.5 Nucleosome spacing is different in *S. pombe* and *S. cerevisiae*

A direct comparison of TSS-aligned overlays of nucleosome occupancy for *S. pombe* and *S. cerevisiae* revealed an identical average distance between the TSS and the +1-nucleosome. With regard to the frequency of the nucleosomal arrays, this analysis revealed an interesting difference in *S. pombe* compared to *S. cerevisiae*. The average distance between the nucleosomal peaks is called spacing or nucleosome repeat length (NRL) and was shorter in *S. pombe* than in *S. cerevisiae* (Fig. 22A). A valuable tool for the analysis of genome-wide data sets is the spectral analysis, also called Fourier transformation, which allows searching a large data set for prominent and regularly recurring patterns along the genome. The application of the spectral analysis revealed a prominent frequency of 6.5 nucleosomes per 1000 bp for *S. pombe* translating to a NRL of 154 bp (Fig. 22B). For *S. cerevisiae*, this analysis revealed a frequency of 6 nucleosomes per 1000 bp which translates to a NRL of 167 bp (Fig. 22B) and confirms a reported NRL of 165 $\pm$ 5 bp<sup>[94, 109, 162]</sup>. The shorter spacing was also confirmed by MNase ladder analysis, where the tetranucleosomal band of *S. pombe* was slightly smaller compared to *S. cerevisiae* as marked by asterisks (Fig. 22C).

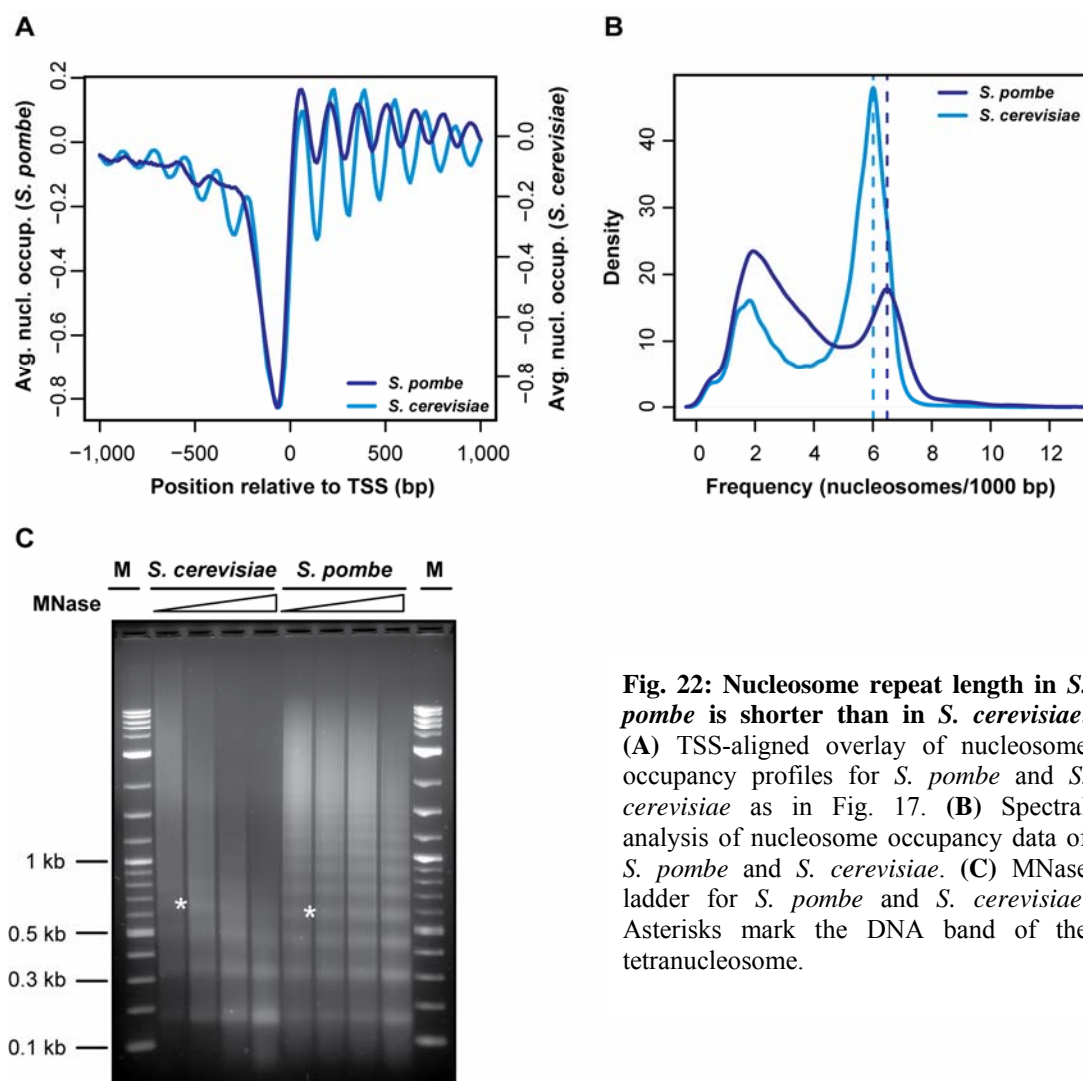


**Fig. 22: Nucleosome repeat length in *S. pombe* is shorter than in *S. cerevisiae*.** (A) TSS-aligned overlay of nucleosome occupancy profiles for *S. pombe* and *S. cerevisiae* as in Fig. 17. (B) Spectral analysis of nucleosome occupancy data of *S. pombe* and *S. cerevisiae*. (C) MNase ladder for *S. pombe* and *S. cerevisiae*. Asterisks mark the DNA band of the tetranucleosome.

For the majority of the data analyses, redundant probes were omitted, since signals arising from these probes cannot be assigned unambiguously to the correct genomic region and could obscure nucleosome occupancy signals. However, for the analysis of heterochromatic regions, which are highly enriched in repetitive DNA sequences, redundant probes were included. This was necessary to implement sufficient data points into the analysis. On the other hand, removing these probes would have led to an interrupted data set at heterochromatic regions, thereby preventing spectral analysis. Heterochromatic regions were defined by the enrichment of the heterochromatic H3K9 dimethyl mark using data from Cam et al. [26]. Spectral analysis of these heterochromatic regions revealed a spacing of 6.1 nucleosomes per 1000 bp, translating to a NRL of 164 bp, compared to 6.5 nucleosomes per 1000 bp (NRL: 154 bp) in euchromatin (Fig. 23A). This result was confirmed by box plot analysis revealing lower nucleosome occupancy for heterochromatin than for euchromatin (Fig. 23B).

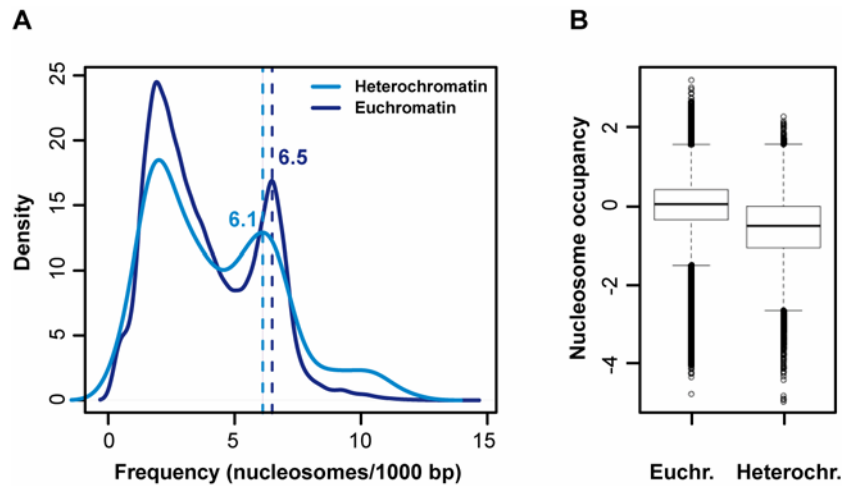


**Fig. 23: Heterochromatic regions of *S. pombe* display wider spacing and lower nucleosome occupancy than euchromatic regions.**

Heterochromatic regions were determined according to the presence of the H3K9 dimethyl mark <sup>[26]</sup>. Redundant probes reflecting repetitive sequences were included into heterochromatin analysis. **(A)** Spectral analysis for heterochromatic and euchromatic regions. **(B)** Box plot analysis for euchromatic and heterochromatic regions.

### 3.6 No pronounced regular nucleosomal arrays upstream of TSSs in *S. pombe*

The TSS-aligned overlay of nucleosome occupancy for *S. pombe* and *S. cerevisiae* (Fig. 22A) revealed yet another difference between the chromatin organization in *S. pombe* and *S. cerevisiae*: the lack of a positioned -1-nucleosome and of a regular nucleosomal array upstream of the NDR in *S. pombe*. However, regularly positioned nucleosomes could be present on the level of individual genes or within subgroups of genes, but might occur with different registers. In the overlay pattern of more than 4000 *S. pombe* genes this would obscure nucleosomal arrays. A valuable approach to search for such subgroups is to cluster genes on the basis of similar nucleosome occupancy patterns, thereby obtaining several subgroups of genes of characteristic nucleosome occupancy patterns. Therefore, genes were clustered according to similar nucleosome occupancy patterns around the TSS into six subgroups. This approach revealed a -1-nucleosome for a subset of gene clusters (1, 3, 4, 6) at different positions relative to the TSS (Fig. 24A and B). However, none of the *S. pombe* clusters showed a regular upstream nucleosomal array (Fig. 24A and B) whereas they were very prominent and almost symmetrical around the TSS in *S. cerevisiae* (Fig. 24D and E; cluster 2, 3, 4 and 5). In *S. pombe*, the nucleosome occupancy pattern around the TSS was more asymmetrical and only visible in the downstream direction of the TSS.

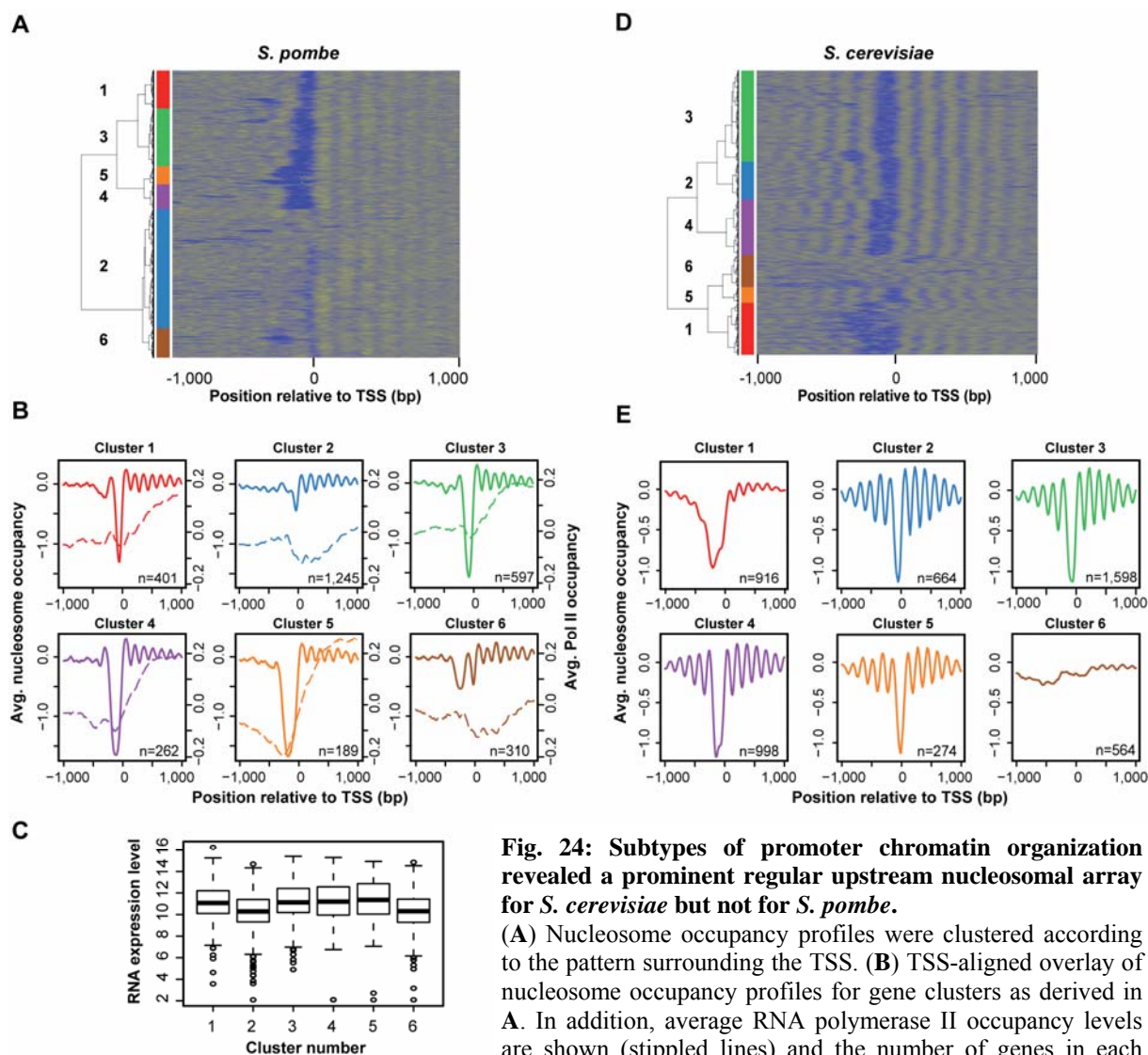


**Fig. 24: Subtypes of promoter chromatin organization revealed a prominent regular upstream nucleosomal array for *S. cerevisiae* but not for *S. pombe*.**

(A) Nucleosome occupancy profiles were clustered according to the pattern surrounding the TSS. (B) TSS-aligned overlay of nucleosome occupancy profiles for gene clusters as derived in A. In addition, average RNA polymerase II occupancy levels are shown (stippled lines) and the number of genes in each cluster (n) is given. (C) Box plot analysis of expression data for gene clusters as in A. (D and E) Analogous to A and B, but for *S. cerevisiae*.

The missing upstream nucleosomal arrays in *S. pombe* could be due to technical limitations, since the *S. pombe* tiling array used in this study had a lower resolution of 20 bp compared to the 4 bp resolution of the *S. cerevisiae* tiling array used by Lee et al. [94]. Therefore, *S. cerevisiae* nucleosome occupancy data of the same 20 bp resolution from another study were analyzed [192]. In general, lower array resolution compromises the amplitude of nucleosomal arrays (Fig. 22A). However, *S. cerevisiae* data with the lower resolution of 20 bp still revealed prominent regular upstream arrays (Fig. 25A). So the lack of regular upstream nucleosomal arrays was unlikely due to the lower resolution.

Another explanation for the lack of upstream nucleosomal arrays in *S. pombe* could be proximal upstream genes that disturb the upstream nucleosomal array of closely downstream localized genes. However, the median intergenic distance of 442 bp in *S. pombe* is even longer than in *S.*

*cerevisiae* with 366 bp. Also the alignment of *S. pombe* genes without an upstream gene within 1 kb showed no regular upstream array (Fig. 25B).

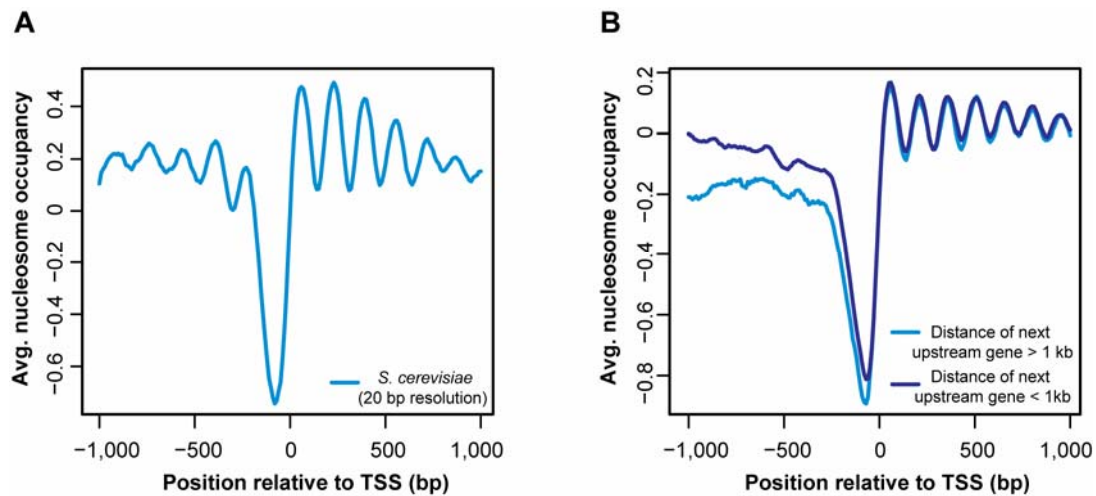


**Fig. 25: Lack of regular upstream nucleosomal arrays in *S. pombe* is neither due to lower resolution of the tiling array nor to proximal upstream genes.**

(A) TSS-aligned overlay of *S. cerevisiae* nucleosome occupancy data from Yuan et al.<sup>[192]</sup> revealed a regular upstream array even at a lower resolution of 20 bp. (B) TSS-aligned overlay of nucleosome occupancy data for *S. pombe* revealed no regular upstream array in *S. pombe* even for far distances (1 kb) of next upstream genes. 744 genes had a distance of more than 1 kb, 3269 genes had a distance of less than 1 kb to the next upstream gene.

### 3.7 Different trans-factors determine nucleosome positioning

#### 3.7.1 Transcription correlates with regular nucleosomal arrays

The process of transcription is often discussed to play a role in nucleosome positioning<sup>[124]</sup>. In this context, the cluster analysis revealed regular nucleosomal arrays only downstream of the TSS in *S. pombe*, but in both directions from the NDR in *S. cerevisiae* (Fig. 24B vs. E). Thus, in *S. pombe*, regular nucleosomal arrays were only visible in the direction of transcription over the gene bodies. Further arguments supported the role of transcription in nucleosome positioning in *S. pombe*.

First, the TSS-aligned RNA polymerase II occupancy profiles, as shown for the individual gene clusters of *S. pombe*, displayed polymerase enrichment over the region of the downstream nucleosomal array (Fig. 24B).

Second, if nucleosome occupancy data were aligned at all NDRs, as defined by HMM (see 2.9.6) instead of the TSS, regular nucleosomal arrays became visible neither in the downstream nor in the upstream direction. A regular nucleosomal array in the downstream direction became only

visible after alignment at promoter NDRs and only if the direction of transcription was considered (Fig. 26A). The alignment at the NDRs pronounced more the NDR depth whereas the alignment at the TSS revealed a more pronounced amplitude of the nucleosomal array. Also the alignment at the ATG, the translation start point, revealed a less pronounced amplitude of the nucleosomal array than the alignment at the TSS (Fig. 26B). In general, the distinctness of composite alignment patterns correlates with the relevance of the alignment point. The more distinct arrays after TSS alignment suggested that the transcription related point of alignment, the TSS, is more relevant for the formation of the regular array than the NDR or the ATG, which are not related to transcription.

Third, clustering genes according to their transcript length into four groups showed a good correlation between the transcript length and nucleosomal array extent (Fig. 26C).

Fourth, the alignment of silent genes showed almost no regular nucleosomal array formation compared to active genes. Due to the missing TSS information, the 262 silent genes were aligned at the ATG. In order to exclude that the lack of regular nucleosomal arrays was due to the smaller sample size of only 262 genes, two randomly selected sets of 262 active genes were included as comparison (Fig. 26D). Despite the smaller sample size these two randomly selected groups of active genes gave a regular nucleosomal array, arguing that the lack of regular nucleosomal arrays appears to be specific for silent genes. It is true for composite patterns in general, and was also observed here for both active and silent genes, that the sample size influences the ‘noisiness’ of the signal, i.e. small sample sizes appear ‘noisier’ than large sample sizes.

All these arguments supported a role of transcription in nucleosome positioning.

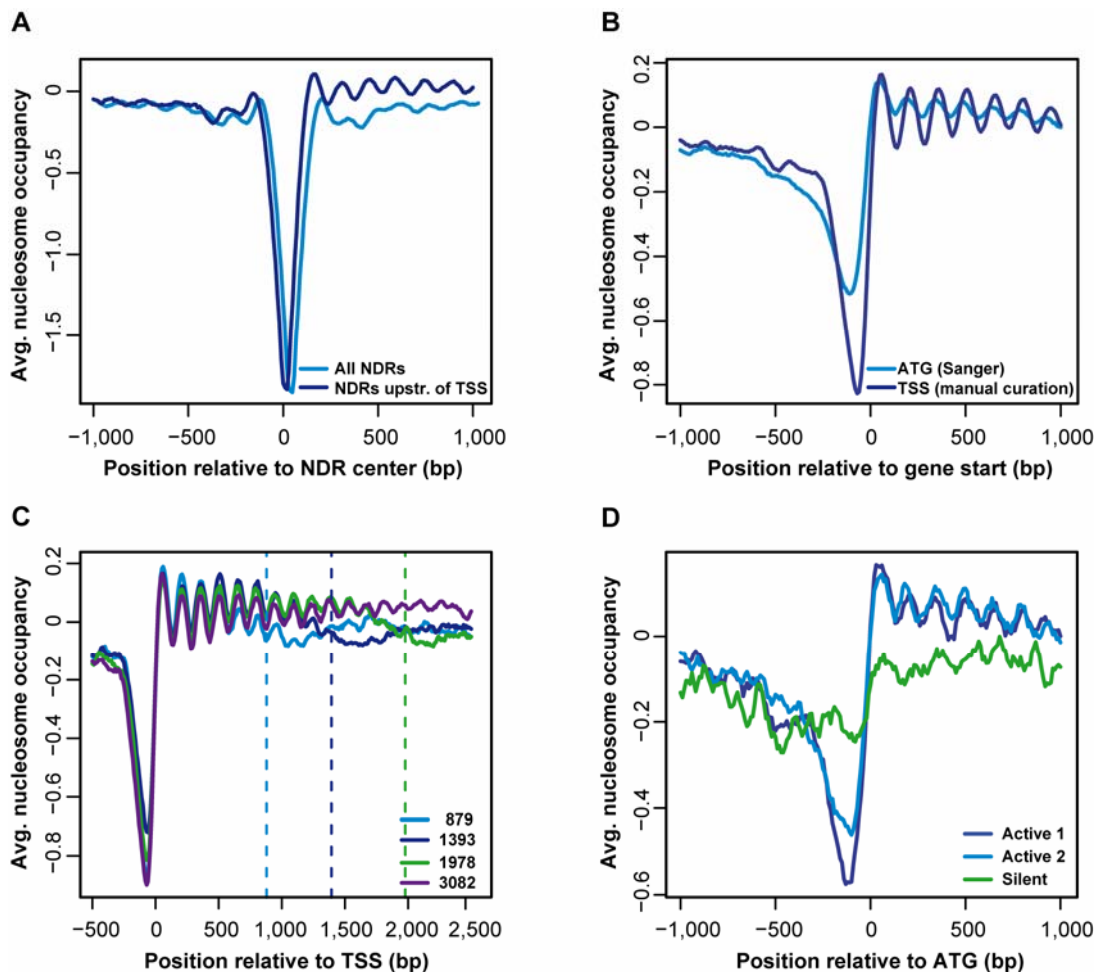


**Fig. 26: Regular nucleosomal arrays emanate from promoter NDRs mainly in the direction of transcription.**

(A) Overlay of nucleosome occupancy profiles after alignment at the center of all NDRs or only of promoter NDRs directly upstream of TSSs. (B) Overlay of nucleosome occupancy profiles after alignment at the start codon or the TSS. (C) Overlay of nucleosome occupancy profiles after alignment at the TSS for genes grouped according to the average transcript length of 879 bp, 1393 bp, 1978 bp and 3082 bp (indicated by the stippled vertical lines), respectively. (D) Overlay of nucleosome occupancy profiles after alignment at the start codon ATG for 262 silent genes and two randomly selected sets of 262 active genes, ensuring comparison of equal sample sizes.

### 3.7.2 H2A.Z-containing promoters show regular upstream arrays in *S. pombe*

H2A.Z was shown to be enriched in the +1- and -1-nucleosomes flanking NDRs at gene promoters in *S. cerevisiae*, especially of inducible genes in their silent state<sup>[56]</sup>. In *S. pombe*, it has been shown recently that H2A.Z is mainly enriched at the +1-nucleosome and also generally at genes with on average lower expression levels<sup>[22]</sup>. An analysis of the nucleosome occupancy at promoters targeted by H2A.Z revealed two observations (Fig. 27): first the promoters showed a less pronounced NDR. This is probably due to the fact that H2A.Z is usually found at promoters of less expressed genes, which were characterized by generally higher nucleosome occupancy at promoter NDRs (Fig. 24B, C). Second, H2A.Z containing promoters showed also a regular

nucleosomal array in the upstream direction, although still less pronounced than in the downstream direction.

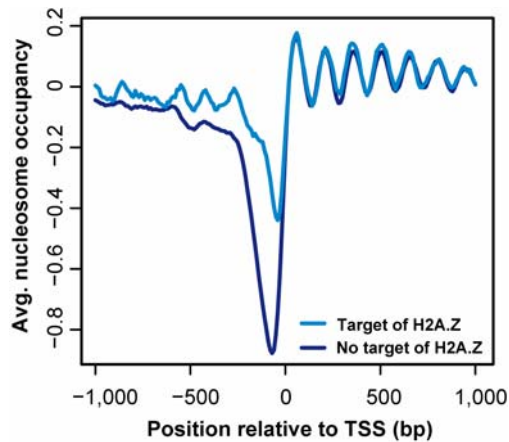


**Fig. 27: H2A.Z target promoters show a regular nucleosomal array upstream of promoter NDRs.**

Overlay of nucleosome occupancy profiles after alignment at the TSS of genes targeted at the promoters by H2A.Z (n=467).

### 3.7.3 Mit1 is important for regular nucleosome spacing in *S. pombe*

Mit1 is a Mi2-type ATP-dependent chromatin remodeling factor with a homolog in humans but not in *S. cerevisiae*. It was purified as part of the SHREC complex, which is involved in transcriptional gene silencing. Indirect end-labeling at the heterochromatic mating type locus showed a different nucleosome positioning pattern in the *mit1* mutant compared to wt. Further, Mit1 was also shown to bind to euchromatic regions <sup>[158]</sup>. Since Mit1 was the first factor implicated in nucleosome positioning in *S. pombe* and its binding was also observable at euchromatic regions, it was considered as a candidate that may generally determine nucleosome positioning. To test for a genome-wide role of Mit1 on nucleosome positioning, a nucleosome occupancy map of the *mit1* mutant was prepared. The TSS-aligned overlay of nucleosome occupancy profiles revealed a strongly compromised amplitude of the nucleosomal array compared to wt and the spectral analysis of the nucleosome occupancy profile did not reveal the prominent frequency of 6.5 nucleosomes per 1000 bp (Fig. 28A and B). Further, not only the downstream arrays but also the weaker upstream arrays at promoters containing H2A.Z were diminished in the *mit1* mutant (Fig. 28C). These findings argue for a role of Mit1 in regular nucleosome spacing up- and downstream of promoter NDRs.



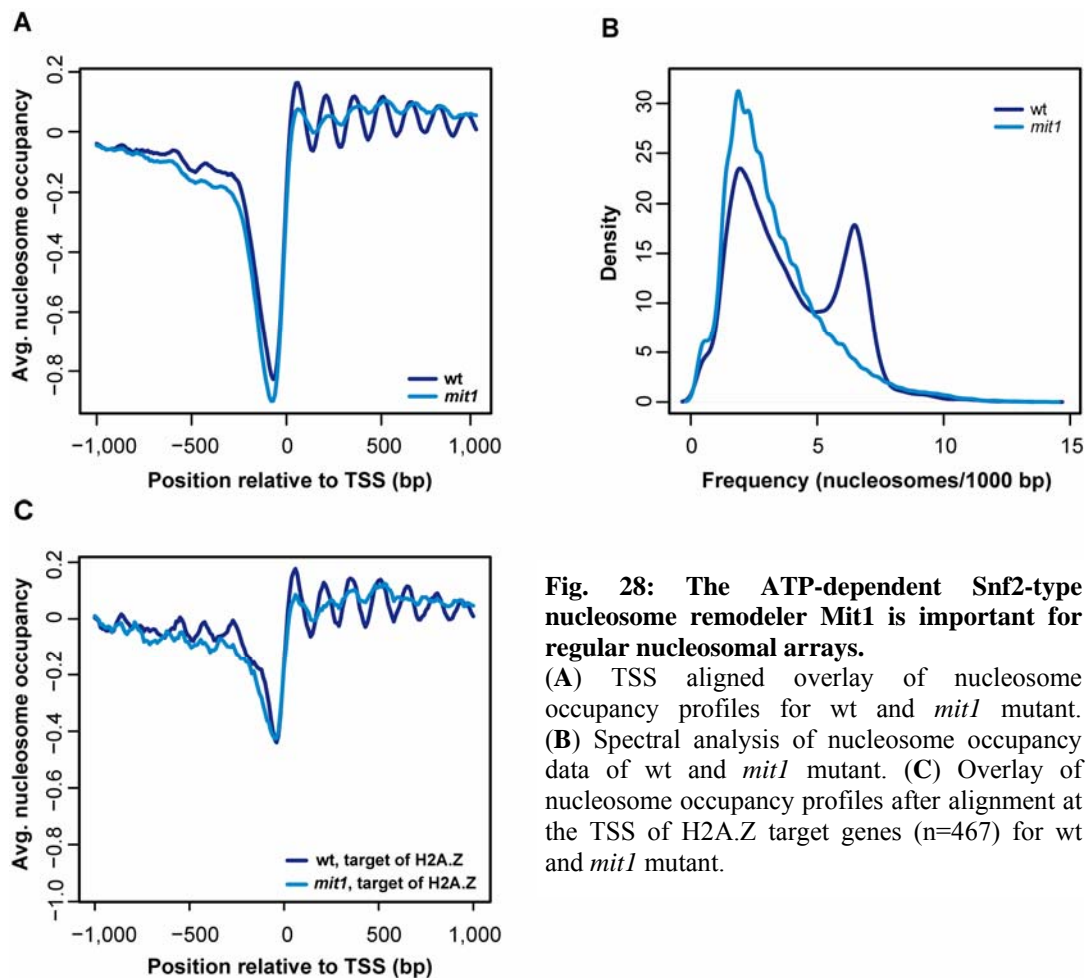


**Fig. 28: The ATP-dependent Snf2-type nucleosome remodeler Mit1 is important for regular nucleosomal arrays.**

(A) TSS aligned overlay of nucleosome occupancy profiles for wt and *mit1* mutant. (B) Spectral analysis of nucleosome occupancy data of wt and *mit1* mutant. (C) Overlay of nucleosome occupancy profiles after alignment at the TSS of H2A.Z target genes (n=467) for wt and *mit1* mutant.

Nucleosome occupancy was also mapped in an *S. pombe* mutant of the remodeler Fft3, which is a homolog of the Fun30 remodeler of the SNF2-type in *S. cerevisiae* and conserved from yeast to humans [48]. Fft3 has so far been not described to have a role in nucleosome positioning, but has been studied in the context of CENP-A deposition at centromeres (Karl Ekwall, personal communication). The TSS-aligned overlay of nucleosome occupancy profiles for the *fft3* mutant did not show a decreased regularity of the nucleosomal arrays compared to wt (Fig. 29A). This finding speaks for a specific role of the ATP-dependent chromatin remodeling factor Mit1 and no effect of the remodeler Fft3 on nucleosome positioning.

Another component of the SHREC complex is the histone deacetylase Clr3 [158]. As Mit1, Clr3 was also shown to influence nucleosome positioning at the heterochromatic mating type locus, but in contrast to Mit1, which also binds to euchromatic regions, the binding of Clr3 appears to be more restricted to heterochromatic regions [158]. In order to look for a genome-wide effect of Clr3 on nucleosome positioning in *S. pombe*, nucleosome occupancy was mapped for the *clr3* mutant. Interestingly, the TSS-aligned overlay did not show important differences to wt (Fig. 29B). This finding argued for a specific effect of Mit1 on the array regularity and not for an effect of the whole SHREC complex.

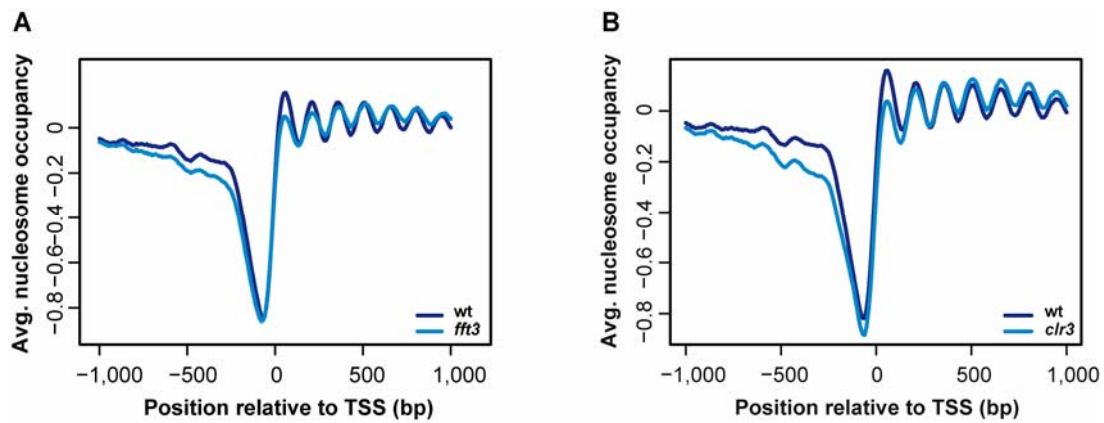


**Fig. 29: The ATP-dependent chromatin remodeler Fft3 and the histone deacetylase Clr3 do not affect nucleosome positioning.**

(A) TSS-aligned overlay of nucleosome occupancy profiles for wt and *fft3* mutant. (B) TSS-aligned overlay of nucleosome occupancy profiles for wt and *clr3* mutant.

### 3.7.4 Tup11/Tup12 target promoters show pronounced NDRs in *S. pombe*

In *S. cerevisiae*, it was observed that the corepressor complex Tup1/Ssn6 generated regular nucleosome positioning at the genes *FLO1*, *RNR2*, *RNR3*, *ANB1*, *SUC2*, and several genes of the **a**-mating type<sup>[104]</sup>. To test for a role of the homologous corepressor complex Tup11/Tup12/Ssn6 on nucleosome positioning in *S. pombe*, nucleosome occupancy at promoters targeted by the corepressors Tup11/Tup12<sup>[42]</sup> was analyzed. The TSS-aligned overlay of nucleosome occupancy profiles at Tup11/Tup12 promoter targets showed very deep and broad promoter NDRs (Fig. 30A). Surprisingly, this characteristic NDR architecture remained unchanged in an *S. pombe* *tup11 tup12* double mutant (Fig. 30B). This finding suggested that the characteristic promoter nucleosome pattern was not due to corepressor binding but either other factors, as for example Ssn6, and/or intrinsic properties encoded in the DNA sequence of the Tup11/12 target promoters.

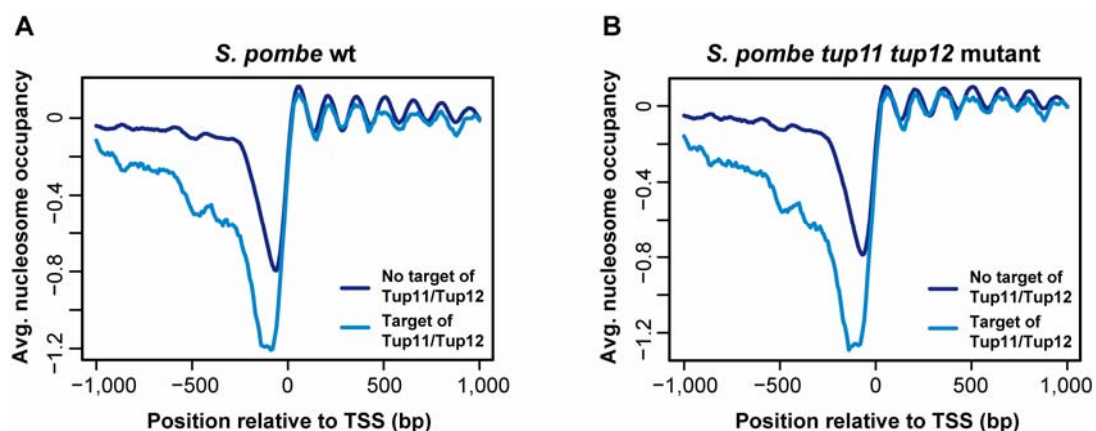


**Fig. 30: Broader and deeper NDRs at Tup11/Tup12 promoter targets are not caused by binding of Tup11 or Tup12.**

(A) TSS-aligned overlay of nucleosome occupancy profiles of promoters with (targets; n=255) and without (n=3758) Tup11/Tup12 binding for *S. pombe* wt. (B) Same as in A, but for the *S. pombe* *tup11 tup12* mutant.

### 3.8 DNA sequence has a different role in nucleosome positioning in *S. pombe* and *S. cerevisiae*

The role of the DNA sequence in nucleosome positioning is not clear yet. In 2006 a universal nucleosome positioning code was postulated supporting a major and conserved role of the DNA sequence in nucleosome positioning in different organisms <sup>[145]</sup>.

To address the question of what role the DNA sequence has in nucleosome positioning in *S. pombe* and how conserved this role is in comparison to *S. cerevisiae*, the N-score, a model that can predict nucleosome occupancy from DNA sequence <sup>[191]</sup>, was applied. Two different N-score models were generated in collaboration with Guo-Cheng Yuan, who developed the algorithm, one for *S. pombe* and one for *S. cerevisiae*, and each 8000 probes corresponding to the highest or lowest nucleosome occupancy signals were selected for training (see 2.9.7 for more detail). These two differently trained models were applied both to the *S. pombe* genome and to the *S. cerevisiae* genome. The TSS-aligned overlay of nucleosome occupancy data obtained by N-score model predictions showed a good prediction of nucleosome occupancy for the organisms the N-score model was trained on, but only poor prediction in the cross-species application (Fig. 31A and B). This became even more apparent in the different gene clusters, where in some clusters peaks and troughs coincided (cluster 1, 2, and 6 in Fig. 31C; cluster 2, 5, and 6 in Fig. 31D). This argued for different roles of the DNA sequence in nucleosome positioning in the two yeasts. Correspondingly, the N-score parameters for each species were different. The structural parameters ‘tip’ (rotation about long base pair axis), ‘minor\_mobility’ (mobility to bend towards minor groove) and ‘minor\_size’ (minor groove size) <sup>[94, 121]</sup> were the most discriminative features in *S. cerevisiae*. In *S. pombe* ‘nucleosome probability’ (probability to contact the nucleosome core), and ‘wedge’ (helix deflection angle) were the most structurally discriminative features.

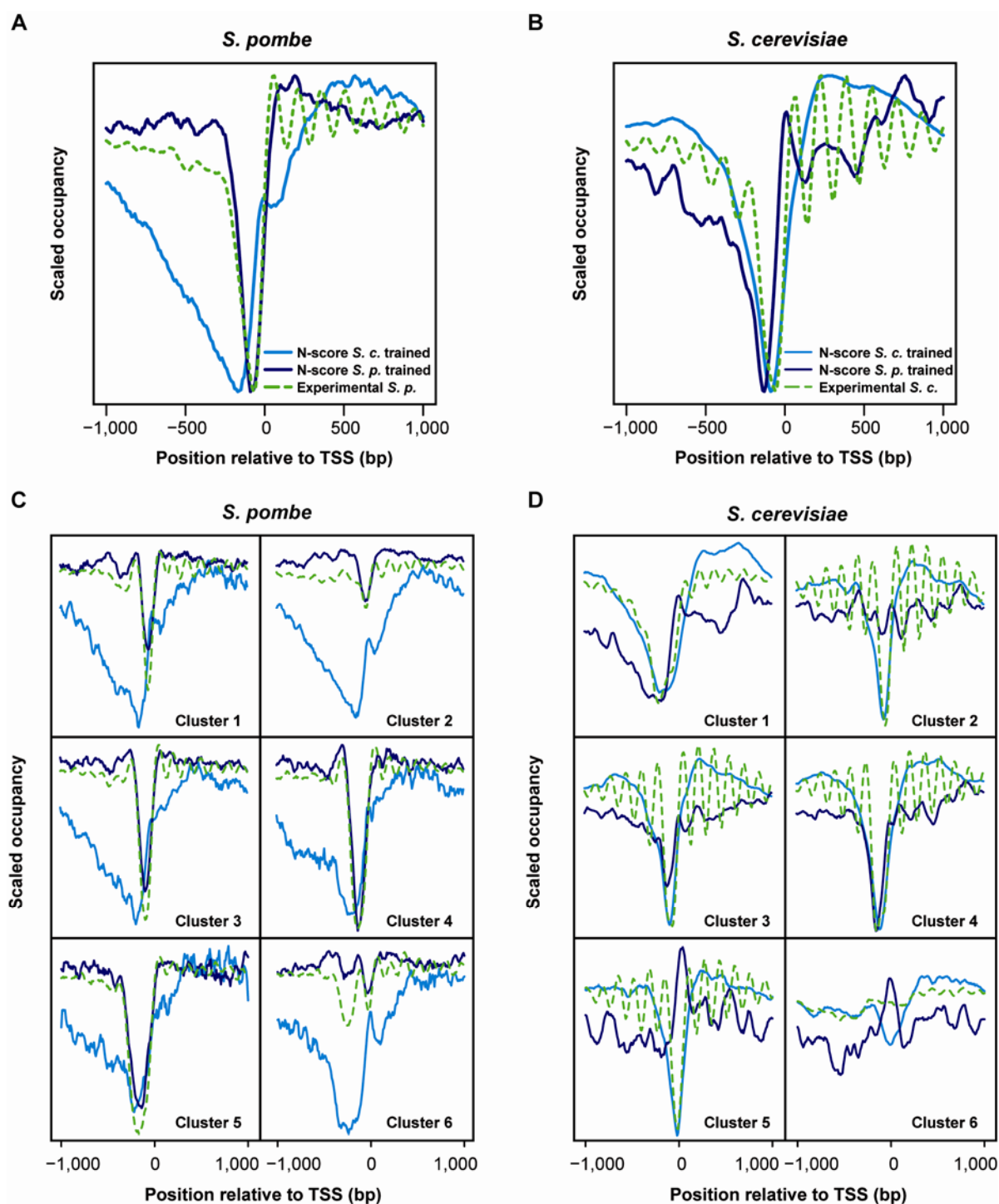


**Fig. 31: DNA sequence influences nucleosome occupancy in *S. pombe* and *S. cerevisiae* differently.** (A) TSS-aligned scaled overlays of nucleosome occupancy and of N-score<sup>[191]</sup> predictions after training with *S. pombe* or *S. cerevisiae* hybridization data and application to the *S. pombe* genome sequence. (B) As A, but with experimental data for *S. cerevisiae* and N-score calculations applied to the *S. cerevisiae* genome sequence. (C) As A, but for genes clustered as in Fig. 24B. (D) As B, but for genes clustered as in Fig. 24E.

Generally, prediction models performed much better when they were trained with nucleosome excluding sequences rather than only with nucleosomal sequences<sup>[124]</sup>. This was also observable for the N-score model. The N-score model trained only with 8000 nucleosomal probes of the

highest signal intensity from *S. pombe* experimental data could not predict the *in vivo* nucleosome occupancy in *S. pombe* (Fig. 32).

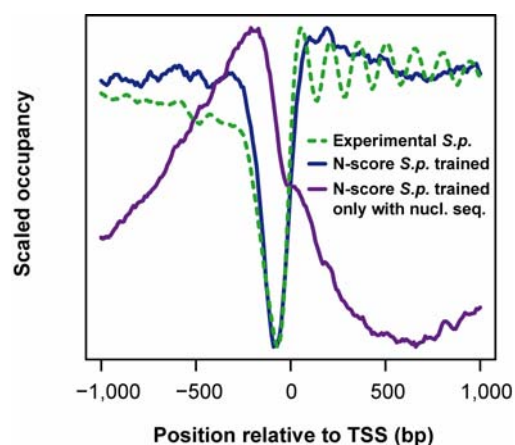


**Fig. 32: N-score model trained only with nucleosomal *S. pombe* sequences does not predict the correct *in vivo* nucleosome occupancy in *S. pombe*.**

TSS-aligned overlay of nucleosome occupancy predicted by N-score model<sup>[191]</sup> that was trained only with nucleosomal sequences, of N-score model trained as in Fig. 31A and of experimental *S. pombe* data.

To exclude any bias implemented in the N-score, another model for the prediction of nucleosome occupancy developed by Kaplan et al.<sup>[75]</sup> was tested. This model was trained only on the intrinsic histone-DNA interaction using the nucleosome occupancy map obtained from *in vitro* assembled salt gradient dialysis chromatin of *S. cerevisiae*. The model predicted well the nucleosome occupancy for *S. cerevisiae* (Fig. 33B). But for *S. pombe*, the model performed only poorly as it predicted a peak of nucleosome occupancy within the promoter NDR (Fig. 33A).

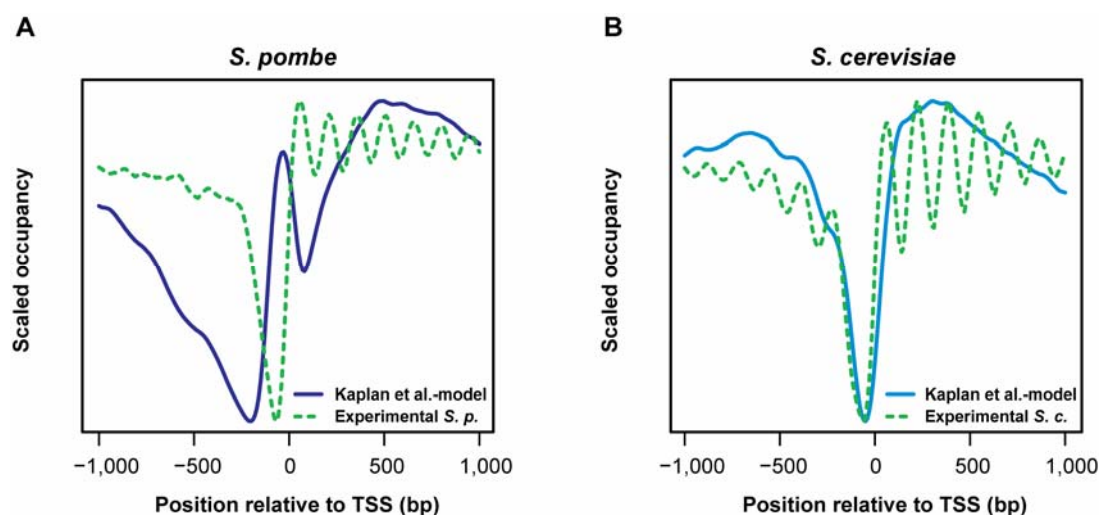


**Fig. 33: The model from Kaplan et al.<sup>[75]</sup> trained on nucleosome occupancy data from *in vitro* assembled chromatin of *S. cerevisiae* predicts the nucleosome occupancy well for *S. cerevisiae* but poorly for *S. pombe*.**

(A) Scaled overlays of experimental nucleosome occupancy data for *S. pombe* and of calculations with the Kaplan et al. model<sup>[75]</sup> applied to the *S. pombe* genome sequence. (B) As A, but with experimental data for *S. cerevisiae* and model calculations applied to the *S. cerevisiae* genome sequence.

Poly(dA:dT) sequences are a strong nucleosome exclusion signal and their role on nucleosome positioning was studied in other organisms. Poly(dA:dT) sequences were shown to be enriched in

NDRs of *S. cerevisiae* and *C. elegans* but not in NDRs of humans, chicken and fly [46, 147, 192]. Searching the *S. pombe* NDRs for frequent ‘DNA sequence words’ revealed that poly(dA:dT) sequences occurred less frequently in NDRs than elsewhere in the genome. For example, the pentamer AAAAA occurred in 8.8% of NDR probes, compared to 12.4% elsewhere in the genome (Tab. 4). Thus, *S. pombe* appears to belong to the same group as humans, chicken and fly, where poly(dA:dT) rich sequences were described to play less of a role in NDR formation [46]. However, the analysis revealed an enrichment of other ‘DNA sequence words’ in the NDRs. The most prominent hit with a frequency of 6% in NDRs and a four-fold enrichment compared to other genomic regions was the sequence CGTTA (Tab. 4). Interestingly, the second hit, TAACGA, is the complementary strand to this motif. Also some of the following hits are related to CGTTA, but have one or two mismatches (Tab. 4). These sequences could be binding sites of factors, e.g. transcription factors, supporting the role of other factors beyond the DNA sequence in nucleosome positioning.

Sequence word	Frequency in NDRs	Frequency in other genomic regions	Fold-enrichment
CGTTA	6.0%	1.5%	4.0
TAACGA	2.9%	0.6%	5.3
CGCTA	3.3%	1.0%	3.4
CACTA	4.0%	1.4%	2.8
ACACA	2.7%	1.6%	1.7
AACGA	5.2%	2.5%	2.1
GTAAC	3.4%	1.6%	2.1
AACGC	2.7%	1.2%	2.3
GCGTA	2.4%	0.9%	2.8
CGGTA	2.4%	1.0%	2.5
CCTTA	2.9%	1.7%	1.7
Poly(dA:dT) length5	8.8%	12.4%	0.7
Poly(dA:dT) length6	2.3%	3.3%	0.7
Poly(dA:dT) length7	0.0%	0.0%	---
Poly(dA:dT) length8	0.0%	0.0%	---
Poly(dA:dT) length9	0.0%	0.0%	---
Poly(dA:dT) length10	0.0%	0.0%	---
Poly(dA:dT) length11	0.0%	0.0%	---
Poly(dA:dT) length12	0.0%	0.0%	---
Poly(dA:dT) mixed length5	61.0%	61.9%	1.0
Poly(dA:dT) mixed length6	39.0%	40.7%	1.0
Poly(dA:dT) mixed length7	23.1%	26.0%	0.9
Poly(dA:dT) mixed length8	13.0%	16.2%	0.8
Poly(dA:dT) mixed length9	7.3%	9.7%	0.7
Poly(dA:dT) mixed length10	4.1%	6.0%	0.7
Poly(dA:dT) mixed length11	2.3%	3.6%	0.6
Poly(dA:dT) mixed length12	1.5%	2.2%	0.7

**Tab. 4:** Frequency of ‘DNA sequence words’ in NDRs and other genomic regions.

### 3.9 *In vitro* reconstitution of the *S. pombe* locus *SPAC1F8.06* does not generate an *in vivo*-like chromatin structure

*In vitro* salt gradient dialysis chromatin of the *PHO5* and *PHO8* promoters can be reconstituted into an *in vivo*-like chromatin structure by incubation with *S. cerevisiae* whole-cell extract and ATP [64, 82]. In order to test if this approach worked also for *S. pombe*, *in vitro* salt gradient dialysis chromatin of the plasmid-born *S. pombe* locus *SPAC1F8.06* and *S. pombe* whole-cell extract were prepared. The reconstitution assay was performed as described in 2.6.3 using either *S. pombe* whole-cell extract or as comparison *S. cerevisiae* whole-cell extract in the presence and absence of ATP. The DNaseI-digested chromatin pattern of pure salt gradient dialysis chromatin (-*S. p.* extract, -ATP) was different from the free DNA pattern, indicating that the chromatin assembly worked. Addition of only *S. pombe* extract without ATP did not affect the nucleosome positioning pattern of the salt gradient dialysis chromatin at *SPAC1F8.06*. Addition of *S. pombe* extract and ATP changed the chromatin structure at *SPAC1F8.06*, but did not generate the *in vivo*-like indirect end-labeling pattern. Adding *S. cerevisiae* extract and ATP also changed the chromatin structure at *SPAC1F8.06*, but the nucleosome positioning pattern was both different from the *in vivo*-like pattern and from the pattern obtained by incubation with *S. pombe* extract and ATP (Fig. 34). Interestingly, the weak hypersensitive site in the *in vivo* DNaseI indirect end-labeling is present already after salt gradient dialysis chromatin speaking for intrinsic properties within the DNA sequence for determination of the hypersensitive site.

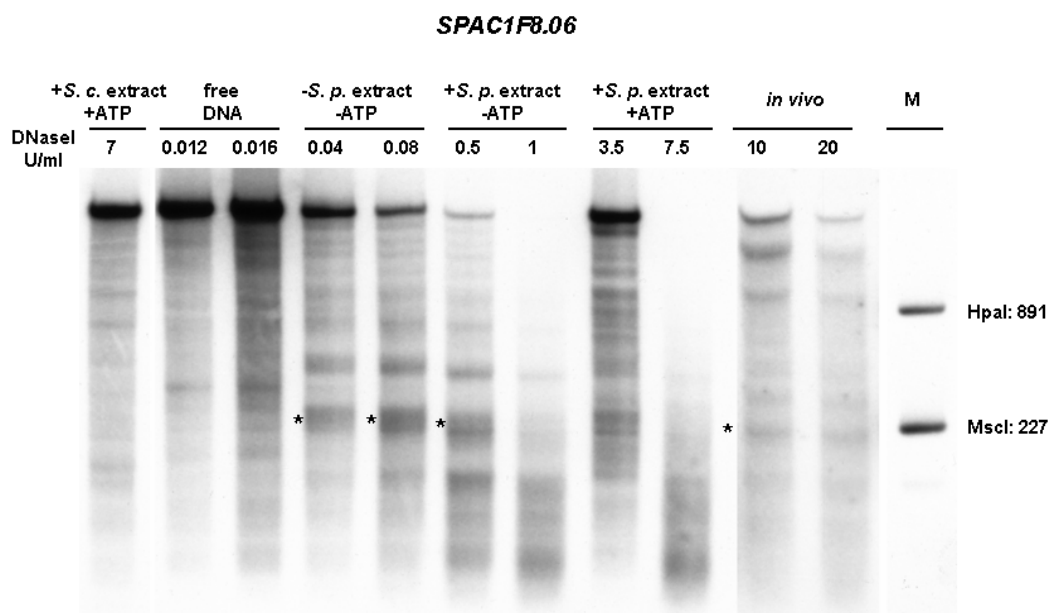


**Fig. 34: *In vitro* reconstitution of the *S. pombe* locus *SPAC1F8.06* does not generate an *in vivo*-like chromatin structure.**

DNaseI indirect end-labeling of free DNA, salt gradient dialysis chromatin after different reconstitution reactions as indicated on top of the lanes and of *in vivo* chromatin. The DNaseI concentrations are given on top of the indirect end-labeling lanes. Secondary cleavage was performed with BglIII. The positions of the marker fragments, generated by HpaI and MscI digestion, relative to the ATG are given. Asterisks mark the hypersensitive site.

## 4 Discussion

### 4.1 Consequences of the short nucleosome spacing in *S. pombe* on higher-order chromatin structure

Contradicting results about the nucleosome repeat length (NRL) in *S. pombe* were reported in the literature. The group of Fritz Thoma measured that *S. pombe* and *S. cerevisiae* had the same NRL of 167 bp<sup>[11]</sup>, whereas Godde and Widom reported a NRL of 156 +/-2 bp<sup>[53]</sup>. Spectral analysis of the nucleosome occupancy map for wt *S. pombe* revealed a NRL of 154 bp confirming the shorter NRL.

Historically, a linker length of ~20 bp was considered the shortest possible, so the nucleosome, containing 166 bp of DNA, was supposed to be the fundamental unit of chromatin structure<sup>[168, 178]</sup>. Therefore, the identification of a shorter spacing of 156 bp +/-2 bp in *S. pombe* was surprising. Nonetheless, also *Aspergillus nidulans* displays a spacing of 157.7 +/-2.3 bp<sup>[53, 113]</sup>.

As mentioned in the Introduction, the nucleosome filament is further packaged into fibers of 30 nm in diameter, in which nucleosomes are closely packed along and radially around the fiber axis<sup>[45, 168, 178]</sup>. These 30 nm fibers were detected in many different cell types and organisms, among them also *S. cerevisiae* and *S. pombe*. In all higher eukaryotes, the linker histone protein H1 is necessary for the formation of the 30 nm fiber, thereby affecting the compaction degree and the NRL<sup>[8]</sup>. For *S. cerevisiae*, a homologous linker histone protein, called Hho1, was identified by sequence similarity to known linker histones<sup>[88]</sup>. Hho1 was shown to be abundant in *S. cerevisiae*, associated with the yeast genome, and to be important for DNA repair and full life span<sup>[35]</sup>. However, it is not clear yet whether Hho1 is associated with the nucleosome in *S. cerevisiae* and whether it plays a role for the formation of the 30 nm fiber. With regard to the NRL the chromatin structure in a *S. cerevisiae hho1* deletion mutant was unchanged<sup>[118]</sup>. For *S. pombe*, a linker histone H1 or any similar protein was not described. Therefore, it is not clear whether yeasts employ the same mechanisms for formation of the 30 nm chromatin fiber as higher eukaryotes.

Also it is not firmly established in what manner the nucleosomal array is folded into the 30 nm fiber<sup>[34, 45]</sup> and two different models were proposed for fiber formation: the crossed linker model and the solenoid model<sup>[34, 180, 182]</sup>. Interestingly, *in vitro* experiments provided evidence for both models dependent on the NRL of the nucleosomal array. The crystal structure of a tetranucleosome with a NRL of 167 bp supported the crossed linker model<sup>[140]</sup>, but it was unclear whether this short nucleosomal array without linker histones resembled a physiological chromatin fiber. But also electron microscopy (EM) measurements of long fibers of 80 nucleosomes with a NRL of 167 bp in the presence of linker histones supported the crossed linker model<sup>[135]</sup>. In



contrast, EM measurements of long fibers of 50-70 nucleosomes of longer NRLs between 177 and 207 bp containing one linker histone per nucleosome supported the solenoid model [134, 135]. The structure of the 167 NRL fiber was less compact and smaller in diameter than fibers with NRLs of 177-207 bp. Nucleosomal arrays with a NRL of 167 bp were only able to bind 0.5 linker histones per nucleosome core, which is probably due to the short linker of 20 bp. Long fibers of 177-207 bp NRL with a linker length between 30 and 60 bp bound stoichiometric amounts of linker histone. Unfortunately, these *in vitro* studies did not examine the structure of 30 nm fibers resulting from nucleosomal arrays of shorter NRLs, as for example 154 bp, the NRL measured in *S. pombe*. Early calculations based on the structure of DNA and of the nucleosome core particle revealed that a short NRL of 156 +/-2 bp, as shown for *S. pombe*, does not allow the formation of a 30 nm fiber according to the crossed linker model [53, 133]. In contrast, the solenoid model is compatible with this short NRL, but only if the solenoidal structure of the 30 nm fiber is right-handed [47, 53, 180]. It will be interesting to further elucidate the higher-order structure of chromatin in *S. pombe*, since the short spacing appears to request a special compaction mechanism. However, it is conceivable that, depending on linker DNA length and the presence of linker histones, alternative structures of the 30 nm fiber exist *in vivo* in different organisms [134]. Intriguingly, heterochromatic regions were characterized by a longer NRL of 164 bp than euchromatic regions in *S. pombe*. These findings are interesting as they are contradictory to the intuitive expectation of repressive heterochromatin being more condensed. However, the larger spacing in *S. pombe* heterochromatin might allow more dense packaging of chromatin in the 30 nm fiber, thereby leading to a more repressed state [7]. If this was true, the shorter spacing in *S. pombe* euchromatin compared to *S. cerevisiae* could lead to a more open chromatin structure, which in turn could allow a generally higher expression level in *S. pombe* than in *S. cerevisiae*. Furthermore, the CHD/Mi-2 type remodeler Mit1 was shown in this work to affect the regular spacing of nucleosomes in *S. pombe*. In *Drosophila* and *S. cerevisiae*, the remodeler complexes of the ISWI family, namely ACF and CHRAC in *Drosophila* and Isw1 in *S. cerevisiae*, are involved in the regular spacing of nucleosomes after their deposition [90]. Also the *Drosophila* remodeler CHD1 in conjunction with the histone chaperone NAP1 was able to assemble chromatin *in vitro*, but dCHD1 generated a shorter NRL (162 bp) than dACF (175 bp) [103]. This finding is interesting given that *S. pombe* has a short spacing and lacks remodeling factors of the ISWI class. Instead, *S. pombe* provides an expanded CHD family of remodeler complexes [29] and the CHD/Mi-2 remodeler Mit1 affected the regularity of the nucleosomal array. It will be interesting to see if the different remodeler composition might be the reason for the shorter NRL in *S. pombe*.

## 4.2 The role of transcription in nucleosome positioning

Intuitively, the transcription process influences nucleosome positioning. However, it is not clear how the processes of transcription and nucleosome positioning are connected, i.e. if a certain chromatin structure over the promoter or the coding regions is necessary for or a consequence of successful transcription.

In *S. cerevisiae*, *Drosophila* and human cells, the distance between the +1-nucleosome and the TSS was found to be different<sup>[94, 110, 142]</sup>. This observation led to speculations about a possible role of this promoter organization and especially about the role of the +1-nucleosome in transcription initiation. In *S. cerevisiae*, the center of the +1-nucleosome is localized ~50-60 bp downstream of the TSS, so that the TSS is buried under the left border of the +1-nucleosome (~10 bp) and remodeling might be necessary for transcription initiation. In contrast, in active genes of human cells and *Drosophila* the center of the +1-nucleosome is localized 115 bp and 135 bp, respectively, downstream of the TSS, so that the TSS is freely accessible, and transcription initiation appears not to be controlled by the position of the +1-nucleosome<sup>[110, 142]</sup>. In *S. pombe*, the distance between the TSS and the +1-nucleosome was the same as in *S. cerevisiae*, so here the +1-nucleosome might have the same role in transcriptional initiation as in *S. cerevisiae*, if there is any. However, with regard to promoter melting during the process of transcription initiation, *S. pombe* and *S. cerevisiae* are different, with *S. pombe* being more similar to humans. In human cells and *S. pombe*, the TSS is localized ~25 bp downstream of the TATA box, and the TSS lies within a small melted bubble of 15 to 20 bp. In contrast, the location of the TSS is more heterogenous in *S. cerevisiae* (40-120 bp from the TATA box) and the bubble extends approximately 100 bp to cover the TSS.

Genes in human cells and *Drosophila* often have an initiated, but paused RNA polymerase II immediately upstream of and in contact with the +1-nucleosome<sup>[110, 142]</sup>. At genes occupied by paused RNA polymerase II, the +1-nucleosome was slightly shifted by 30 bp into the upstream direction compared to active genes in human cells, but 10 bp into the downstream direction compared to active genes in *Drosophila*<sup>[110, 142]</sup>. In *S. cerevisiae*, depletion of Rpb1, the large subunit of the RNA polymerase, also caused a downstream shift of the +1-nucleosome with propagation of this effect into the subsequent nucleosomal array<sup>[174]</sup>. However, in both cases, the observed nucleosome shifts were only small (~10 bp). The new sequencing techniques used for these analyses have a 1 bp resolution, but the MNase digest does not have bp precision and probably limits the resolution. Therefore, it is not clear whether the small effects are significant and reflect the *in vivo* situation.

Silent genes did not show a regular nucleosomal array in humans<sup>[142]</sup>, and also in *S. pombe* hardly any regular nucleosomal array appeared over silent genes (Fig. 26D). Last, in *S. pombe* a

nucleosomal array was only visible over the transcript and not further beyond. All these findings suggested a connection between the process of transcription and the position of the +1-nucleosome and the subsequent nucleosomes.

One intriguing difference that came up between *S. pombe* and *S. cerevisiae* was the asymmetry of the nucleosomal array in respect to the TSS in *S. pombe* compared to *S. cerevisiae*. In *S. pombe*, a nucleosomal array was only visible downstream of the TSS where transcription of annotated genes occurred, whereas in *S. cerevisiae*, nucleosomal arrays appeared both upstream and downstream of the TSS. An interesting observation made in some eukaryotic organisms and analyzed in detail in *S. cerevisiae* is that genomes are extensively transcribed, thereby generating a highly interspersed transcriptome and a large number of non-coding RNAs [188]. A comparison of these transcriptome data with nucleosome occupancy data revealed that many of the unannotated transcripts occur as transcripts antisense to protein coding transcripts, i.e. as part of divergent transcript pairs. Most of these unannotated transcripts were shown to initiate from 5' NDRs associated with the promoters of protein coding genes. But also many protein coding genes are orientated in a divergent manner in *S. cerevisiae* and were shown to frequently share a common 5' NDR for transcription initiation. So in *S. cerevisiae*, bidirectional promoter usage is a common feature and leads to transcription into both directions from NDRs [188]. If transcription is the cause of regular nucleosomal arrays, then a high abundance of bidirectionality may explain symmetrical arrays at promoter NDRs (Fig. 35). Conversely, low abundance of bidirectionality might mainly lead to asymmetrical arrays. It is not clear if NDR sharing and bidirectional promoter usage is common in *S. pombe*. But if bidirectionality of promoters is less frequent in *S. pombe* this could explain the asymmetry of nucleosomal arrays with respect to the TSS and support the role of transcription in forming regular nucleosomal arrays.

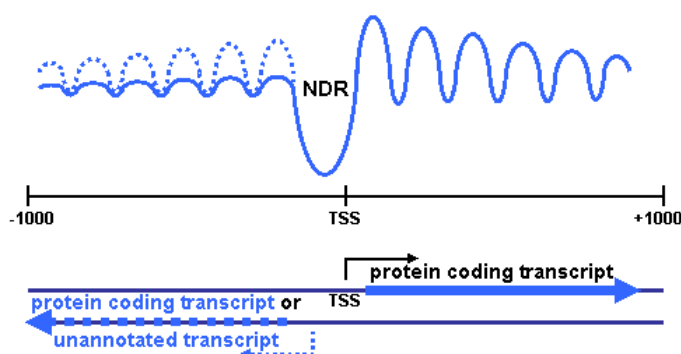


**Fig. 35: Bidirectional promoter usage might generate symmetrical nucleosomal arrays in *S. cerevisiae*.**

Transcription of divergently orientated transcripts that initiate from a shared promoter NDR might lead to symmetrical nucleosomal arrays in *S. cerevisiae*. Stippled line in the upstream direction indicates increased upstream nucleosomal array as a possible consequence of transcription also in the upstream direction.

### 4.3 The role of H2A.Z in nucleosome positioning

Mapping H2A.Z distribution in different species revealed an enrichment of H2A.Z in the nucleosomes flanking the NDR at gene promoters. This distribution suggested a role of H2A.Z in formation of the NDR and of the stereotypical promoter architecture.

However, a large scale study mapping nucleosome occupancy on *S. cerevisiae* chromosome 3 in mutants deleted for the genes encoding H2A.Z or the H2A.Z-specific remodeler Swr1 did not show a changed nucleosome positioning pattern<sup>[61]</sup>. This finding was in line with a previous single gene study analyzing nucleosome positioning at four *S. cerevisiae* promoters being highly enriched for H2A.Z<sup>[96]</sup>. In contrast, a 20 bp shift of a nucleosome at the *GAL1* promoter was reported in a deletion mutant for H2A.Z<sup>[56]</sup>. But all in all, H2A.Z appears not to have a general effect on nucleosome positioning in *S. cerevisiae*<sup>[61]</sup>.

The fact that H2A.Z is not important for nucleosome positioning in *S. cerevisiae* does not exclude a role of H2A.Z in nucleosome positioning in *S. pombe*. Differences between organisms were also described for other properties of H2A.Z. For example, in *S. cerevisiae* and humans, H2A.Z is enriched both at the +1- and at the -1-nucleosomes flanking the promoter NDR<sup>[1, 6]</sup>, whereas in *S. pombe* and fly H2A.Z is mainly present at the +1-nucleosome<sup>[22, 110]</sup>. Further, H2A.Z is essential for cell survival in vertebrates and metazoans, whereas it is dispensable in *S. pombe* and *S. cerevisiae*<sup>[197]</sup>.

*S. pombe* genome-wide nucleosome occupancy data revealed an upstream nucleosomal array at H2A.Z target promoters, speaking for a role of H2A.Z in nucleosome positioning at *S. pombe* promoters. This observation might be connected to interesting features of promoters harbouring H2A.Z. Recently, H2A.Z has been described to have a role in suppressing antisense transcription in *S. pombe*<sup>[198]</sup>. Combining these two findings, i.e. less antisense transcription but at the same point more prominent nucleosomal array in the upstream direction at H2A.Z target promoters, contradicts the hypothesis discussed in 4.2. Here transcription is postulated to be important for the formation of regular nucleosomal arrays. However, it is questionable if there is at all a connection between these two observations, i.e. between the upstream arrays at H2A.Z target genes and the role of H2A.Z in suppressing antisense transcription. First, only at a small number of genes, namely 4.7% of 842 analyzed *S. pombe* genes, antisense transcripts were upregulated in a *pht1* (*S. pombe htz1* (H2A.Z)) deletion mutant<sup>[198]</sup>. Second, it is not clear whether the genes showing upregulation of antisense transcripts are exclusively H2A.Z targets, or alternatively, how many H2A.Z target genes did not show upregulated antisense transcripts<sup>[198]</sup>. Therefore, it is difficult to say how big the overlap is between H2A.Z target genes with upstream nucleosomal arrays and genes with upregulated antisense transcripts in a *pht1* deletion mutant. Further experiments will be

necessary to examine the connection between H2A.Z, sense/antisense transcription and the formation of upstream nucleosomal arrays.

#### 4.4 The role of DNA sequence in nucleosome positioning

The role of DNA sequence in determining nucleosome positioning has been of great interest over the last years and has been controversially discussed. One major study reported a ‘genomic code’ for nucleosome positioning, stating that genomes encode an intrinsic nucleosome organization that can explain ~50% of the *in vivo* nucleosome positions <sup>[145]</sup>. However, more and more studies emphasize a major role of trans-factors in determining translational nucleosome positioning.

To investigate the role of the DNA sequence in *S. pombe* in comparison to *S. cerevisiae*, the N-score algorithm <sup>[191]</sup>, trained both with nucleosomal and linker sequences of either *S. pombe* or *S. cerevisiae in vivo* nucleosome occupancy signals, was applied. These differently trained N-score models predicted well the nucleosome occupancy for the species it was trained on, but performed poorly in the cross-species application. This argues for a role of the DNA sequence in nucleosome positioning, otherwise model training with DNA sequence could not predict nucleosome occupancy at all. However, the role of the DNA sequence in nucleosome positioning appears to be different in the two yeasts, arguing against the proposed universal ‘genomic code’. These findings are consistent with the different nucleosome positioning patterns at one and the same DNA sequence on shuttle vectors in *S. pombe* and *S. cerevisiae* <sup>[12]</sup>, and at the *S. cerevisiae HIS3* locus after integration into the *S. pombe* genome <sup>[147]</sup>. However, since the two N-score models were trained with experimental *in vivo* nucleosome occupancy data, this approach does not exclusively address the intrinsic features of DNA. For example, certain motives for DNA binding proteins, enriched in the DNA sequences used for model training, would influence the outcome of the prediction. In this case, the effect on nucleosome positioning would not be caused by intrinsic features of the underlying DNA sequence, but rather by the binding of a trans-factor to the respective motif.

To test for intrinsic DNA features that would intrinsically favour and disfavour nucleosome formation, the *S. pombe* genome was searched for sequence motifs. In contrast to *S. cerevisiae* and *C. elegans*, *S. pombe* promoter NDRs were not characterized by an enrichment of poly(dA:dT) sequences, sequences that intrinsically disfavor nucleosome formation. Also in humans, *Drosophila*, and chicken, no enrichment of these sequences was found in the promoter NDRs <sup>[46]</sup>. Another approach to examine the role of intrinsic DNA features on nucleosome positioning is *in vitro* assembly of chromatin by salt gradient dialysis, which is based on the pure biophysical interaction of histones and DNA. In *S. cerevisiae*, two studies mapped nucleosomes

after such *in vitro* reconstitution of the whole genome into chromatin [75, 194]. The data from one study were used to generate a model for predicting nucleosome positioning [75]. Although these *in vitro* approaches strongly depend on the experimental conditions which might influence the outcome [7], the *in vitro* based model was able to predict the nucleosome occupancy in *S. cerevisiae*, where it predicted the promoter NDRs, but was not able to predict the nucleosome occupancy in *S. pombe*. Together, these data show that also intrinsic DNA sequence features appear to play a different role in nucleosome positioning in the two yeasts.

In general, prediction models performed better when also nucleosome excluding sequences (linker sequences) were included into the training set [124]. This was also confirmed for the *S. pombe* based N-score model, which was not able to predict the promoter NDR for *S. pombe* when it was only trained with nucleosomal and not with linker DNA sequences from *S. pombe*. From the *in vivo* based N-score model [191] and the *in vitro* based Kaplan et al. model [75] it was also evident that only the position of the promoter NDR can be predicted but not the exact nucleosome positions – not even the position of the usually best positioned +1-nucleosome [75, 124]. Together, these findings suggest that DNA sequence (non-intrinsic features in *S. pombe* and rather intrinsic features in *S. cerevisiae*) is used to exclude nucleosomes from specific regions rather than to precisely position nucleosomes, suggesting a minor universal importance of nucleosome positioning sequences.

If the ‘genomic code’ of nucleosome positioning existed, one would expect a conserved role of the DNA sequence in determining nucleosome positioning or occupancy across species. The differences in the model predictions in the cross-species application, in the role of poly(dA:dT) rich sequences in different organisms, and the impossibility to predict the exact nucleosome positions argue against a universal ‘genomic code’ for nucleosome positioning. Nucleosome positioning trans-factors may override intrinsic DNA sequence features, thereby limiting the power of models based only on the interaction of histones and DNA for predicting nucleosome positions *in vivo*.

#### 4.5 The model of statistical nucleosome positioning

The statistical nucleosome positioning model proposes that positioning of nucleosomes arises from a boundary element in the DNA sequence that establishes the ordering or positioning of the neighboring nucleosomes due to their high density on DNA. This model calls only for a few determined sites within the genome from which a passive and statistical queuing process establishes non-randomly positioned nucleosomes [84]. Intuitively, packaging of the genome by this model appears to be more appropriate for the cell than independent nucleosome positioning,

since the statistical nucleosome positioning model, for which only boundary elements need to be determined, is less demanding in terms of sequence constraint during evolution. However, the nature of the boundary is not clear yet, and the promoter NDR and/or the +1-nucleosome were proposed as possible candidates.

Analysis of DNA sequence rules in *S. pombe* and *S. cerevisiae* revealed that DNA sequence co-defined nucleosome positioning only at promoter NDRs, possible boundary elements, but not for the majority of individual nucleosomes, suggesting that rather the concept of statistical and not of independent nucleosome positioning might be correct.

For *S. cerevisiae*, even further evidence exists for statistical nucleosome positioning. For example, deletion of *Isw2* in *S. cerevisiae* caused not only a shift of the +1-nucleosome, but also a shift of the adjacent nucleosomes to the downstream direction at *Isw2* target loci <sup>[176]</sup>. Similarly, depletion of *Rpb1*, leading to inhibition of transcription, caused a shift of the +1-nucleosome and the adjacent nucleosomes to the downstream direction <sup>[174]</sup>. After depletion of the transcription factors *Reb1* and *Abf1*, which are involved in NDR formation, a shift of both the +1-nucleosome and the adjacent nucleosomes slightly into the upstream direction was observable <sup>[61]</sup>. Accordingly, the positioning of one nucleosome in the array forces the positioning of all other nucleosomes, probably as a consequence of the tight packaging of nucleosomes in the array.

For *S. pombe*, so far no such clear observations have been made that would evidence statistical nucleosome positioning. However, if statistical nucleosome positioning occurred in *S. pombe*, then it appears to be a rather modified form as suggested from observations made in this work, and this might also be true for other organisms. Assuming that promoter NDRs acted as boundary and that the alignment of nucleosomes to promoter NDRs is a completely passive and statistical queuing process, one would expect symmetrical ordering of nucleosomes to both sides of the NDR. However, the observed asymmetry of nucleosomal arrays arising from the NDR only to the downstream direction in *S. pombe* indicates that the statistical nucleosome positioning process becomes modified by an additional mechanism that sets the direction of the array formation. Further, nucleosomal arrays of different species are characterized by a different spacing despite of the highly conserved nucleosome core particle between species. Therefore, there also needs to be a mechanism that determines the spacing of nucleosomes in the nucleosomal array. This work suggests that in *S. pombe* the transcriptional machinery is involved in setting the direction and the ATPase subunit *Mit1* of the SHREC complex is critical for actively generating the regular spacing.

## 4.6 The evolution of nucleosome positioning mechanisms

Considering the high conservation of the histone proteins and the need for DNA packaging in all eukaryotes, one could assume that eukaryotic organisms use the same nucleosome positioning mechanisms. On the other hand, nucleosome positioning is also important for regulating gene expression, and gene expression divergence, often as consequence of DNA sequence variation, largely influences phenotypic diversity <sup>[27]</sup>. The mechanisms of how DNA sequence variation affects gene expression divergence are multifaceted. At promoters, two main principles of DNA sequence variation were described to cause gene expression divergence, namely changes in transcription factor binding motifs <sup>[164]</sup> and changes in intrinsic DNA sequence features, which cause differences in nucleosome positioning <sup>[27]</sup>. For example, the analysis of transcriptional responses in three closely related yeast species revealed that differential gene expression frequently correlates with the loss of transcription factor binding sites in orthologous gene promoters. However, many genes displayed gene expression divergence, although the transcription factor binding sites were unchanged. In these genes, the DNA sequence next to the transcription factor binding site had diverged in the three species, thereby causing changes in the predicted nucleosome occupancy <sup>[164]</sup>.

Along the same line, the detailed comparison of nucleosome positioning mechanisms between the evolutionary far diverged *S. pombe* and *S. cerevisiae* also revealed many differences in nucleosome positioning mechanisms with respect to the use of intrinsic DNA sequence, remodelers, the histone variant H2A.Z, and the role of the corepressor complex Tup11/Tup12/Ssn6. A summary of the stereotypical promoter chromatin structure in *S. pombe* and of the factors that were found to influence chromatin structure is given in Fig. 36.

Differences in nucleosome positioning mechanisms both in terms of employing intrinsic DNA sequence features and transcription factors were also reported for other organisms. For example, *S. cerevisiae* and *C. elegans* often use poly(dA:dT) DNA stretches, which intrinsically disfavor nucleosome formation, for NDR formation, whereas humans, chicken, fly and *S. pombe* show no enrichment of these DNA stretches in promoter NDRs. In addition, the transcription factors Reb1, Abf1 and Rsc3, which play key roles in NDR formation in *S. cerevisiae*, are not conserved throughout eukaryotes <sup>[5]</sup>. Obvious orthologs of these proteins are not found outside of fungi and also in *S. pombe*, Abf1 and Rsc3 are not conserved <sup>[5]</sup>. The differences observed between *S. pombe* and *S. cerevisiae* in this work argue for evolutionary plasticity of nucleosome positioning mechanisms rather than a universal nucleosome positioning code. Probably, nucleosome positioning mechanisms coevolve with DNA sequence variations and in turn regulate gene expression profiles <sup>[5]</sup>.



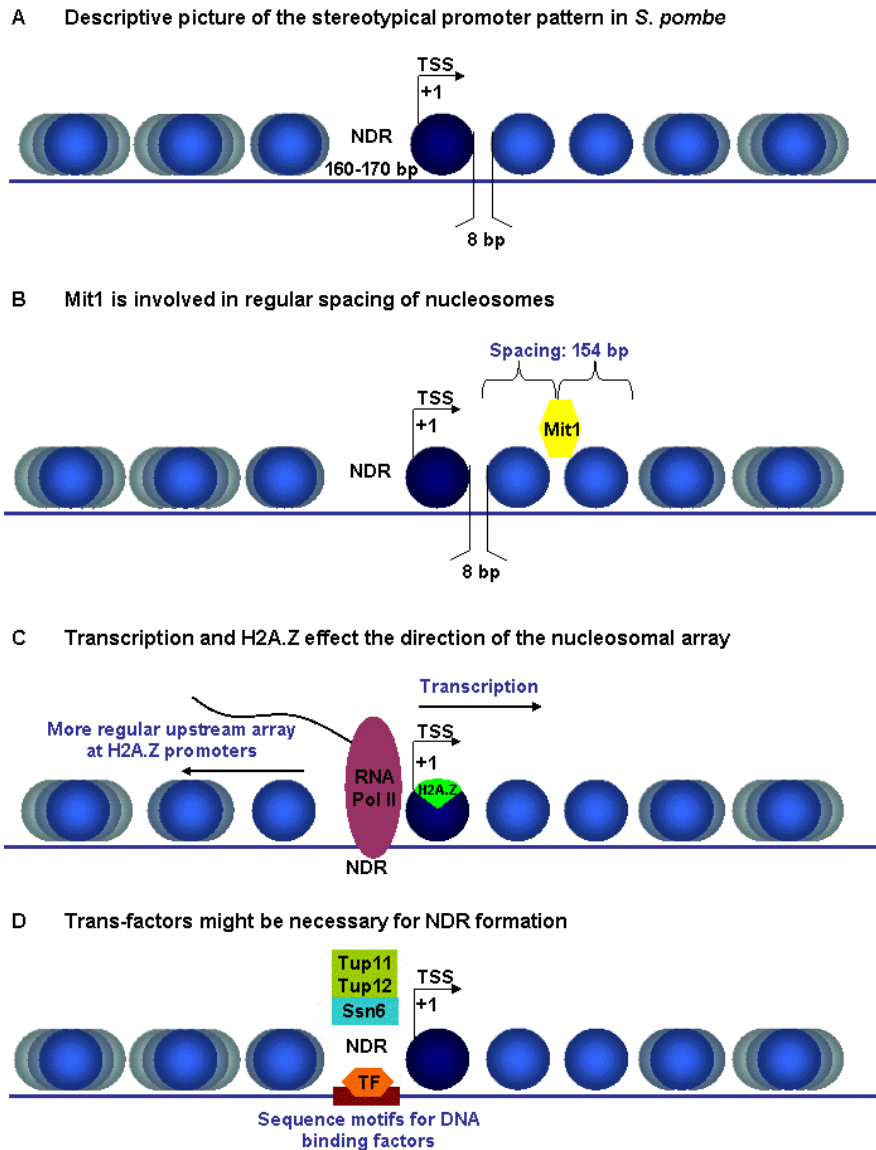


**Fig. 36: Descriptive and dynamic view of nucleosome positioning in *S. pombe*.**

(A) Descriptive picture of the stereotypical promoter pattern in *S. pombe*. An NDR is closely upstream of the TSS followed by a positioned +1-nucleosome. Darker nucleosomes are positioned more strongly than lighter nucleosomes. Weaker positioning with increasing distance from the NDR is illustrated by grey shadows around the nucleosomes. The average nucleosome spacing in *S. pombe* (8 bp) is given. (B) The ATP-dependent chromatin remodeling factor Mit1 appears to be necessary for regular spacing in *S. pombe*. (C) Transcription by RNA polymerase II is correlated with regular downstream nucleosomal arrays. Promoters harbouring H2A.Z correlated with a more regular upstream nucleosomal array. (D) Trans-factors might be necessary for NDR formation, e.g. Ssn6, associated with the corepressors Tup11/Tup12 or transcription factors.

[Modified after Radman-Livaja and Rando <sup>[124]</sup>]

## 4.7 Outlook

The analysis of nucleosome positioning mechanisms and their determinants is still at its beginning. Many factors probably act in concert to obtain the nucleosome organization needed for controlled gene expression. *S. pombe* differs in its nucleosome positioning mechanisms from *S. cerevisiae* and the evolutionary divergence between the two yeasts allows examining how nucleosome positioning mechanisms evolved. This work brought insight into a number of mechanisms - both trans-factors and DNA sequence - involved in nucleosome positioning in *S. pombe*, but important questions are still open: How many nucleosomes are translationally perfectly positioned or rather delocalized? Does this positioning state influence gene expression? An HMM<sup>[192]</sup> was tested to search for positioned and delocalized nucleosomes, however, it failed to recognize many translationally positioned nucleosomes. More efficient models will be required to address this question.

Does statistical nucleosome positioning occur in *S. pombe*? If yes, what defines the boundary in molecular terms? And which factors, i.e. DNA sequence and/or trans-factors are implicated in NDR formation and nucleosome positioning? All these aspects are connected and might be regulated by the interplay of a variety of factors. It was suggested that the boundary function could be provided by the NDR. However, genome-wide *in vitro* reconstitution experiments by salt gradient dialysis that were able to recapitulate the NDR were neither able to obtain the positioned +1-nucleosome nor the subsequent downstream nucleosomal array, suggesting that an NDR per se is not sufficient to act as boundary.

*S. pombe* NDRs, in contrast to *S. cerevisiae* NDRs, were not enriched in poly(dA:dT) rich sequences, suggesting a less prominent role of intrinsic DNA sequence features in *S. pombe*. However, more detailed examination of the role of the intrinsic DNA sequence in nucleosome positioning is necessary, and *in vitro* reconstitution of the whole *S. pombe* genome by salt gradient dialysis probably provides a potent approach.

Moreover, NDR screening revealed interesting sequence motives that are possible candidates for trans-factor binding sites. A yeast-one-hybrid screen could allow the identification of factors binding to these motives. The ATP-dependent remodeler RSC and the transcription factor Reb1 were shown to be important for NDR formation in *S. cerevisiae*. Since both components are conserved in *S. pombe*, these factors might serve the same role in nucleosome positioning in *S. pombe*. Further analysis of the role of H2A.Z and the role of transcription might help to understand their importance for nucleosomal arrays and how they are connected.

Last, what does the higher-order structure of a nucleosomal array with a NRL of 154 bp look like? *In vitro* experiments and subsequent EM measurements as performed for nucleosome fibers of longer NRLs<sup>[135]</sup> could answer this question.

## 5 References

1. Albert, I., T.N. Mavrich, L.P. Tomsho, J. Qi, S.J. Zanton, S.C. Schuster, and B.F. Pugh, Translational and rotational settings of H2A.Z nucleosomes across the *Saccharomyces cerevisiae* genome. *Nature*, 2007. 446(7135): p. 572-6.
2. Almer, A. and W. Horz, Nuclease hypersensitive regions with adjacent positioned nucleosomes mark the gene boundaries of the PHO5/PHO3 locus in yeast. *EMBO J*, 1986. 5(10): p. 2681-7.
3. Almer, A., H. Rudolph, A. Hinnen, and W. Horz, Removal of positioned nucleosomes from the yeast PHO5 promoter upon PHO5 induction releases additional upstream activating DNA elements. *EMBO J*, 1986. 5(10): p. 2689-96.
4. Anderson, J.D. and J. Widom, Sequence and position-dependence of the equilibrium accessibility of nucleosomal DNA target sites. *J Mol Biol*, 2000. 296(4): p. 979-87.
5. Badis, G., E.T. Chan, H. van Bakel, L. Pena-Castillo, D. Tillo, K. Tsui, C.D. Carlson, A.J. Gossett, M.J. Hasinoff, C.L. Warren, M. Gebbia, S. Talukder, A. Yang, S. Mnaimneh, D. Terterov, D. Coburn, A. Li Yeo, Z.X. Yeo, N.D. Clarke, J.D. Lieb, A.Z. Ansari, C. Nislow, and T.R. Hughes, A library of yeast transcription factor motifs reveals a widespread function for Rsc3 in targeting nucleosome exclusion at promoters. *Mol Cell*, 2008. 32(6): p. 878-87.
6. Barski, A., S. Cuddapah, K. Cui, T.Y. Roh, D.E. Schones, Z. Wang, G. Wei, I. Chepelev, and K. Zhao, High-resolution profiling of histone methylations in the human genome. *Cell*, 2007. 129(4): p. 823-37.
7. Bassett, A., S. Cooper, C. Wu, and A. Travers, The folding and unfolding of eukaryotic chromatin. *Curr Opin Genet Dev*, 2009. 19(2): p. 159-65.
8. Bates, D.L. and J.O. Thomas, Histones H1 and H5: one or two molecules per nucleosome? *Nucleic Acids Res*, 1981. 9(22): p. 5883-94.
9. Belikov, S., B. Gelius, G. Almouzni, and O. Wrangé, Hormone activation induces nucleosome positioning in vivo. *EMBO J*, 2000. 19(5): p. 1023-33.
10. Belikov, S., B. Gelius, and O. Wrangé, Hormone-induced nucleosome positioning in the MMTV promoter is reversible. *EMBO J*, 2001. 20(11): p. 2802-11.
11. Bernardi, F., T. Koller, and F. Thoma, The *ade6* gene of the fission yeast *Schizosaccharomyces pombe* has the same chromatin structure in the chromosome and in plasmids. *Yeast*, 1991. 7(6): p. 547-58.
12. Bernardi, F., M. Zatchej, and F. Thoma, Species specific protein--DNA interactions may determine the chromatin units of genes in *S.cerevisiae* and in *S.pombe*. *EMBO J*, 1992. 11(3): p. 1177-85.
13. Bernstein, B.E., E.L. Humphrey, R.L. Erlich, R. Schneider, P. Bouman, J.S. Liu, T. Kouzarides, and S.L. Schreiber, Methylation of histone H3 Lys 4 in coding regions of active genes. *Proc Natl Acad Sci U S A*, 2002. 99(13): p. 8695-700.

14. Bernstein, B.E., C.L. Liu, E.L. Humphrey, E.O. Perlstein, and S.L. Schreiber, Global nucleosome occupancy in yeast. *Genome Biol*, 2004. 5(9): p. R62.
15. Bernstein, B.E., A. Meissner, and E.S. Lander, The mammalian epigenome. *Cell*, 2007. 128(4): p. 669-81.
16. Bernstein, E. and S.B. Hake, The nucleosome: a little variation goes a long way. *Biochem Cell Biol*, 2006. 84(4): p. 505-17.
17. Bird, A., DNA methylation patterns and epigenetic memory. *Genes Dev*, 2002. 16(1): p. 6-21.
18. Boeger, H., J. Griesenbeck, J.S. Strattan, and R.D. Kornberg, Nucleosomes unfold completely at a transcriptionally active promoter. *Mol Cell*, 2003. 11(6): p. 1587-98.
19. Bolivar, F., R.L. Rodriguez, P.J. Greene, M.C. Betlach, H.L. Heyneker, H.W. Boyer, J.H. Crosa, and S. Falkow, Construction and characterization of new cloning vehicles. II. A multipurpose cloning system. *Gene*, 1977. 2(2): p. 95-113.
20. Bonisch, C., S.M. Nieratschker, N.K. Orfanos, and S.B. Hake, Chromatin proteomics and epigenetic regulatory circuits. *Expert Rev Proteomics*, 2008. 5(1): p. 105-19.
21. Bruno, M., A. Flaus, C. Stockdale, C. Rencurel, H. Ferreira, and T. Owen-Hughes, Histone H2A/H2B dimer exchange by ATP-dependent chromatin remodeling activities. *Mol Cell*, 2003. 12(6): p. 1599-606.
22. Buchanan, L., M. Durand-Dubief, A. Roguev, C. Sakalar, B. Wilhelm, A. Stralfors, A. Shevchenko, R. Aasland, K. Ekwall, and A. Francis Stewart, The *Schizosaccharomyces pombe* JmjC-protein, Msc1, prevents H2A.Z localization in centromeric and subtelomeric chromatin domains. *PLoS Genet*, 2009. 5(11): p. e1000726.
23. Cairns, B.R., The logic of chromatin architecture and remodelling at promoters. *Nature*, 2009. 461(7261): p. 193-8.
24. Cairns, B.R., Y. Lorch, Y. Li, M. Zhang, L. Lacomis, H. Erdjument-Bromage, P. Tempst, J. Du, B. Laurent, and R.D. Kornberg, RSC, an essential, abundant chromatin-remodeling complex. *Cell*, 1996. 87(7): p. 1249-60.
25. Cairns, B.R., A. Schlichter, H. Erdjument-Bromage, P. Tempst, R.D. Kornberg, and F. Winston, Two functionally distinct forms of the RSC nucleosome-remodeling complex, containing essential AT hook, BAH, and bromodomains. *Mol Cell*, 1999. 4(5): p. 715-23.
26. Cam, H.P., T. Sugiyama, E.S. Chen, X. Chen, P.C. FitzGerald, and S.I. Grewal, Comprehensive analysis of heterochromatin- and RNAi-mediated epigenetic control of the fission yeast genome. *Nat Genet*, 2005. 37(8): p. 809-19.
27. Choi, J.K. and Y.J. Kim, Intrinsic variability of gene expression encoded in nucleosome positioning sequences. *Nat Genet*, 2009. 41(4): p. 498-503.
28. Choi, W.S., Y.C. Lin, and J.D. Gralla, The *Schizosaccharomyces pombe* open promoter bubble: mammalian-like arrangement and properties. *J Mol Biol*, 2004. 340(5): p. 981-9.
29. Clapier, C.R. and B.R. Cairns, The biology of chromatin remodeling complexes. *Annu Rev Biochem*, 2009. 78: p. 273-304.

30. Dalal, Y., T. Furuyama, D. Vermaak, and S. Henikoff, Structure, dynamics, and evolution of centromeric nucleosomes. *Proc Natl Acad Sci U S A*, 2007. 104(41): p. 15974-81.
31. Davey, C.A., D.F. Sargent, K. Luger, A.W. Maeder, and T.J. Richmond, Solvent mediated interactions in the structure of the nucleosome core particle at 1.9 Å resolution. *J Mol Biol*, 2002. 319(5): p. 1097-113.
32. David, L., W. Huber, M. Granovskaia, J. Toedling, C.J. Palm, L. Bofkin, T. Jones, R.W. Davis, and L.M. Steinmetz, A high-resolution map of transcription in the yeast genome. *Proc Natl Acad Sci U S A*, 2006. 103(14): p. 5320-5.
33. Dion, M.F., T. Kaplan, M. Kim, S. Buratowski, N. Friedman, and O.J. Rando, Dynamics of replication-independent histone turnover in budding yeast. *Science*, 2007. 315(5817): p. 1405-8.
34. Dorigo, B., T. Schalch, A. Kulangara, S. Duda, R.R. Schroeder, and T.J. Richmond, Nucleosome arrays reveal the two-start organization of the chromatin fiber. *Science*, 2004. 306(5701): p. 1571-3.
35. Downs, J.A., E. Kosmidou, A. Morgan, and S.P. Jackson, Suppression of homologous recombination by the *Saccharomyces cerevisiae* linker histone. *Mol Cell*, 2003. 11(6): p. 1685-92.
36. Drew, H.R. and A.A. Travers, DNA bending and its relation to nucleosome positioning. *J Mol Biol*, 1985. 186(4): p. 773-90.
37. Durrin, L.K., R.K. Mann, and M. Grunstein, Nucleosome loss activates CUP1 and HIS3 promoters to fully induced levels in the yeast *Saccharomyces cerevisiae*. *Mol Cell Biol*, 1992. 12(4): p. 1621-9.
38. Dutrow, N., D.A. Nix, D. Holt, B. Milash, B. Dalley, E. Westbroek, T.J. Parnell, and B.R. Cairns, Dynamic transcriptome of *Schizosaccharomyces pombe* shown by RNA-DNA hybrid mapping. *Nat Genet*, 2008. 40(8): p. 977-86.
39. Eberharter, A. and P.B. Becker, ATP-dependent nucleosome remodelling: factors and functions. *J Cell Sci*, 2004. 117(Pt 17): p. 3707-11.
40. Elgin, S.C., DNAase I-hypersensitive sites of chromatin. *Cell*, 1981. 27(3 Pt 2): p. 413-5.
41. Erard, M. and D.G. Barker, Electron microscopic studies of condensed mitotic chromosomes in the fission yeast *Schizosaccharomyces pombe*. *Biol Cell*, 1985. 55(1-2): p. 27-34.
42. Fagerstrom-Billai, F., M. Durand-Dubief, K. Ekwall, and A.P. Wright, Individual subunits of the Ssn6-Tup11/12 corepressor are selectively required for repression of different target genes. *Mol Cell Biol*, 2007. 27(3): p. 1069-82.
43. Fazio, T.G. and T. Tsukiyama, Chromatin remodeling in vivo: evidence for a nucleosome sliding mechanism. *Mol Cell*, 2003. 12(5): p. 1333-40.
44. Felsenfeld, G. and M. Groudine, Controlling the double helix. *Nature*, 2003. 421(6921): p. 448-53.

45. Felsenfeld, G. and J.D. McGhee, Structure of the 30 nm chromatin fiber. *Cell*, 1986. 44(3): p. 375-7.
46. Field, Y., N. Kaplan, Y. Fondufe-Mittendorf, I.K. Moore, E. Sharon, Y. Lubling, J. Widom, and E. Segal, Distinct modes of regulation by chromatin encoded through nucleosome positioning signals. *PLoS Comput Biol*, 2008. 4(11): p. e1000216.
47. Finch, J.T. and A. Klug, Solenoidal model for superstructure in chromatin. *Proc Natl Acad Sci U S A*, 1976. 73(6): p. 1897-901.
48. Flaus, A., D.M. Martin, G.J. Barton, and T. Owen-Hughes, Identification of multiple distinct Snf2 subfamilies with conserved structural motifs. *Nucleic Acids Res*, 2006. 34(10): p. 2887-905.
49. Fuks, F., DNA methylation and histone modifications: teaming up to silence genes. *Curr Opin Genet Dev*, 2005. 15(5): p. 490-5.
50. Furuyama, T. and S. Henikoff, Centromeric nucleosomes induce positive DNA supercoils. *Cell*, 2009. 138(1): p. 104-13.
51. Gavin, A.C., M. Bosche, R. Krause, P. Grandi, M. Marzioch, A. Bauer, J. Schultz, J.M. Rick, A.M. Michon, C.M. Cruciat, M. Remor, C. Hofert, M. Schelder, M. Brajenovic, H. Ruffner, A. Merino, K. Klein, M. Hudak, D. Dickson, T. Rudi, V. Gnau, A. Bauch, S. Bastuck, B. Huhse, C. Leutwein, M.A. Heurtier, R.R. Copley, A. Edelmann, E. Querfurth, V. Rybin, G. Drewes, M. Raida, T. Bouwmeester, P. Bork, B. Seraphin, B. Kuster, G. Neubauer, and G. Superti-Furga, Functional organization of the yeast proteome by systematic analysis of protein complexes. *Nature*, 2002. 415(6868): p. 141-7.
52. Giga-Hama, Y. and H. Kumagai, Foreign Gene Expression in Fission Yeast *Schizosaccharomyces Pombe*. Springer, Landes Bioscience, 1997.
53. Godde, J.S. and J. Widom, Chromatin structure of *Schizosaccharomyces pombe*. A nucleosome repeat length that is shorter than the chromosomal DNA length. *J Mol Biol*, 1992. 226(4): p. 1009-25.
54. Gottesfeld, J.M. and L.S. Bloomer, Nonrandom alignment of nucleosomes on 5S RNA genes of *X. laevis*. *Cell*, 1980. 21(3): p. 751-60.
55. Grewal, S.I. and S. Jia, Heterochromatin revisited. *Nat Rev Genet*, 2007. 8(1): p. 35-46.
56. Guillemette, B., A.R. Bataille, N. Gevry, M. Adam, M. Blanchette, F. Robert, and L. Gaudreau, Variant histone H2A.Z is globally localized to the promoters of inactive yeast genes and regulates nucleosome positioning. *PLoS Biol*, 2005. 3(12): p. e384.
57. Gupta, S., J. Dennis, R.E. Thurman, R. Kingston, J.A. Stamatoyannopoulos, and W.S. Noble, Predicting human nucleosome occupancy from primary sequence. *PLoS Comput Biol*, 2008. 4(8): p. e1000134.
58. Hake, S.B. and C.D. Allis, Histone H3 variants and their potential role in indexing mammalian genomes: the "H3 barcode hypothesis". *Proc Natl Acad Sci U S A*, 2006. 103(17): p. 6428-35.
59. Han, M. and M. Grunstein, Nucleosome loss activates yeast downstream promoters in vivo. *Cell*, 1988. 55(6): p. 1137-45.

60. Han, M., U.J. Kim, P. Kayne, and M. Grunstein, Depletion of histone H4 and nucleosomes activates the PHO5 gene in *Saccharomyces cerevisiae*. *EMBO J*, 1988. 7(7): p. 2221-8.
61. Hartley, P.D. and H.D. Madhani, Mechanisms that specify promoter nucleosome location and identity. *Cell*, 2009. 137(3): p. 445-58.
62. Heichinger, C., C.J. Penkett, J. Bahler, and P. Nurse, Genome-wide characterization of fission yeast DNA replication origins. *EMBO J*, 2006. 25(21): p. 5171-9.
63. Hendrich, B. and A. Bird, Identification and characterization of a family of mammalian methyl-CpG binding proteins. *Mol Cell Biol*, 1998. 18(11): p. 6538-47.
64. Hertel, C.B., G. Langst, W. Horz, and P. Korber, Nucleosome stability at the yeast PHO5 and PHO8 promoters correlates with differential cofactor requirements for chromatin opening. *Mol Cell Biol*, 2005. 25(24): p. 10755-67.
65. Horn, P.J. and C.L. Peterson, Molecular biology. Chromatin higher order folding--wrapping up transcription. *Science*, 2002. 297(5588): p. 1824-7.
66. Huber, W., A. von Heydebreck, H. Sultmann, A. Poustka, and M. Vingron, Variance stabilization applied to microarray data calibration and to the quantification of differential expression. *Bioinformatics*, 2002. 18 Suppl 1: p. S96-104.
67. Igo-Kemenes, T., A. Omori, and H.G. Zachau, Non-random arrangement of nucleosomes in satellite I containing chromatin of rat liver. *Nucleic Acids Res*, 1980. 8(22): p. 5377-90.
68. Ioshikhes, I.P., I. Albert, S.J. Zanton, and B.F. Pugh, Nucleosome positions predicted through comparative genomics. *Nat Genet*, 2006. 38(10): p. 1210-5.
69. Jiang, C. and B.F. Pugh, Nucleosome positioning and gene regulation: advances through genomics. *Nat Rev Genet*, 2009. 10(3): p. 161-72.
70. Jin, C. and G. Felsenfeld, Nucleosome stability mediated by histone variants H3.3 and H2A.Z. *Genes Dev*, 2007. 21(12): p. 1519-29.
71. Jin, C., C. Zang, G. Wei, K. Cui, W. Peng, K. Zhao, and G. Felsenfeld, H3.3/H2A.Z double variant-containing nucleosomes mark 'nucleosome-free regions' of active promoters and other regulatory regions. *Nat Genet*, 2009. 41(8): p. 941-5.
72. Johnson, S.M., F.J. Tan, H.L. McCullough, D.P. Riordan, and A.Z. Fire, Flexibility and constraint in the nucleosome core landscape of *Caenorhabditis elegans* chromatin. *Genome Res*, 2006. 16(12): p. 1505-16.
73. Kamakaka, R.T. and S. Biggins, Histone variants: deviants? *Genes Dev*, 2005. 19(3): p. 295-310.
74. Kan, P.Y., T.L. Caterino, and J.J. Hayes, The H4 tail domain participates in intra- and internucleosome interactions with protein and DNA during folding and oligomerization of nucleosome arrays. *Mol Cell Biol*, 2009. 29(2): p. 538-46.
75. Kaplan, N., I.K. Moore, Y. Fondufe-Mittendorf, A.J. Gossett, D. Tillo, Y. Field, E.M. LeProust, T.R. Hughes, J.D. Lieb, J. Widom, and E. Segal, The DNA-encoded nucleosome organization of a eukaryotic genome. *Nature*, 2009. 458(7236): p. 362-6.

76. Karlin, S., B.E. Blaisdell, R.J. Sapolsky, L. Cardon, and C. Burge, Assessments of DNA inhomogeneities in yeast chromosome III. *Nucleic Acids Res*, 1993. 21(3): p. 703-11.
77. Kent, N.A., N. Karabetsou, P.K. Politis, and J. Mellor, In vivo chromatin remodeling by yeast ISWI homologs Isw1p and Isw2p. *Genes Dev*, 2001. 15(5): p. 619-26.
78. Kim, H.S., V. Vanoosthuysen, J. Fillingham, A. Roguev, S. Watt, T. Kislinger, A. Treyer, L.R. Carpenter, C.S. Bennett, A. Emili, J.F. Greenblatt, K.G. Hardwick, N.J. Krogan, J. Bahler, and M.C. Keogh, An acetylated form of histone H2A.Z regulates chromosome architecture in *Schizosaccharomyces pombe*. *Nat Struct Mol Biol*, 2009. 16(12): p. 1286-93.
79. Kiyama, R. and E.N. Trifonov, What positions nucleosomes?--A model. *FEBS Lett*, 2002. 523(1-3): p. 7-11.
80. Kobor, M.S., S. Venkatasubrahmanyam, M.D. Meneghini, J.W. Gin, J.L. Jennings, A.J. Link, H.D. Madhani, and J. Rine, A protein complex containing the conserved Swi2/Snf2-related ATPase Swr1p deposits histone variant H2A.Z into euchromatin. *PLoS Biol*, 2004. 2(5): p. E131.
81. Komura, J. and T. Ono, Disappearance of nucleosome positioning in mitotic chromatin in vivo. *J Biol Chem*, 2005. 280(15): p. 14530-5.
82. Korber, P. and W. Horz, In vitro assembly of the characteristic chromatin organization at the yeast PHO5 promoter by a replication-independent extract system. *J Biol Chem*, 2004. 279(33): p. 35113-20.
83. Korber, P., T. Luckenbach, D. Blaschke, and W. Horz, Evidence for histone eviction in trans upon induction of the yeast PHO5 promoter. *Mol Cell Biol*, 2004. 24(24): p. 10965-74.
84. Kornberg, R.D. and L. Stryer, Statistical distributions of nucleosomes: nonrandom locations by a stochastic mechanism. *Nucleic Acids Res*, 1988. 16(14A): p. 6677-90.
85. Kouzarides, T., Chromatin modifications and their function. *Cell*, 2007. 128(4): p. 693-705.
86. Krogan, N.J., M.C. Keogh, N. Datta, C. Sawa, O.W. Ryan, H. Ding, R.A. Haw, J. Pootoolal, A. Tong, V. Canadien, D.P. Richards, X. Wu, A. Emili, T.R. Hughes, S. Buratowski, and J.F. Greenblatt, A Snf2 family ATPase complex required for recruitment of the histone H2A variant Htz1. *Mol Cell*, 2003. 12(6): p. 1565-76.
87. Kurdistani, S.K., S. Tavazoie, and M. Grunstein, Mapping global histone acetylation patterns to gene expression. *Cell*, 2004. 117(6): p. 721-33.
88. Landsman, D., Histone H1 in *Saccharomyces cerevisiae*: a double mystery solved? *Trends Biochem Sci*, 1996. 21(8): p. 287-8.
89. Langst, G. and P.B. Becker, ISWI induces nucleosome sliding on nicked DNA. *Mol Cell*, 2001. 8(5): p. 1085-92.
90. Langst, G. and P.B. Becker, Nucleosome mobilization and positioning by ISWI-containing chromatin-remodeling factors. *J Cell Sci*, 2001. 114(Pt 14): p. 2561-8.



91. Langst, G., E.J. Bonte, D.F. Corona, and P.B. Becker, Nucleosome movement by CHRAC and ISWI without disruption or trans-displacement of the histone octamer. *Cell*, 1999. 97(7): p. 843-52.
92. Lantermann, A., A. Stralfors, F. Fagerstrom-Billai, P. Korber, and K. Ekwall, Genome-wide mapping of nucleosome positions in *Schizosaccharomyces pombe*. *Methods*, 2009. 48(3): p. 218-25.
93. Lee, C.K., Y. Shibata, B. Rao, B.D. Strahl, and J.D. Lieb, Evidence for nucleosome depletion at active regulatory regions genome-wide. *Nat Genet*, 2004. 36(8): p. 900-5.
94. Lee, W., D. Tillo, N. Bray, R.H. Morse, R.W. Davis, T.R. Hughes, and C. Nislow, A high-resolution atlas of nucleosome occupancy in yeast. *Nat Genet*, 2007. 39(10): p. 1235-44.
95. Levy, A. and M. Noll, Multiple phases of nucleosomes in the hsp 70 genes of *Drosophila melanogaster*. *Nucleic Acids Res*, 1980. 8(24): p. 6059-68.
96. Li, B., S.G. Pattenden, D. Lee, J. Gutierrez, J. Chen, C. Seidel, J. Gerton, and J.L. Workman, Preferential occupancy of histone variant H2AZ at inactive promoters influences local histone modifications and chromatin remodeling. *Proc Natl Acad Sci U S A*, 2005. 102(51): p. 18385-90.
97. Lohr, D., T. Torchia, and J. Hopper, The regulatory protein GAL80 is a determinant of the chromatin structure of the yeast GAL1-10 control region. *J Biol Chem*, 1987. 262(32): p. 15589-97.
98. Lorch, Y., J.W. LaPointe, and R.D. Kornberg, Nucleosomes inhibit the initiation of transcription but allow chain elongation with the displacement of histones. *Cell*, 1987. 49(2): p. 203-10.
99. Louis, C., P. Schedl, B. Samal, and A. Worcel, Chromatin structure of the 5S RNA genes of *D. melanogaster*. *Cell*, 1980. 22(2 Pt 2): p. 387-92.
100. Luger, K., A.W. Mader, R.K. Richmond, D.F. Sargent, and T.J. Richmond, Crystal structure of the nucleosome core particle at 2.8 Å resolution. *Nature*, 1997. 389(6648): p. 251-60.
101. Luger, K. and T.J. Richmond, DNA binding within the nucleosome core. *Curr Opin Struct Biol*, 1998. 8(1): p. 33-40.
102. Lusser, A. and J.T. Kadonaga, Strategies for the reconstitution of chromatin. *Nat Methods*, 2004. 1(1): p. 19-26.
103. Lusser, A., D.L. Urwin, and J.T. Kadonaga, Distinct activities of CHD1 and ACF in ATP-dependent chromatin assembly. *Nat Struct Mol Biol*, 2005. 12(2): p. 160-6.
104. Malave, T.M. and S.Y. Dent, Transcriptional repression by Tup1-Ssn6. *Biochem Cell Biol*, 2006. 84(4): p. 437-43.
105. Malik, H.S. and S. Henikoff, Phylogenomics of the nucleosome. *Nat Struct Biol*, 2003. 10(11): p. 882-91.

106. Martienssen, R.A., M. Zaratiegui, and D.B. Goto, RNA interference and heterochromatin in the fission yeast *Schizosaccharomyces pombe*. *Trends Genet*, 2005. 21(8): p. 450-6.
107. Martinez-Garcia, J.F., F. Estruch, and J.E. Perez-Ortin, Chromatin structure of the 5' flanking region of the yeast *LEU2* gene. *Mol Gen Genet*, 1989. 217(2-3): p. 464-70.
108. Maundrell, K., A. Hutchison, and S. Shall, Sequence analysis of ARS elements in fission yeast. *EMBO J*, 1988. 7(7): p. 2203-9.
109. Mavrich, T.N., I.P. Ioshikhes, B.J. Venters, C. Jiang, L.P. Tomsho, J. Qi, S.C. Schuster, I. Albert, and B.F. Pugh, A barrier nucleosome model for statistical positioning of nucleosomes throughout the yeast genome. *Genome Res*, 2008. 18(7): p. 1073-83.
110. Mavrich, T.N., C. Jiang, I.P. Ioshikhes, X. Li, B.J. Venters, S.J. Zanton, L.P. Tomsho, J. Qi, R.L. Glaser, S.C. Schuster, D.S. Gilmour, I. Albert, and B.F. Pugh, Nucleosome organization in the *Drosophila* genome. *Nature*, 2008. 453(7193): p. 358-62.
111. Miele, V., C. Vaillant, Y. d'Aubenton-Carafa, C. Thermes, and T. Grange, DNA physical properties determine nucleosome occupancy from yeast to fly. *Nucleic Acids Res*, 2008. 36(11): p. 3746-56.
112. Mizuguchi, G., X. Shen, J. Landry, W.H. Wu, S. Sen, and C. Wu, ATP-driven exchange of histone H2AZ variant catalyzed by SWR1 chromatin remodeling complex. *Science*, 2004. 303(5656): p. 343-8.
113. Morris, N.R., Nucleosome structure in *Aspergillus nidulans*. *Cell*, 1976. 8(3): p. 357-63.
114. Nelson, H.C., J.T. Finch, B.F. Luisi, and A. Klug, The structure of an oligo(dA).oligo(dT) tract and its biological implications. *Nature*, 1987. 330(6145): p. 221-6.
115. Oshima, Y., The phosphatase system in *Saccharomyces cerevisiae*. *Genes Genet Syst*, 1997. 72(6): p. 323-34.
116. Ozsolak, F., J.S. Song, X.S. Liu, and D.E. Fisher, High-throughput mapping of the chromatin structure of human promoters. *Nat Biotechnol*, 2007. 25(2): p. 244-8.
117. Parnell, T.J., J.T. Huff, and B.R. Cairns, RSC regulates nucleosome positioning at Pol II genes and density at Pol III genes. *EMBO J*, 2008. 27(1): p. 100-10.
118. Patterton, H.G., C.C. Landel, D. Landsman, C.L. Peterson, and R.T. Simpson, The biochemical and phenotypic characterization of Hho1p, the putative linker histone H1 of *Saccharomyces cerevisiae*. *J Biol Chem*, 1998. 273(13): p. 7268-76.
119. Peckham, H.E., R.E. Thurman, Y. Fu, J.A. Stamatoyannopoulos, W.S. Noble, K. Struhl, and Z. Weng, Nucleosome positioning signals in genomic DNA. *Genome Res*, 2007. 17(8): p. 1170-7.
120. Perez-Ortin, J.E., F. Estruch, E. Matallana, and L. Franco, Fine analysis of the chromatin structure of the yeast *SUC2* gene and of its changes upon derepression. Comparison between the chromosomal and plasmid-inserted genes. *Nucleic Acids Res*, 1987. 15(17): p. 6937-56.

121. Ponomarenko, J.V., M.P. Ponomarenko, A.S. Frolov, D.G. Vorobyev, G.C. Overton, and N.A. Kolchanov, Conformational and physicochemical DNA features specific for transcription factor binding sites. *Bioinformatics*, 1999. 15(7-8): p. 654-68.
122. Prunell, A., Nucleosome reconstitution on plasmid-inserted poly(dA) . poly(dT). *EMBO J*, 1982. 1(2): p. 173-9.
123. Pusarla, R.H. and P. Bhargava, Histones in functional diversification. Core histone variants. *FEBS J*, 2005. 272(20): p. 5149-68.
124. Radman-Livaja, M. and O.J. Rando, Nucleosome positioning: How is it established, and why does it matter? *Dev Biol*, 2009.
125. Raisner, R.M., P.D. Hartley, M.D. Meneghini, M.Z. Bao, C.L. Liu, S.L. Schreiber, O.J. Rando, and H.D. Madhani, Histone variant H2A.Z marks the 5' ends of both active and inactive genes in euchromatin. *Cell*, 2005. 123(2): p. 233-48.
126. Rando, O.J. and K. Ahmad, Rules and regulation in the primary structure of chromatin. *Curr Opin Cell Biol*, 2007. 19(3): p. 250-6.
127. Rando, O.J. and H.Y. Chang, Genome-wide views of chromatin structure. *Annu Rev Biochem*, 2009. 78: p. 245-71.
128. Reinke, H. and W. Horz, Histones are first hyperacetylated and then lose contact with the activated PHO5 promoter. *Mol Cell*, 2003. 11(6): p. 1599-607.
129. Rhodes, D., Nucleosome cores reconstituted from poly (dA-dT) and the octamer of histones. *Nucleic Acids Res*, 1979. 6(5): p. 1805-16.
130. Richard-Foy, H. and G.L. Hager, Sequence-specific positioning of nucleosomes over the steroid-inducible MMTV promoter. *EMBO J*, 1987. 6(8): p. 2321-8.
131. Richmond, E. and C.L. Peterson, Functional analysis of the DNA-stimulated ATPase domain of yeast SWI2/SNF2. *Nucleic Acids Res*, 1996. 24(19): p. 3685-92.
132. Richmond, T.J. and C.A. Davey, The structure of DNA in the nucleosome core. *Nature*, 2003. 423(6936): p. 145-50.
133. Richmond, T.J., J.T. Finch, B. Rushton, D. Rhodes, and A. Klug, Structure of the nucleosome core particle at 7 Å resolution. *Nature*, 1984. 311(5986): p. 532-7.
134. Robinson, P.J. and D. Rhodes, Structure of the '30 nm' chromatin fibre: a key role for the linker histone. *Curr Opin Struct Biol*, 2006. 16(3): p. 336-43.
135. Routh, A., S. Sandin, and D. Rhodes, Nucleosome repeat length and linker histone stoichiometry determine chromatin fiber structure. *Proc Natl Acad Sci U S A*, 2008. 105(26): p. 8872-7.
136. Sambrook, J. and D.W. Russell, *Molecular Cloning - A Laboratory Manual*, 3. edn. (Cold Spring Harbor, Cold Spring Harbor Laboratory Press). 2001.

137. Sasaki, S., C.C. Mello, A. Shimada, Y. Nakatani, S. Hashimoto, M. Ogawa, K. Matsushima, S.G. Gu, M. Kasahara, B. Ahsan, A. Sasaki, T. Saito, Y. Suzuki, S. Sugano, Y. Kohara, H. Takeda, A. Fire, and S. Morishita, Chromatin-associated periodicity in genetic variation downstream of transcriptional start sites. *Science*, 2009. 323(5912): p. 401-4.
138. Satchwell, S.C., H.R. Drew, and A.A. Travers, Sequence periodicities in chicken nucleosome core DNA. *J Mol Biol*, 1986. 191(4): p. 659-75.
139. Satchwell, S.C. and A.A. Travers, Asymmetry and polarity of nucleosomes in chicken erythrocyte chromatin. *EMBO J*, 1989. 8(1): p. 229-38.
140. Schalch, T., S. Duda, D.F. Sargent, and T.J. Richmond, X-ray structure of a tetranucleosome and its implications for the chromatin fibre. *Nature*, 2005. 436(7047): p. 138-41.
141. Schmitt, M.E., T.A. Brown, and B.L. Trumpower, A rapid and simple method for preparation of RNA from *Saccharomyces cerevisiae*. *Nucleic Acids Res*, 1990. 18(10): p. 3091-2.
142. Schones, D.E., K. Cui, S. Cuddapah, T.Y. Roh, A. Barski, Z. Wang, G. Wei, and K. Zhao, Dynamic regulation of nucleosome positioning in the human genome. *Cell*, 2008. 132(5): p. 887-98.
143. Schultz, M.C., Chromatin assembly in yeast cell-free extracts. *Methods*, 1999. 17(2): p. 161-72.
144. Schultz, M.C., D.J. Hockman, T.A. Harkness, W.I. Garinther, and B.A. Altheim, Chromatin assembly in a yeast whole-cell extract. *Proc Natl Acad Sci U S A*, 1997. 94(17): p. 9034-9.
145. Segal, E., Y. Fondufe-Mittendorf, L. Chen, A. Thastrom, Y. Field, I.K. Moore, J.P. Wang, and J. Widom, A genomic code for nucleosome positioning. *Nature*, 2006. 442(7104): p. 772-8.
146. Segal, E. and J. Widom, What controls nucleosome positions? *Trends Genet*, 2009. 25(8): p. 335-43.
147. Sekinger, E.A., Z. Moqtaderi, and K. Struhl, Intrinsic histone-DNA interactions and low nucleosome density are important for preferential accessibility of promoter regions in yeast. *Mol Cell*, 2005. 18(6): p. 735-48.
148. Shivaswamy, S., A. Bhinge, Y. Zhao, S. Jones, M. Hirst, and V.R. Iyer, Dynamic remodeling of individual nucleosomes across a eukaryotic genome in response to transcriptional perturbation. *PLoS Biol*, 2008. 6(3): p. e65.
149. Shrader, T.E. and D.M. Crothers, Artificial nucleosome positioning sequences. *Proc Natl Acad Sci U S A*, 1989. 86(19): p. 7418-22.
150. Simon, R.H. and G. Felsenfeld, A new procedure for purifying histone pairs H2A + H2B and H3 + H4 from chromatin using hydroxylapatite. *Nucleic Acids Res*, 1979. 6(2): p. 689-96.

151. Simpson, R.T. and H. Shindo, Conformation of DNA in chromatin core particles containing poly(dAdT)-poly(dAdT) studied by <sup>31</sup>P NMR spectroscopy. *Nucleic Acids Res*, 1979. 7(2): p. 481-92.
152. Sipiczki, M., Where does fission yeast sit on the tree of life? *Genome Biol*, 2000. 1(2): p. REVIEWS1011.
153. Stein, A., T.E. Takasuka, and C.K. Collings, Are nucleosome positions in vivo primarily determined by histone-DNA sequence preferences? *Nucleic Acids Res*, 2010. 38(3): p. 709-19.
154. Struhl, K., Naturally occurring poly(dA-dT) sequences are upstream promoter elements for constitutive transcription in yeast. *Proc Natl Acad Sci U S A*, 1985. 82(24): p. 8419-23.
155. Studitsky, V.M., D.J. Clark, and G. Felsenfeld, A histone octamer can step around a transcribing polymerase without leaving the template. *Cell*, 1994. 76(2): p. 371-82.
156. Studitsky, V.M., G.A. Kassavetis, E.P. Geiduschek, and G. Felsenfeld, Mechanism of transcription through the nucleosome by eukaryotic RNA polymerase. *Science*, 1997. 278(5345): p. 1960-3.
157. Stunkel, W., I. Kober, and K.H. Seifart, A nucleosome positioned in the distal promoter region activates transcription of the human U6 gene. *Mol Cell Biol*, 1997. 17(8): p. 4397-405.
158. Sugiyama, T., H.P. Cam, R. Sugiyama, K. Noma, M. Zofall, R. Kobayashi, and S.I. Grewal, SHREC, an effector complex for heterochromatic transcriptional silencing. *Cell*, 2007. 128(3): p. 491-504.
159. Svaren, J. and W. Horz, Transcription factors vs nucleosomes: regulation of the PHO5 promoter in yeast. *Trends Biochem Sci*, 1997. 22(3): p. 93-7.
160. Thoma, F., Nucleosome positioning. *Biochim Biophys Acta*, 1992. 1130(1): p. 1-19.
161. Thoma, F. and R.T. Simpson, Local protein-DNA interactions may determine nucleosome positions on yeast plasmids. *Nature*, 1985. 315(6016): p. 250-2.
162. Thomas, J.O. and V. Furber, Yeast chromatin structure. *FEBS Lett*, 1976. 66(2): p. 274-80.
163. Tirosh, I. and N. Barkai, Two strategies for gene regulation by promoter nucleosomes. *Genome Res*, 2008. 18(7): p. 1084-91.
164. Tirosh, I., A. Weinberger, D. Bezalet, M. Kaganovich, and N. Barkai, On the relation between promoter divergence and gene expression evolution. *Mol Syst Biol*, 2008. 4: p. 159.
165. Travers, A., M. Caserta, M. Churcher, E. Hiriart, and E. Di Mauro, Nucleosome positioning-what do we really know? *Mol Biosyst*, 2009. 5(12): p. 1582-92.
166. Tschumper, G. and J. Carbon, Sequence of a yeast DNA fragment containing a chromosomal replicator and the TRP1 gene. *Gene*, 1980. 10(2): p. 157-66.

167. Valouev, A., J. Ichikawa, T. Tonthat, J. Stuart, S. Ranade, H. Peckham, K. Zeng, J.A. Malek, G. Costa, K. McKernan, A. Sidow, A. Fire, and S.M. Johnson, A high-resolution, nucleosome position map of *C. elegans* reveals a lack of universal sequence-dictated positioning. *Genome Res*, 2008. 18(7): p. 1051-63.
168. van Holde, K.E., *Chromatin* (New York, Springer Verlag), 1988.
169. Venter, U., J. Svaren, J. Schmitz, A. Schmid, and W. Horz, A nucleosome precludes binding of the transcription factor Pho4 in vivo to a critical target site in the PHO5 promoter. *EMBO J*, 1994. 13(20): p. 4848-55.
170. Vogelauer, M., J. Wu, N. Suka, and M. Grunstein, Global histone acetylation and deacetylation in yeast. *Nature*, 2000. 408(6811): p. 495-8.
171. Wang, J.C., The path of DNA in the nucleosome. *Cell*, 1982. 29(3): p. 724-6.
172. Wasylyk, B. and P. Chambon, Transcription by eukaryotic RNA polymerases A and B of chromatin assembled in vitro. *Eur J Biochem*, 1979. 98(2): p. 317-27.
173. Wasylyk, B., G. Thevenin, P. Oudet, and P. Chambon, Transcription of in vitro assembled chromatin by *Escherichia coli* RNA polymerase. *J Mol Biol*, 1979. 128(3): p. 411-40.
174. Weiner, A., A. Hughes, M. Yassour, O.J. Rando, and N. Friedman, High-resolution nucleosome mapping reveals transcription-dependent promoter packaging. *Genome Res*, 2010. 20(1): p. 90-100.
175. Weintraub, H. and M. Groudine, Chromosomal subunits in active genes have an altered conformation. *Science*, 1976. 193(4256): p. 848-56.
176. Whitehouse, I., O.J. Rando, J. Delrow, and T. Tsukiyama, Chromatin remodelling at promoters suppresses antisense transcription. *Nature*, 2007. 450(7172): p. 1031-5.
177. Whitehouse, I. and T. Tsukiyama, Antagonistic forces that position nucleosomes in vivo. *Nat Struct Mol Biol*, 2006. 13(7): p. 633-40.
178. Widom, J., Toward a unified model of chromatin folding. *Annu Rev Biophys Biophys Chem*, 1989. 18: p. 365-95.
179. Widom, J., Role of DNA sequence in nucleosome stability and dynamics. *Q Rev Biophys*, 2001. 34(3): p. 269-324.
180. Widom, J. and A. Klug, Structure of the 300A chromatin filament: X-ray diffraction from oriented samples. *Cell*, 1985. 43(1): p. 207-13.
181. Wilhelm, B.T., S. Marguerat, S. Watt, F. Schubert, V. Wood, I. Goodhead, C.J. Penkett, J. Rogers, and J. Bahler, Dynamic repertoire of a eukaryotic transcriptome surveyed at single-nucleotide resolution. *Nature*, 2008. 453(7199): p. 1239-43.
182. Williams, S.P., B.D. Athey, L.J. Muglia, R.S. Schappe, A.H. Gough, and J.P. Langmore, Chromatin fibers are left-handed double helices with diameter and mass per unit length that depend on linker length. *Biophys J*, 1986. 49(1): p. 233-48.

183. Wippo, C.J., B.S. Krstulovic, F. Ertel, S. Musladin, D. Blaschke, S. Sturzl, G.C. Yuan, W. Horz, P. Korber, and S. Barbaric, Differential cofactor requirements for histone eviction from two nucleosomes at the yeast PHO84 promoter are determined by intrinsic nucleosome stability. *Mol Cell Biol*, 2009. 29(11): p. 2960-81.
184. Wittig, B. and S. Wittig, A phase relationship associates tRNA structural gene sequences with nucleosome cores. *Cell*, 1979. 18(4): p. 1173-83.
185. Wolffe, A., *Chromatin - Structure & Function*, 3. edn. (London, Academic Press). 1998.
186. Woodcock, C.L. and S. Dimitrov, Higher-order structure of chromatin and chromosomes. *Curr Opin Genet Dev*, 2001. 11(2): p. 130-5.
187. Wu, C., Y.C. Wong, and S.C. Elgin, The chromatin structure of specific genes: II. Disruption of chromatin structure during gene activity. *Cell*, 1979. 16(4): p. 807-14.
188. Xu, Z., W. Wei, J. Gagneur, F. Perocchi, S. Clauder-Munster, J. Camblong, E. Guffanti, F. Stutz, W. Huber, and L.M. Steinmetz, Bidirectional promoters generate pervasive transcription in yeast. *Nature*, 2009. 457(7232): p. 1033-7.
189. Yang, X., R. Zaurin, M. Beato, and C.L. Peterson, Swi3p controls SWI/SNF assembly and ATP-dependent H2A-H2B displacement. *Nat Struct Mol Biol*, 2007. 14(6): p. 540-7.
190. Yuan, G.C., Targeted recruitment of histone modifications in humans predicted by genomic sequences. *J Comput Biol*, 2009. 16(2): p. 341-55.
191. Yuan, G.C. and J.S. Liu, Genomic sequence is highly predictive of local nucleosome depletion. *PLoS Comput Biol*, 2008. 4(1): p. e13.
192. Yuan, G.C., Y.J. Liu, M.F. Dion, M.D. Slack, L.F. Wu, S.J. Altschuler, and O.J. Rando, Genome-scale identification of nucleosome positions in *S. cerevisiae*. *Science*, 2005. 309(5734): p. 626-30.
193. Zhang, H., D.N. Roberts, and B.R. Cairns, Genome-wide dynamics of Htz1, a histone H2A variant that poises repressed/basal promoters for activation through histone loss. *Cell*, 2005. 123(2): p. 219-31.
194. Zhang, Y., Z. Moqtaderi, B.P. Rattner, G. Euskirchen, M. Snyder, J.T. Kadonaga, X.S. Liu, and K. Struhl, Intrinsic histone-DNA interactions are not the major determinant of nucleosome positions in vivo. *Nat Struct Mol Biol*, 2009. 16(8): p. 847-52.
195. Zhang, Z. and J.C. Reese, Ssn6-Tup1 requires the ISW2 complex to position nucleosomes in *Saccharomyces cerevisiae*. *EMBO J*, 2004. 23(11): p. 2246-57.
196. Zhao, X., P.S. Pendergrast, and N. Hernandez, A positioned nucleosome on the human U6 promoter allows recruitment of SNAPc by the Oct-1 POU domain. *Mol Cell*, 2001. 7(3): p. 539-49.
197. Zlatanova, J. and A. Thakar, H2A.Z: view from the top. *Structure*, 2008. 16(2): p. 166-79.
198. Zofall, M., T. Fischer, K. Zhang, M. Zhou, B. Cui, T.D. Veenstra, and S.I. Grewal, Histone H2A.Z cooperates with RNAi and heterochromatin factors to suppress antisense RNAs. *Nature*, 2009. 461(7262): p. 419-22.

## 6 Abbreviations

A	Absorption
ACF	ATP-utilizing chromatin assembly and remodeling factor
ADP	Adenosindiphosphate
ATP	Adenosintriphosphate
bp	Base pair
β-ME	β-mercaptoethanol
BSA	Bovine serum albumine
<i>C. elegans</i>	<i>Caenorhabditis elegans</i>
CENP-A	Centromere protein A
CHD	Chromodomain-helicase-DNA-binding
ChIP	Chromatin immunoprecipitation
CK	Creatine kinase
CP	Creatine phosphate
DMSO	Dimethylsulfoxide
DNA	Deoxyribonucleic acid
DNase I	Bovine deoxyribonucleaseI
DNMT	DNA methyltransferase
dNTP	Deoxyribonucleotidetriphosphate
<i>Drosophila/D. melanogaster</i>	<i>Drosophila melanogaster</i>
DTT	Dithiothreitol
<i>E. coli</i>	<i>Escherichia coli</i>
EDTA	Ethylendiamintetraacetic acid
EGTA	Ethylenglycol-bis(2-aminoethyl)-N,N,N',N'-tetraacetic acid
EM	Electron microscopy
EMM	Edinburgh minimal medium
EthBr	Ethidiumbromide
EtOH	Ethanol
h	Hour
H1/H2A/H2B/H3/ H4	Histone proteins
HAT	Histone acetyltransferase
HDAC	Histone deacetylase
HEPES	N-(2-Hydroxyethyl)piperazine-H <sup>+</sup> -2-ethanesulfonic acid
HMM	Hidden Markov model
IAC	Isoamylalcohol/chloroform
INO80	Inositol requiring
ISWI	Imitation switch ( <i>Drosophila, Xenopus</i> )
ISW2	Imitation switch ( <i>Sacharomyces cerevisiae</i> )
l	Liter
M	Molar
min	Minute(s)
ml	Milli liter
mM	Milli molar
MNase	Micrococcal nuclease
MOPS	3-(N-morpholino)propanesulfonic acid
MWCO	Molecular weight cut off
NA	Not available
NDR	Nucleosome depleted region
NFR	Nucleosome free region
NP-40	Nonidet P-40



---

NRL	Nucleosome repeat length
OD	Optical density
o/n	over night
ORF	Open reading frame
PCR	Polymerase chain reaction
PEG	Polyethylene glycol
PMSF	Phenylmethylsulphonylfluoride
PVP40	Polyvinylpyrrolidon 40
PTM	Posttranslational modification
RNA	Ribonucleic acid
RNAi	RNA interference
RNase A	Ribonuclease A
rpm	Revolutions per minute
RSC	Remodels the structure of chromatin
RT	Room temperature
<i>S. cerevisiae/S. c.</i>	<i>Saccharomyces cerevisiae</i>
SDS	Sodium dodecyl sulfate
SNF2	Sucrose non-fermenting protein 2
<i>S. pombe/S. p.</i>	<i>Schizosaccharomyces pombe</i>
Sth1	Snf two homolog 1
SWI/SNF	Switch/sucrose non-fermenting
SWR1	Swi2/Snf2-related 1
TAE	Tris acetate EDTA buffer
TdT	Terminal deoxynucleotidyl transferase
Tris	Tris(hydroxymethyl)aminomethane
TSS	Transcription start site
TTS	Transcription termination site
U	Unit
UTR	Untranslated region
UV	Ultraviolet
v/v	Volume per volume
wt	Wild-type
w/v	Weight per volume

## Curriculum vitae

**Name** Alexandra Bettina Lantermann  
**Date of birth** 20<sup>th</sup> November 1981  
**Place of birth** Deggendorf

### Education

Mar. 2007 – present PhD thesis at the Ludwig-Maximilians-University of Munich  
 Adolf-Butenandt-Institute, Prof. Peter Becker  
 Project: Comparison of genome-wide nucleosome positioning mechanisms  
 in *Schizosaccharomyces pombe* and *Saccharomyces cerevisiae*

2004 – 2006 Studies of Molecular Biotechnology at the TU Munich  
 Master of Science  
 Master's thesis at the Ludwig-Maximilians-University of Munich  
 Max-von-Pettenkofer Institute, PD. Frank Ebel  
 Project: Analysis of the pathogenicity of the human mould  
*Aspergillus fumigatus*

2001 – 2004 Studies of Molecular Biotechnology at the TU Munich  
 Bachelor of Science  
 Bachelor's thesis at the TU Munich  
 Department of Biosciences, Prof. Siegfried Scherer  
 Project: Binding studies of cell wall binding domains from phage  
 endolysins to cell walls of *Listeria monocytogenes*

1999 – 2001 Descartes Gymnasium Neuburg an der Donau  
 Abitur

1992 – 1999 Comenius Gymnasium Deggendorf

### Publications

Lantermann, A., T. Straub, A. Stralfors, G. C. Yuan, K. Ekwall and P. Korber (2010). *Schizosaccharomyces pombe* genome-wide nucleosome mapping reveals positioning mechanisms distinct from those of *Saccharomyces cerevisiae*. Nat Struct Mol Biol 17(2): 251-257.

Lantermann, A., A. Stralfors, F. Fagerstrom-Billai, P. Korber and K. Ekwall (2009). Genome-wide mapping of nucleosome positions in *Schizosaccharomyces pombe*. Methods 48(3): 218-225.